

# Modelling the Deposition and Concentration of Long Range Air Pollutants: Final Report

Anthony Dore<sup>1</sup>, Massimo Vieno<sup>1</sup>, Margaret MacDougal<sup>1</sup>, Maciej Kryza<sup>2</sup>, Marek Błaś<sup>2</sup>, Jane Hall<sup>3</sup>, Alessandro Dosio<sup>1</sup>, Sim Tang<sup>1</sup>, Ron Smith<sup>1</sup>, Bill Bealey<sup>1</sup> and Mark Sutton<sup>1</sup>

<sup>1</sup>*Centre for Ecology and Hydrology, Edinburgh Research Station  
Bush Estate, Penicuik, Midlothian EH26 0QB*

<sup>2</sup>*Department of Meteorology and Climatology, University of Wroclaw,  
ul. Kosiby 8, 51-670 Wroclaw, Poland*

<sup>3</sup>*Centre for Ecology and Hydrology, Monks Wood Research Station  
Abbots Ripton, Huntingdon, PE28 2LS*

February 2006

Client: DEFRA	
Client Project number: EPG 1/3/302	CEH Project number: C02159
Project Title: Modelling the Deposition and Concentration of Long Range Air Pollutants	
Start date: 1 December 2002	Completion date: 30 November 2005
Client Project Officer: Samantha Baker	
CEH Project Officer: Anthony Dore	
Main authors: Anthony Dore, Massimo Vieno, Margaret MacDougal, Maciej Kryza, Marek Błaś, Jane Hall, Alessandro Dosio, Sim Tang, Ron Smith, Bill Bealey and Mark Sutton	
Report approved for release by: Mark Sutton	
Reporting period: 1 December 2002 – 30 November 2005	
Report date: 5 April 2006	
Report Number: AS 06/05	
Report Status: Final	

This report is a confidential document prepared under contract between [client] and the Natural Environment Research Council (NERC). It should not be distributed or quoted without the permission of both the Centre for Ecology and Hydrology (CEH) and [client].

# **Executive Summary**

## **Objectives of the Project**

1. Research has been conducted by a consortium of CEH, University of Edinburgh, and the University of Wroclaw to model the deposition and concentrations of long range air pollutants for DEFRA. The work had the following objectives:
  - To develop a model to make maps of deposition of sulphur and oxidised and reduced nitrogen across the United Kingdom.
  - To compare the model with results from other UK and European models.
  - To compare the results of the model with measurements of gas and aerosol concentrations and wet deposition from the UK national monitoring networks.
  - To improve the meteorological parameterisations employed by the model.
  - To incorporate emissions from international shipping in the model.
  - To improve the parameterisation of emissions from high and low level sources in the model.
  - To investigate the sensitivity of model parameters.
  - To apply the model to investigate past and future trends in sulphur and nitrogen deposition.
  - To apply the model to future emissions abatement scenarios.
  - To generate source-receptor data for input to the United Kingdom Integrated Assessment model.
  - To make model information, data and reports accessible on a website.

## **Scientific and operational performance of FRAME**

2. A good correlation is demonstrated between FRAME and measurements of gas concentrations ( $\text{SO}_2$ ,  $\text{NO}_x$ ,  $\text{NH}_3$ ,  $\text{HNO}_3$ ), as well as the wet deposition and aerosol concentrations of  $\text{SO}_4^{2-}$ ,  $\text{NO}_3^{-}$  and  $\text{NH}_4^+$ . This shows that the model, despite its relatively simple meteorological parameterisations, is well suited to calculating average annual concentrations and deposition of acidifying and eutrophying pollutants.
3. As emissions of  $\text{SO}_2$  and  $\text{NO}_x$  have reduced significantly in recent decades, with further decreases forecast over the next 15 years, the relative importance of  $\text{NH}_3$  and its contribution to nutrient nitrogen and acidic deposition has increased. FRAME was originally developed as an ammonia specialist model and is well suited to tackle this challenge. The good performance of FRAME for  $\text{NH}_3$  depends on the fine-vertical structure, allowing simulation of ground level (1-2 m) air concentrations, coupled with its land-use-specific treatment of dry deposition.
4. The operational performance of FRAME has been improved by restructuring the model code. The output format allows a smooth interface to emissions data of the NAEI, to calculations of exceedance of critical loads conducted at CEH-Monkswood and input to the United Kingdom Integrated Assessment Model, for calculation of the cost benefits of different emissions abatement strategies. An input parameter file was

developed to allow all new parameterisations to be selected as model simulation options.

5. An operational package of post-processing routines has been developed for FRAME using IDL graphics to automate the plotting of UK sulphur and nitrogen deposition maps, scatter graphs showing model-measurement calculations, exceedance of critical levels for ammonia concentrations, UK deposition budgets and population-weighted particulate concentrations.

## Developments to parameterisations in FRAME

6. Emissions of  $\text{SO}_2$  and  $\text{NO}_x$  from international shipping are increasing and therefore rapidly becoming an important source of air pollution as land-based emissions are brought under control. Shipping emissions were explicitly included in the FRAME domain and were estimated to make a contribution of 10% to total sulphur deposition in the UK.
7. A plume rise model was introduced to FRAME for point source emissions, resulting in improved correlation with measurements of  $\text{SO}_2$  concentrations
8.  $\text{NH}_3$  emissions were input to the model according to different categories of agricultural emissions and non-agricultural emissions, each with a specific emissions height. Surface layer concentrations of ammonia were found to be sensitive to the height at which individual emissions sources were input to the model.
9. Background emissions of  $\text{SO}_2$  and  $\text{NO}_x$  were input to the model according to SNAP emissions code. This proved useful in creating future emissions scenarios using individual SNAP abatement factors.
10.  $\text{HNO}_3$  has been identified as an important source of oxidised nitrogen deposition in the UK. Changes to a number of physical and chemical parameterisations in FRAME led to underestimates in modelled nitric acid concentrations being reduced from a factor of 8 to a factor of 2

## Application of FRAME

11. FRAME was used to estimate past and future deposition of nitrogen and sulphur to the UK. During the period 1970 it was estimated that deposition of sulphur, oxidised nitrogen and reduced nitrogen to the UK have fallen by 90%, 56% and 20% respectively. For certain vegetation types, the exceedance of critical loads has improved significantly during this period (i.e. for dwarf shrub heath the percentage of area with exceedance of critical loads for acid deposition has fallen from 96% to 22% during this period). For other vegetation types, exceedances are forecast to remain high (i.e. for unmanaged woodland, exceedance of critical loads for nitrogen deposition is forecast to decrease from 98% to 94% between 1970 and 2020).
12. Wet and dry deposition maps of  $\text{SO}_x$ ,  $\text{NO}_y$  and  $\text{NH}_x$  from FRAME were compared with the measurement based CBED data. The two data sets generally showed good agreement. FRAME gave lower values of  $\text{NO}_y$  dry deposition than CBED and lower wet deposition than CBED in the north of Scotland. These differences may be accounted for by an underestimate of  $\text{HNO}_3$  concentrations in FRAME and by an underestimate of long range transport to the remote far north. Alternatively, it is possible that some overestimate exists in CBED due to extrapolation of measurements from a sparse network of monitoring stations
13. A sensitivity study was undertaken to assess the importance of 25 individual physical and chemical model parameters in influencing nitrogen and sulphur deposition. It was

concluded that emissions rates, dry deposition velocities and wet removal rates were the most important parameters in introducing uncertainty to estimates of acidifying and nitrogen deposition

14. FRAME was applied to assessing the influence of eight separate emissions abatement scenarios for the year 2020 for the Air Quality Strategy. The ‘Euro High’ scenario (involving a high level of control to NO<sub>x</sub> emissions from petrol and diesel vehicles) resulted in the largest effect, with NO<sub>y</sub> deposition reduced by 12%.
15. FRAME was applied to generating source receptor relationships between emissions and national scale N and S deposition for 75 counties, 20 point sources, international shipping and European import. The data was used as input to the UK Integrated Assessment Model

## **Recommendations for future developments**

16. It was recognised that concentrations of NH<sub>3</sub> and NH<sub>x</sub> dry deposition in source regions, as well as wet deposition in upland regions vary significantly on a scale unresolved by a model 5km grid square. The future development of a finer 1km resolution of FRAME is recommended
17. Currently, emissions of SO<sub>2</sub> and NO<sub>x</sub> from international shipping are gridded at a 50 km resolution. This leads to the need to re-grid emissions in coastal areas where a 5 km grid square is classified as land, and results in uncertainty in emissions from ports and coastal regions. The assessment of the contribution to acid deposition from international shipping would benefit from a finer resolution of emissions data in ports and coastal regions.
18. In assessing the temporal trends in nitrogen and sulphur deposition in the UK, a 50 year time series (1970-2020) exists for SO<sub>2</sub> and NO<sub>x</sub> emissions. However, the NH<sub>3</sub> emissions time series dates back only till 1990. Future work on time trends would benefit from an extension to the historical record of NH<sub>3</sub> emissions.
19. A future need exists for a Lagrangian model such as FRAME to provide a fast response in assessing the effects of emissions abatement scenarios and generating source-receptor data from multiple simulations. However, comparison of FRAME with state of the art Eulerian models, such as EMEP4UK and Models-3, will be important in assessing the potential future role of the new models for calculating S and N deposition in the UK.

# Table of Contents

<b>MODELLING THE DEPOSITION AND CONCENTRATION OF LONG RANGE AIR POLLUTANTS:</b> .....	<b>1</b>
<b>FINAL REPORT</b> .....	<b>1</b>
<b>EXECUTIVE SUMMARY</b> .....	<b>2</b>
OBJECTIVES OF THE PROJECT .....	3
SCIENTIFIC AND OPERATIONAL PERFORMANCE OF FRAME .....	3
DEVELOPMENTS TO PARAMETERISATIONS IN FRAME .....	4
APPLICATION OF FRAME .....	4
FUTURE RECOMMENDATIONS .....	5
<b>TABLE OF CONTENTS</b> .....	<b>6</b>
<b>1. BACKGROUND</b> .....	<b>8</b>
<b>2. DESCRIPTION OF FRAME</b> .....	<b>11</b>
2.1 HISTORY .....	11
2.2 FRAME MODEL DOMAIN .....	11
2.3 EMISSIONS .....	11
2.4 PLUME RISE.....	12
2.5 DIFFUSION .....	12
2.6 CHEMISTRY .....	12
2.7 WET DEPOSITION .....	12
2.8 DRY DEPOSITION.....	13
2.9 DIURNAL CYCLE.....	13
2.10 WIND ROSE .....	13
2.11 COMPUTATIONAL PERFORMANCE.....	13
<b>3 INTER-COMPARISON OF FRAME WITH EMEP AND CBED DEPOSITION</b> .....	<b>16</b>
<b>4 CORRELATION OF FRAME WITH MEASUREMENTS FROM THE NATIONAL MONITORING NETWORKS</b> .....	<b>21</b>
<b>5 WIND FREQUENCY AND WIND SPEED ROSE</b> .....	<b>25</b>
5.1 RADIOSONDE DATA.....	25
5.2 WIND FREQUENCY ROSE .....	25
5.3 WIND SPEED ROSE .....	26
5.4 APPLICATION OF RADIOSONDE WIND DATA IN FRAME .....	33
<b>6 EMISSIONS FROM INTERNATIONAL SHIPPING</b> .....	<b>36</b>
<b>7 REPRESENTATION OF EMISSIONS HEIGHT IN FRAME</b> .....	<b>41</b>
7.1 PLUME RISE FOR POINT SOURCE EMISSIONS OF SO <sub>2</sub> AND NO <sub>x</sub> .....	41
7.2 INTRODUCTION OF SECTOR DEPENDENT HEIGHT OF AMMONIA EMISSIONS .....	43
<b>8 COMPARISON OF FRAME WITH MEASUREMENTS FROM THE AMMONIA MONITORING NETWORK</b> .....	<b>44</b>
<b>9 SENSITIVITY STUDY</b> .....	<b>46</b>
9.1 INTRODUCTION .....	46
9.2 PARAMETERS STUDIED .....	46

9.3 RESULTS .....	49
9.4 CONCLUSION .....	53
<b>10. IMPROVEMENT OF THE PARAMETERISATION OF HNO<sub>3</sub> IN FRAME .....</b>	<b>54</b>
10.1 INTRODUCTION .....	54
10.2 CHANGES TO PRODUCTION AND LOSS MECHANISMS OF HNO <sub>3</sub> .....	54
<b>11 THE AIR QUALITY STRATEGY .....</b>	<b>58</b>
11.1 RATIONALE AND BACKGROUND.....	58
11.2 RESULTS .....	58
11.3 CALCULATION OF EXCEEDANCE OF CRITICAL LOADS .....	60
<b>12 PAST AND FUTURE TRENDS FOR NITROGEN AND SULPHUR .....</b>	<b>64</b>
12.1 PAST AND FUTURE TRENDS IN EMISSIONS OF SO <sub>2</sub> , NO <sub>x</sub> AND NH <sub>3</sub> .....	64
12.2 TRENDS IN DEPOSITION OF SULPHUR AND NITROGEN .....	65
12.3 PAST AND FUTURE TRENDS IN THE EXCEEDANCE OF CRITICAL LOADS .....	66
<b>13 SOURCE-RECEPTOR RELATIONSHIPS FOR THE UKIAM.....</b>	<b>72</b>
<b>14. FRAME WEB SITE.....</b>	<b>72</b>
<b>14. REFERENCES .....</b>	<b>73</b>
<b>APPENDIX 1: SUMMARY LOG OF MAJOR DEVELOPMENTS IN FRAME IN RELATION TO MODEL VERSIONS .....</b>	<b>1</b>
<b>APPENDIX 2: FLOW CHART ILLUSTRATING THE FRAME MECHANISM.....</b>	<b>5</b>

## 1. Background

The emission of pollutant gases ( $\text{SO}_2$ ,  $\text{NO}_x$  and  $\text{NH}_3$ ) from the United Kingdom, from European sources and from international shipping results in the deposition of acidifying and eutrophying species to sensitive ecosystems. The emitted gases are chemically transformed in the atmosphere to particulate matter, comprising sulphate, nitrate and ammonium aerosol, which is subject to long range transport. Deposition exceeding the critical loads for acidification and eutrophication may occur, even in regions remote from the source of emissions, such as the Scottish Highlands. Acidification affects soils and freshwater, particularly in upland areas where soils tend to be derived from base-poor rocks and annual precipitation is high. Deposition of both reduced and oxidised nitrogen results in eutrophication leading to changes in plant species composition and water quality in semi-natural habitats. In addition, secondary aerosols are of concern both regarding their potential impacts on human health (COMEAP, 2001) and their effect on visibility and the global radiative balance.

Emissions of  $\text{SO}_2$  and  $\text{NO}_x$  in the United Kingdom have fallen by 88% and 43% during the period 1970-2005 (pers. comm, Chris Dore, AEA Technology), with further reductions of 44% and 38%, respectively, forecast over the next 15 years according to Business-as-Usual scenarios (pers. comm, John Stedman, AEA Technology). Despite these improvements to the quality of the atmosphere, deposition of sulphate and nitrate by precipitation has responded with smaller changes than those in land-based emissions (Fowler *et al.*, 2005). One possible explanation of this observation is the role of shipping emissions of  $\text{SO}_2$  and  $\text{NO}_x$  which, in contrast to land based emissions, have shown increases over recent decades of approximately 2.5% per year (Johnson *et al.*, 2000, Vestreng and Fagerli, 2005). Furthermore, emissions of ammonia in the UK have shown more modest decreases of 19% between 1990 and 2003 (pers. comm, Chris Dore, NETCEN). Emissions of  $\text{SO}_2$  and  $\text{NO}_x$  from Europe have shown similar decreases to those from the UK. However, estimating their role in contributing to acid and nutrient-nitrogen deposition in the United Kingdom has recently received more attention. The focus for future studies of modelling emissions and deposition of nitrogen and sulphur in the United Kingdom will therefore increasingly be on shipping emissions and ammonia emissions, as land based emissions of  $\text{SO}_2$  and  $\text{NO}_x$  become relatively less important.

Sulphur and nitrogen compounds can be removed from the atmosphere by direct turbulent deposition to vegetation (dry deposition) which is an important pathway for deposition of gaseous species,  $\text{SO}_2$ ,  $\text{NO}_2$  and  $\text{NH}_3$ . For ammonia the deposition rate is particularly sensitive to the vegetation type, with high deposition rates to forest and moorland. For aerosols, as well as soluble gases ( $\text{SO}_2$ ,  $\text{HNO}_3$ ,  $\text{NH}_3$ ) removal by precipitation (wet deposition) is an important pathway for deposition. Transport distances of chemicals may be several thousand km from their emissions source before they are deposited, depending on the chemical reactions and dry and wet removal rates of individual chemical species. Numeric atmospheric transport models are increasingly being used as a key tool to estimate the transport and deposition of nitrogen and sulphur.

The model currently used by DEFRA to estimate sulphur and nitrogen deposition in the United Kingdom is the **Fine Resolution Atmospheric Multi-pollutant Exchange** model (**FRAME**). Estimates of present day S and N deposition may be derived from measurements, for example as shown for the UK by the **National Expert Group on Transboundary Air Pollution (NEGTAP, 2001)**. The use of a canopy compensation point to generate maps of gaseous deposition to vegetation for the United Kingdom is described in Smith *et al.* (2000). Smith and Fowler (2001) describe a technique to generate maps of wet deposition for the United Kingdom by interpolation of measured concentrations of ions in precipitation. The

combination of these two measurement-based data sets is referred to as **CBED** (Concentration Based Estimated Deposition) and is used to inform DEFRA about current levels of nitrogen and sulphur deposition in the United Kingdom.

The importance of protecting sensitive ecosystems from environmental damage has led to several international and European agreements. These include the 1999 Protocol to Abate Acidification, Eutrophication and Ground-level Ozone, under the UNECE Convention on Long-Range Transboundary Air Pollution (**CLRTAP**) and the European Community National Emissions Ceiling Directive (**NECD**). These agreements lay down targets for nation states to achieve reductions of emissions of SO<sub>2</sub>, NO<sub>x</sub> and NH<sub>3</sub> by the year 2010. The UK Government and the devolved administrations published an Air Quality Strategy for England, Scotland, Wales and Northern Ireland (**AQS**) in 2000 (DETR, 2000) in January 2000. It sets air quality standards and objectives for eight key pollutants to be achieved between 2003 and 2008. For seven of these pollutants local authorities are charged with the task of working towards the objectives in a cost effective way. The standards and objectives are subject to regular review to take account of the latest information on the health effects of air pollution and technical and policy developments.

Measurement-based estimates have been used successfully as an environmental assessment tool for past or present conditions. Assessment of future scenarios, however, requires the application of models linked to atmospheric emission changes. Measurements also have a limited spatial resolution, and uncertainty arises in the interpolation of concentrations and deposition between measurement sites. The spatial resolution of model estimates is limited either by the resolution of input data such as land use and emissions (which are available at a 1 km resolution for the United Kingdom) or by computational restrictions. Furthermore, for the assessment of the terms in mass-consistent budgets (emissions, deposition, import and export), atmospheric transport models are invaluable. Models are necessary for the establishment of source–receptor relationships for integrated assessment modelling and for estimating the contribution to S and N deposition from international shipping and from import from European sources.

The EMEP Eulerian Unified model (Tarrasón, et al., 2003) is used to estimate sulphur and nitrogen deposition across Europe. Calculations are driven by PARLAM-PS, a Numerical Weather Prediction Model (NWP). The model incorporates emissions of SO<sub>2</sub>, NO<sub>x</sub>, NH<sub>3</sub>, NMVOC, CO and PM<sub>2.5</sub> and PM<sub>10</sub>. The EMEP model includes a detailed treatment of three-dimensional transport and diffusion of air pollutants, as well as atmospheric chemical reactions and particle size distribution. Due to the continent scale size of the EMEP domain, it is restricted to operating on a 50 km grid with a vertical resolution in the lowest layer of 92 m. For national scale assessments, a 50 km scale is insufficient to resolve the finer scale distribution of land use, precipitation and emissions of pollutant gases. For accurate estimation of ammonia concentrations and dry deposition of ammonia, a model with a fine vertical resolution is essential. Increasingly there is a need to apply atmospheric transport models to estimating the relative roles of different emissions sources in contributing to acid and nutrient nitrogen deposition. The results of such simulations may be used as input to integrated assessment calculations in order to derive the most cost efficient means of abating pollutant emissions and protecting environmental and human health. The **United Kingdom Integrated Assessment Model, UKIAM** (Oxley *et al.*, 2003) has been developed to estimate the relative cost efficiency of abating emissions from different regions, at a county level, and point sources using sulphur and nitrogen deposition footprints from the FRAME model. Based on the above considerations, the requirements for a model capable of accurately estimating ground level gas and particulate concentrations, capturing the fine scale features of emissions of NO<sub>x</sub> and NH<sub>3</sub> and of wet deposition in upland regions, as well as performing multiple simulations (of up to 100) for source-receptor applications may be specified simply as:

- (i) Fine horizontal resolution
- (ii) Fine near-surface vertical resolution
- (iii) Fast run time
- (iv) Good comparison with measurements of gas and aerosol concentrations and wet deposition

FRAME is well suited to fit these needs. It is important however to consider this work in the context of parallel developments with Eulerian models driven by real time meteorology. United Kingdom versions of both the EMEP model (“EMEP4UK”) and the US EPA model, Models-3, at a 4-5 km resolution are currently under development at CEH funded by other DEFRA contracts. These models use detailed meteorological data to simulate atmospheric transport, including the effects of curved movement of air trajectories and lateral dispersion. They would therefore, in principle, be capable of achieving a better representation of nitrogen and sulphur deposition than FRAME, assuming that their future development is successful. The time scale for the Eulerian models to surpass FRAME in accuracy of representing wet and dry deposition, as well as gas and particle concentrations, is not known, but can realistically be expected to occur within the next five years. It is important to note, however, that a Eulerian model is unlikely to entirely replace FRAME in the short term. Future parallel development and regular inter-comparison of these modelling systems will be important. The following points emphasise the need for parallel development of modelling applications:

- (1) In the Eulerian chemical transport models, wet deposition is calculated using precipitation generated from a Numerical Weather Prediction Model (NWP). In a Lagrangian trajectory model such as FRAME, wet deposition is calculated using measurements of precipitation. Significant improvements in NWP models may therefore be necessary before the Eulerian models are capable of estimating wet deposition as effectively as FRAME.
- (2) The execution time for a full year by a Eulerian model, such as EMEP run on a similar horizontal grid to FRAME, is estimated at approximately two weeks using the CEH Nemesis parallel supercomputer. This compares with 25 minutes for a FRAME simulation. Eulerian models are therefore unsuitable for source-receptor calculations involving approximately 100 model runs with current computer technology.
- (3) The development of a 1 km version of FRAME is currently being undertaken. This fine scale resolution is currently an unrealistic aspiration for a Eulerian model with a UK domain.

## 2. Description of FRAME

### 2.1 History

The **FRAME** (Fine Resolution Atmospheric Multi-pollutant Exchange) model is a Lagrangian atmospheric transport model used to assess the long-term annual mean deposition of reduced and oxidised nitrogen and sulphur over the United Kingdom. A detailed description of the FRAME model is contained in Singles *et al.* (1998). Fournier *et al.* (2003) describe the development of a parallelised version of the model with an extended domain that includes Northern Ireland and the Republic of Ireland. The model was developed from an earlier European scale model, **TERN** (Transport over Europe of Reduced Nitrogen, ApSimon *et al.* 1994). FRAME was developed initially to focus, in particular, on transport and deposition of reduced nitrogen and was named the **Fine Resolution AMmonia Exchange** model. Subsequently, FRAME was developed to improve the representation of sulphur and oxidised nitrogen (Fournier *et al.*, 2005). The developments included: the introduction of a fine angular resolution of 1° between trajectories; the generation of a point source database including stack parameters (stack height, stack diameter, exit temperature, exit velocity); the introduction of shipping emissions of SO<sub>2</sub> and NO<sub>x</sub>. Following these changes, a robust multi-chemical species tool was developed. The new name reflects these changes whilst preserving the familiar acronym. The current version of FRAME is 5.8

### 2.2 FRAME Model Domain

The domain of FRAME covers the British Isles with a grid resolution of 5 km and grid dimensions of 172 x 244. Input gas and aerosol concentrations at the edge of the UK FRAME domain are calculated using **FRAME-EUROPE**, a larger scale European simulation which was developed from TERN to run a statistical model over the entirety of Europe with a 150 km scale resolution.

While FRAME is usually referred to as a Lagrangian model, strictly speaking it combines elements of both Lagrangian and Eulerian approaches: the lateral dispersion is Lagrangian, so that the model simulates an air column moving along straight-line trajectories over the UK. However, the model atmosphere is divided into 33 separate layers extending from the ground to an altitude of 2500 m, and the diffusion between these layers (using the finite volume approach) is effectively Eulerian in nature. FRAME is unique in regional scale dispersion models in having an extremely detailed vertical resolution: Layer thicknesses vary from 1 m at the surface to 100 m at the top of the domain. Separate trajectories are run at a 1° resolution for all grid edge points. Wind frequency and wind speed roses (Dore *et al.* 2005) are used to give the appropriate weighting to directional deposition and concentration for calculation of total deposition and average concentration.

### 2.3 Emissions

Emissions of ammonia are estimated for each 5 km grid square using the AENEID model (Atmospheric Emissions for National Environmental Impacts Determination) that combines data on farm animal numbers (cattle, poultry, pigs, sheep and horses), with land cover information, as well as fertiliser application, crops and non-agricultural emissions (including traffic and contributions from human sources, wild animals etc). The AENEID model is described in Dragosits *et al.* (1998) and is now updated as a contribution of CEH to the National Atmospheric Emissions Inventory (NAEI, <http://www.naei.org.uk/>) and the National Ammonia Reduction and Strategies Evaluation System (NARSES). NH<sub>3</sub> is input to the lowest layer for emissions from sheep, fertiliser application and non-agricultural sources.

Emissions from cattle, poultry and pigs are input to deeper surface layers depending on the relative time spent grazing and in housing. Emissions of SO<sub>2</sub> and NO<sub>x</sub> are taken directly from the National Atmospheric Emissions Inventory (NAEI, [www.naei.org.uk](http://www.naei.org.uk)). 900 individual point sources are included with detailed information on stack parameters from 250 of these. SO<sub>2</sub> and NO<sub>x</sub> background emissions are divided into **SNAP** (Source Nomenclature Activity Profile) code emissions sector with the depth of surface layer into which emissions are input selected according to emissions source. This division of emissions in FRAME directly into the SNAP codes allows ready exchange of information with the NAEI, and smooth running of scenarios based on emission controls applied to particular source sectors.

## 2.4 Plume Rise

Point source emissions of SO<sub>2</sub> and NO<sub>x</sub> are treated individually with a plume rise model which uses stack height, stack diameter, exit temperature and exit velocity to calculate an ‘effective emissions height’. The plume reaches its maximum height when its temperature is equal to that of the surrounding environment and its momentum is dissipated. Buoyancy forces dominate the plume rise, which is parameterised separately for stable conditions and for neutral and unstable conditions according to the Pasquill-Gifford stability classes. The incorporation of this model into FRAME has led to a substantial improvement in model performance for predicted SO<sub>2</sub> concentrations in relation to measurements from the rural SO<sub>2</sub> network (Vieno, 2005)

## 2.5 Diffusion

Diffusion of gaseous and particulate species in the vertical is calculated using K-theory eddy diffusivity and solved with a Finite Volume Method (Vieno, 2005). The vertical diffusivity K<sub>Z</sub> has a linearly increasing value up to a specified height H<sub>Z</sub> and then remains constant (K<sub>max</sub>) to the top of the boundary layer. During daytime, when diffusivity depends on a combination of mechanical and convective mixing, H<sub>Z</sub> is taken as 200 m and K<sub>max</sub> is a function of the boundary layer depth and the geostrophic wind speed. At night time these values depend on the Pasquill stability class.

## 2.6 Chemistry

The chemical scheme in FRAME is similar to that employed in the EMEP Lagrangian model (Barrett and Seland, 1995). The prognostic chemical variables calculated in FRAME are: NH<sub>3</sub>, NO, NO<sub>2</sub>, HNO<sub>3</sub>, PAN, SO<sub>2</sub>, H<sub>2</sub>SO<sub>4</sub>, as well as NH<sub>4</sub><sup>+</sup>, NO<sub>3</sub><sup>-</sup> and SO<sub>4</sub><sup>2-</sup> aerosol. For oxidised nitrogen, a suite of gas phase reactions is considered. These include photolytic dissociation of NO<sub>2</sub>, oxidation of NO by ozone, formation of PAN (peroxyacetyl nitrate) and the creation of nitric acid by reaction with the OH· free radical. NH<sub>4</sub>NO<sub>3</sub> aerosol is formed by the equilibrium reaction between HNO<sub>3</sub> and NH<sub>3</sub>. A second category of large nitrate aerosol is present and simulates the deposition of nitric acid on to soil dust or marine aerosol. The formation of H<sub>2</sub>SO<sub>4</sub> by gas phase oxidation of SO<sub>2</sub> is represented by a predefined oxidation rate. H<sub>2</sub>SO<sub>4</sub> then reacts with NH<sub>3</sub> to form ammonium sulphate aerosol. The aqueous phase reactions considered in the model include the oxidation of S(IV) by O<sub>3</sub>, H<sub>2</sub>O<sub>2</sub> and the metal catalysed reaction with O<sub>2</sub>.

## 2.7 Wet Deposition

The FRAME model employs a constant drizzle approach using precipitation rates calculated from a climatological map of average annual precipitation for the British Isles. Wet deposition of chemical species is calculated using scavenging coefficients based on those used in the EMEP model. An enhanced washout rate is assumed over hill areas due to the scavenging of cloud droplets by the seeder-feeder effect. The washout rate for the orographic

component of rainfall is assumed to be twice that calculated for the non-orographic component (Dore *et al.*, 1992). The model incorporates the directional dependence of orographic rainfall by considering two components of rainfall: non-orographic precipitation, which has no directional dependence, and orographic precipitation, which is directionally dependent and stronger for wind directions associated with humid air masses. The directional orographic rainfall model is described in detail by Fournier *et al.* (2005a).

## 2.8 Dry Deposition

Dry deposition of SO<sub>2</sub>, NO<sub>2</sub> and NH<sub>3</sub> is calculated individually to five different land categories (arable, forest, moor-land, grassland and urban). For ammonia, dry deposition is calculated individually at each grid square using a canopy resistance model (Singles *et al.*, 1998). The model includes an optional bi-directional canopy compensation point parameterisation (Vieno 2005) which will be used in combination with monthly emissions and meteorological data. In the standard model version, the NH<sub>3</sub> deposition velocity is generated from the sums of the aerodynamic resistance, the laminar boundary layer resistance and the surface resistance. Dry deposition of SO<sub>2</sub> and NO<sub>2</sub> is calculated using maps of deposition velocity derived by the CEH ‘big leaf’ model, CBED (Smith *et al.* 2000), which takes account of surface properties as well as the geographical and altitudinal variation of wind-speed. Other species are assigned constant values of deposition velocity.

## 2.9 Diurnal Cycle

The depth of the boundary layer in FRAME is calculated using a mixed boundary layer model with constant potential temperature capped by an inversion layer with a discontinuity in potential temperature. Solar irradiance is calculated as a function of latitude, time of the year and time of the day. At night time, a single fixed value is used for the boundary layer depth according to Pasquill stability class and surface wind speed.

## 2.10 Wind Rose

The wind rose now employed in FRAME uses 6-hourly operational radiosonde data from the stations of Stornoway, Hillsborough, Camborne and Valentia spanning a ten-year period (1991-2000) to establish the frequency and harmonic mean wind speed as a function of direction for the British Isles. This is illustrated in Figures 2(a) and 2(b) for data averaged over the ten year period. The radiosonde wind frequency rose was found by Dore *et al.* (2005) to have close agreement with the Jenkinson objective classification for a 120-year data set.

## 2.11 Computational Performance

The FRAME model code is written in High Performance FORTRAN 90 and executed in parallel on a Linux Beowulf cluster comprising of 60 dual processors, (i.e. 120 processors in total). Run time for a simulation employing 100 processors is approximately 25 minutes.

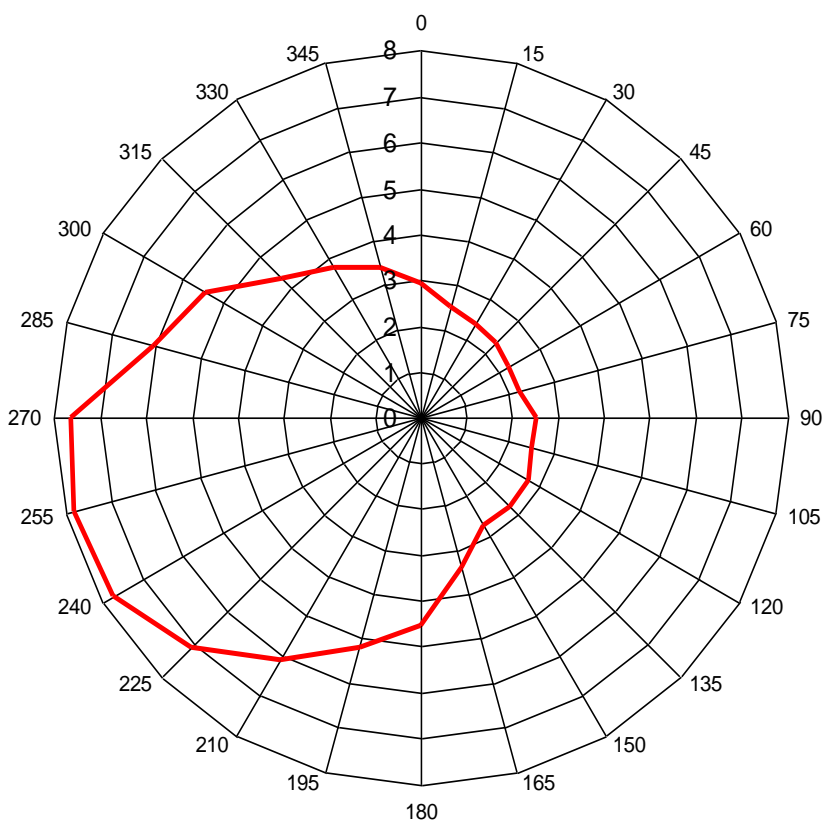


**Figure 2(a)** Wind frequency rose derived from radiosonde data (Dore *et al.* 2005a) as used in FRAME.

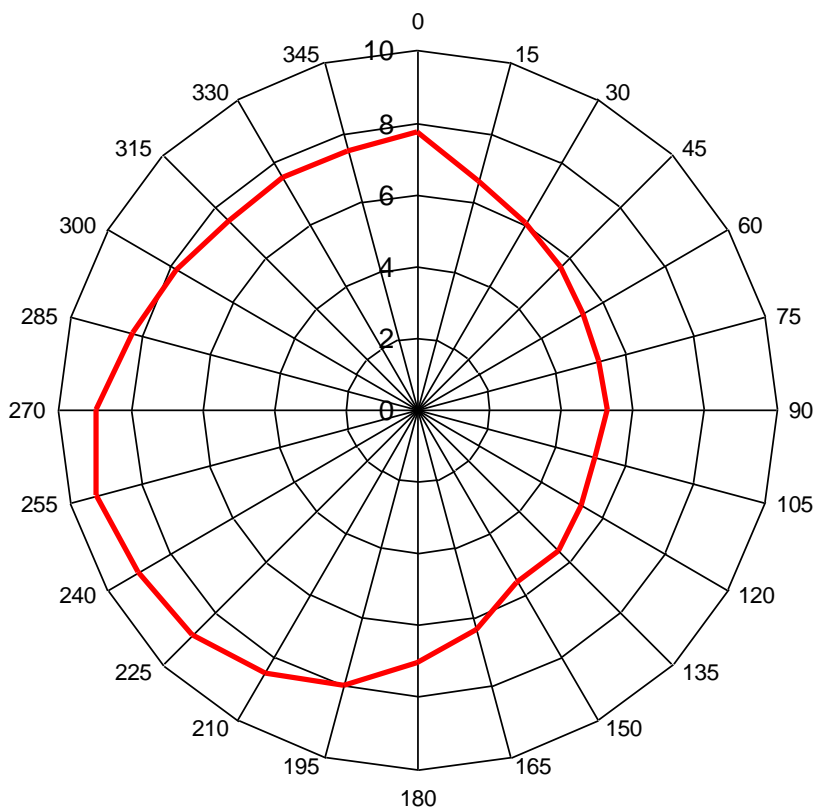


**Figure 2(b)** Wind speed rose derived from radiosonde data (Dore *et al.* 2005a) as used in FRAME.  
Modelling the Deposition and Concentration of Long Range Air Pollutants

### **Box 1: Key features of the FRAME model.**

- \* 5km x 5km resolution over the British Isles (incorporating the Republic of Ireland) grid dimensions: 244 x 172 with a 1° angular resolution in the trajectories.
- \* Input gas and aerosol concentrations at the edge of the model domain are calculated with FRAME-Europe, using European emissions and running on the EMEP 150 km scale grid.
- \* 33 layer Lagrangian model with an air column moving along straight-line trajectories with 24 different wind directions. Variable layer thickness from 1 m at the surface to 100 m at the top of the mixing layer.
- \* Emissions of SO<sub>2</sub> and NO<sub>x</sub>, from 900 major point sources input at height dependent on plume rise calculation. SNAP code dependent background SO<sub>2</sub> and NO<sub>x</sub> sources mixed into appropriate lower layers of the atmosphere. Source-dependent NH<sub>3</sub> emissions mixed into lowest surface layers.
- \* Diffusion in the vertical is calculated using K-theory eddy diffusivity and solved with the Finite Volume Method.
- \* Wet deposition calculated using a diurnally varying scavenging coefficient depending on mixing layer depth. A precipitation model is used to calculate wind-direction-dependent orographic enhancement of wet deposition.
- \* Dry deposition for NH<sub>3</sub> is ecosystem specific, including a version with bi-directional NH<sub>3</sub> exchange. Dry deposition of NO<sub>2</sub> and SO<sub>2</sub> is derived from the CEH deposition model and is ecosystem dependent.
- \* The model chemistry includes gas phase and aqueous phase reactions of oxidised sulphur and oxidised nitrogen and conversion of NH<sub>3</sub> to ammonium sulphate and ammonium nitrate aerosol.
- \* The chemical species treated include: NH<sub>3</sub>, NH<sub>4</sub><sup>+</sup> aerosol, NO, NO<sub>2</sub>, HNO<sub>3</sub>, PAN, NO<sub>3</sub><sup>-</sup> aerosol, SO<sub>2</sub>, H<sub>2</sub>SO<sub>4</sub> and SO<sub>4</sub><sup>2-</sup> aerosol.
- \* Current model run time: 25 minutes on CEH Edinburgh Beowulf cluster using 100 processors.

### **3 Inter-comparison of FRAME with EMEP and CBED deposition**

The mapped deposition of sulphur, oxidised nitrogen and reduced nitrogen calculated by FRAME for emissions year 2002 is shown in Figures 3.1, 3.2 and 3.3, respectively. These maps are compared to the equivalent deposition data for CBED (averaged over years 2001-2003) and for EMEP with emissions year 2002.

In general, the spatial patterns of wet deposition for FRAME and CBED show close agreement. Deposition is highest in the hill areas of the Pennines and Wales, due to a combination of heavy precipitation and orographically enhanced concentrations in precipitation due to the seeder-feeder effect. The main difference in wet deposition between FRAME and CBED occurs in the north of Scotland where FRAME gives much lower estimates. This could be either due to an underestimate in concentrations of secondary particulate matter advected to the north caused by the straight line trajectory approximation in FRAME or an overestimate of orographic enhancement of deposition by the CBED procedure in the mountainous terrain. Although sulphate and nitrate aerosol concentrations are only available at a few sites, ammonium aerosol is measured at more sites and it should be noted that there is good agreement between FRAME and measured ammonium aerosol concentrations in N and W Scotland. The pattern of wet deposition with the EMEP model is quite different. Wet deposition is highest in the lowland source areas of eastern England. The main reason for this difference is that orographic enhancement of ion concentrations in precipitation is not considered in the EMEP model. Furthermore, there are difficulties associated with meteorological modelling of orographic precipitation at a 50 km resolution. As demonstrated by Dore *et al.* (2006), wet deposition in upland regions can vary significantly at a 1km resolution which is unresolved by the model 5 km grid squares. This emphasises the need to develop a future version of FRAME at a finer 1 km resolution.

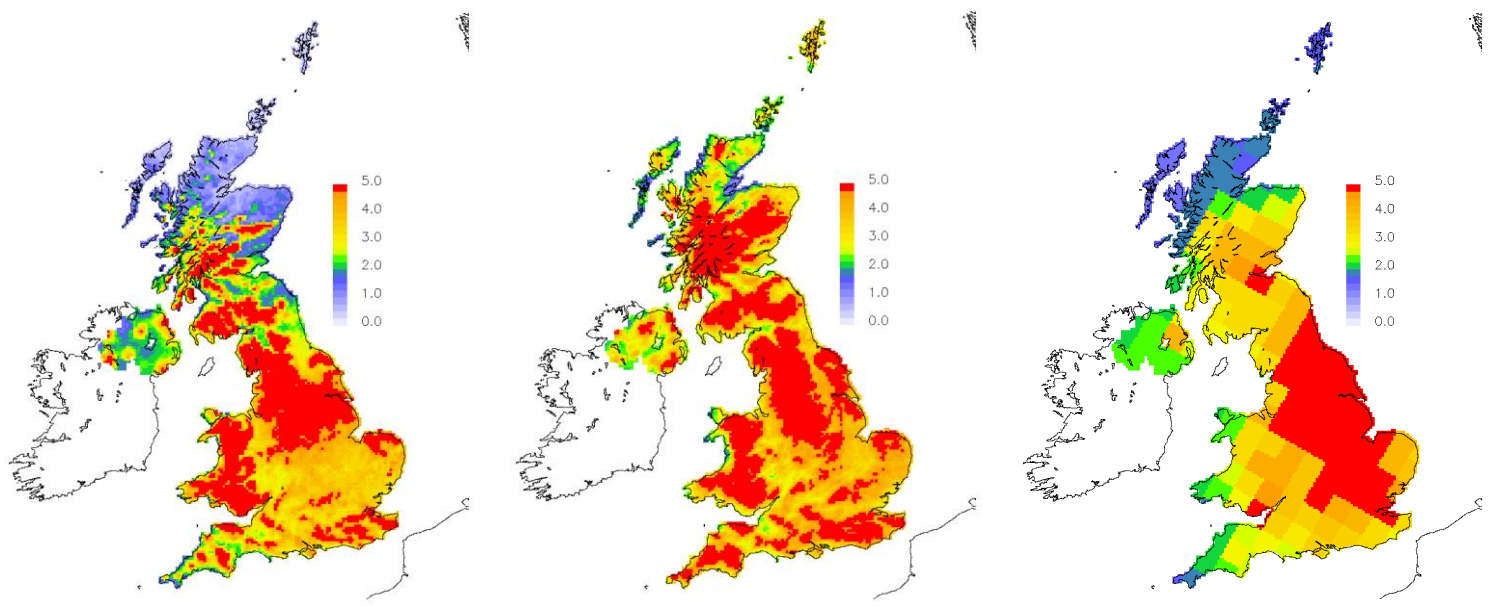
Dry deposition of sulphur (Figures 3.1(d)-(f)) for all three datasets is highest close to the source areas of northern England and Greater London. The EMEP data in addition show a strong SE-NW gradient in sulphur dry deposition, which is due to the greater component of mass imported from Europe than with FRAME. The advantages of running a fine scale trajectory model are clearly illustrated in Figure 3.2(d) for FRAME. Dry deposition of NO<sub>Y</sub> is closely correlated to road transport, and the large urban areas of Greater London, Birmingham, Manchester and the major motorways are clearly visible in this map. Overall, FRAME gives significantly lower estimates of NO<sub>Y</sub> deposition than CBED (as discussed below). A similar spatial structure in dry deposition of reduced nitrogen is evident for the three models (Figures 4(d)-(f)). However the coarse 50 km resolution of the EMEP model means that is not able to capture the fine scale features of ammonia emissions and deposition. CBED and FRAME give very similar reduced nitrogen deposition maps. This, however, is not surprising since CBED uses spatial output of ammonia concentrations from FRAME, compensated by a measurement-model correlation to derive its fine scale spatial pattern in NH<sub>3</sub> dry deposition. One significant difference between FRAME and CBED is the presence of negative deposition with the CBED data in eastern England. This occurs due to the canopy compensation point parameterisation, which may result in net emissions from fertilised fields in agricultural areas. This process is also represented in the bi-directional exchange module of FRAME, which is currently an optional parameterisation, and will be of general application in a future monthly model version following introduction of seasonal meteorology and ammonia emissions to the model.

Table 3.1 illustrates the total deposition budgets to the United Kingdom for the three datasets for sulphur, oxidised nitrogen and reduced nitrogen. In general, there is relatively close agreement in the wet deposition budgets of FRAME and EMEP, but EMEP gives higher dry deposition for SO<sub>X</sub> and NO<sub>Y</sub>. For dry and wet deposition of reduced nitrogen and sulphur

the FRAME and CBED budgets show agreement to within approximately 25%, but significant differences occur for oxidised nitrogen, which is lower for FRAME than with CBED. An important factor in the dry deposition of oxidised nitrogen is nitric acid which contributes approximately 70% of the total NO<sub>y</sub> deposition in CBED. The comparison of modelled HNO<sub>3</sub> concentrations with measurements is discussed below. This suggests that FRAME underestimates HNO<sub>3</sub> concentrations and therefore deposition.

**Table 3.1:** UK annual deposition budgets for FRAME, CBED and EMEP

Budget	FRAME	CBED	EMEP
<b>SO<sub>x</sub> wet (Mg S)</b>	104	117	104
<b>NO<sub>y</sub> wet (Mg N)</b>	64	95	65
<b>NH<sub>x</sub> wet (Mg N)</b>	84	107	73
<b>SO<sub>x</sub> dry (Mg S)</b>	56	64	77
<b>NO<sub>y</sub> dry (Mg N)</b>	46	98	54
<b>NH<sub>x</sub> dry (Mg N)</b>	68	65	61



**Fig. 3.1(a)** FRAME 2002 SO<sub>x</sub> wet deposition  
[kg S ha<sup>-1</sup> yr<sup>-1</sup>]

**Fig. 3.1(b)** CBED 2001-03 SO<sub>x</sub> wet deposition  
[kg S ha<sup>-1</sup> yr<sup>-1</sup>]

**Fig. 3.1(c)** EMEP 2002 SO<sub>x</sub> wet deposition  
[kg S ha<sup>-1</sup> yr<sup>-1</sup>]

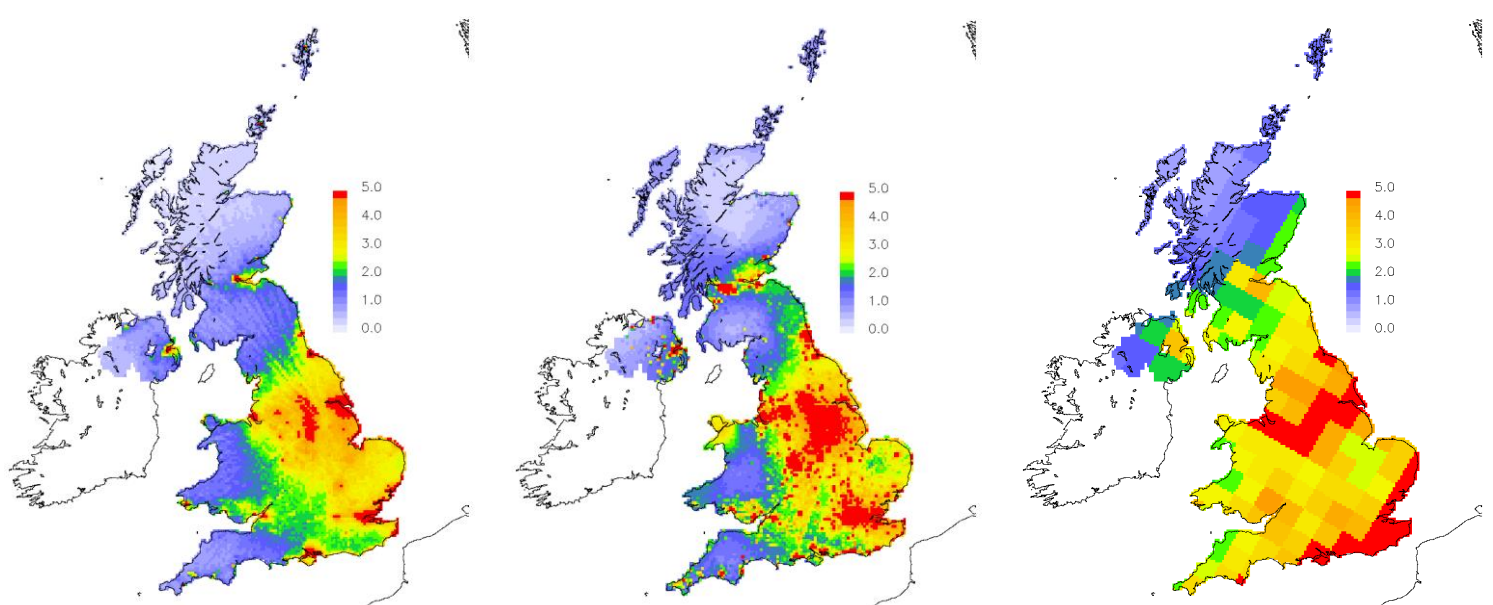


**Fig. 3.1(d)** FRAME 2002 SO<sub>x</sub> dry deposition  
[kg S ha<sup>-1</sup> yr<sup>-1</sup>]

**Fig. 3.1(e)** CBED 2001-03 SO<sub>x</sub> dry deposition  
[kg S ha<sup>-1</sup> yr<sup>-1</sup>]

**Fig. 3.1(f)** EMEP 2002 SO<sub>x</sub> dry deposition  
[kg S ha<sup>-1</sup> yr<sup>-1</sup>]

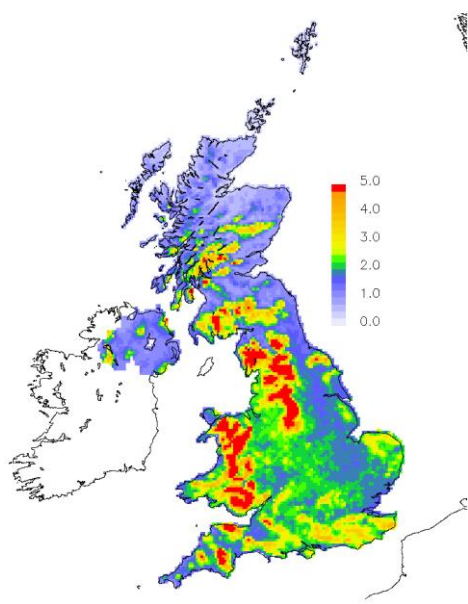


**Fig. 3.2(a)** FRAME 2002 NO<sub>y</sub> wet deposition  
[kg N ha<sup>-1</sup> yr<sup>-1</sup>]

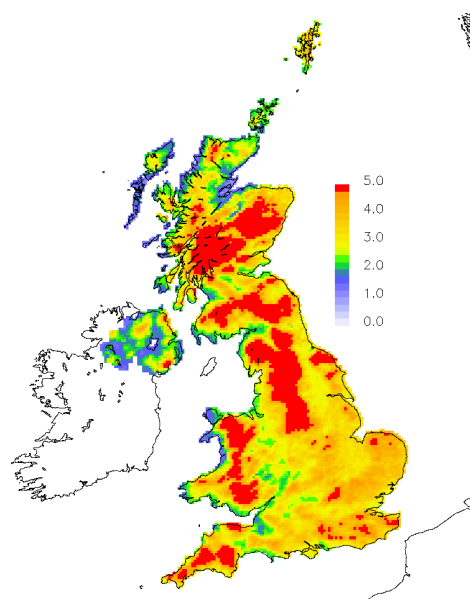


**Fig. 3.2(b)** CBED 2001-03 NO<sub>y</sub> wet deposition  
[kg N ha<sup>-1</sup> yr<sup>-1</sup>]

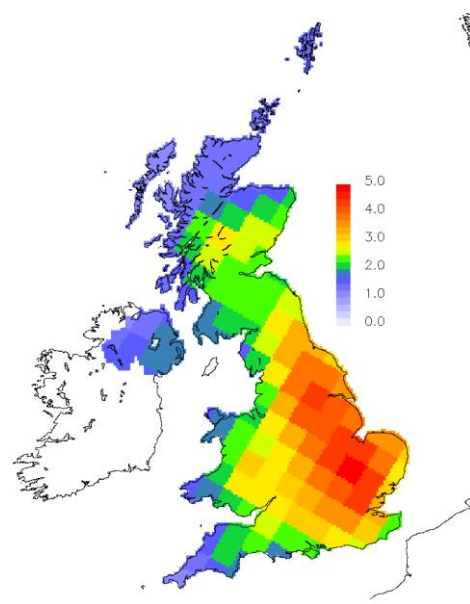


**Fig 3.2(c)** EMEP 2002 NO<sub>y</sub> wet deposition  
[kg N ha<sup>-1</sup> yr<sup>-1</sup>]

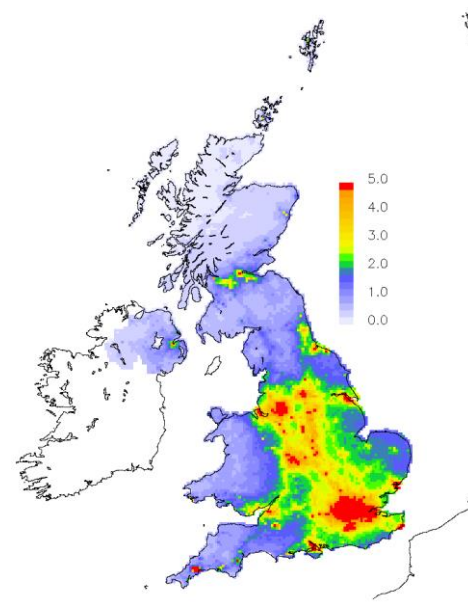


**Fig. 3.2(d)** FRAME 2002 NO<sub>y</sub> dry deposition  
[kg N ha<sup>-1</sup> yr<sup>-1</sup>]

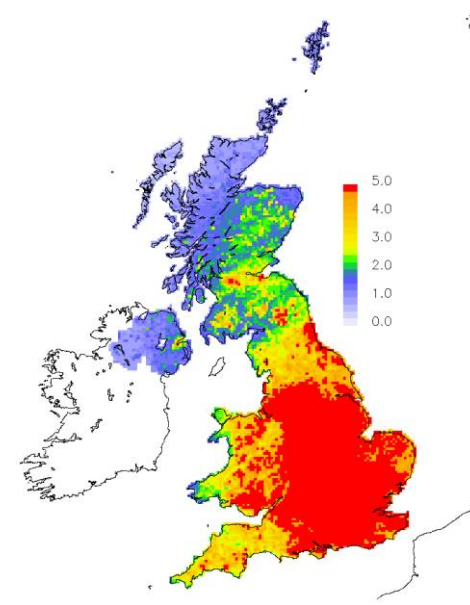


**Fig. 3.2(e)** CBED 2001-3 NO<sub>y</sub> dry deposition  
[kg N ha<sup>-1</sup> yr<sup>-1</sup>]

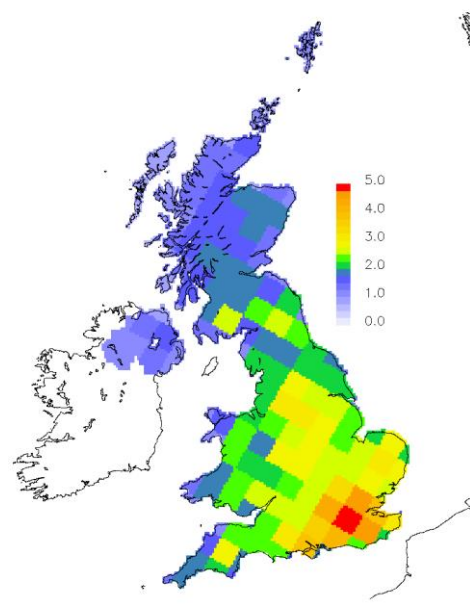


**Fig. 3.2(f)** EMEP 2002 NO<sub>y</sub> dry deposition  
[kg N ha<sup>-1</sup> yr<sup>-1</sup>]

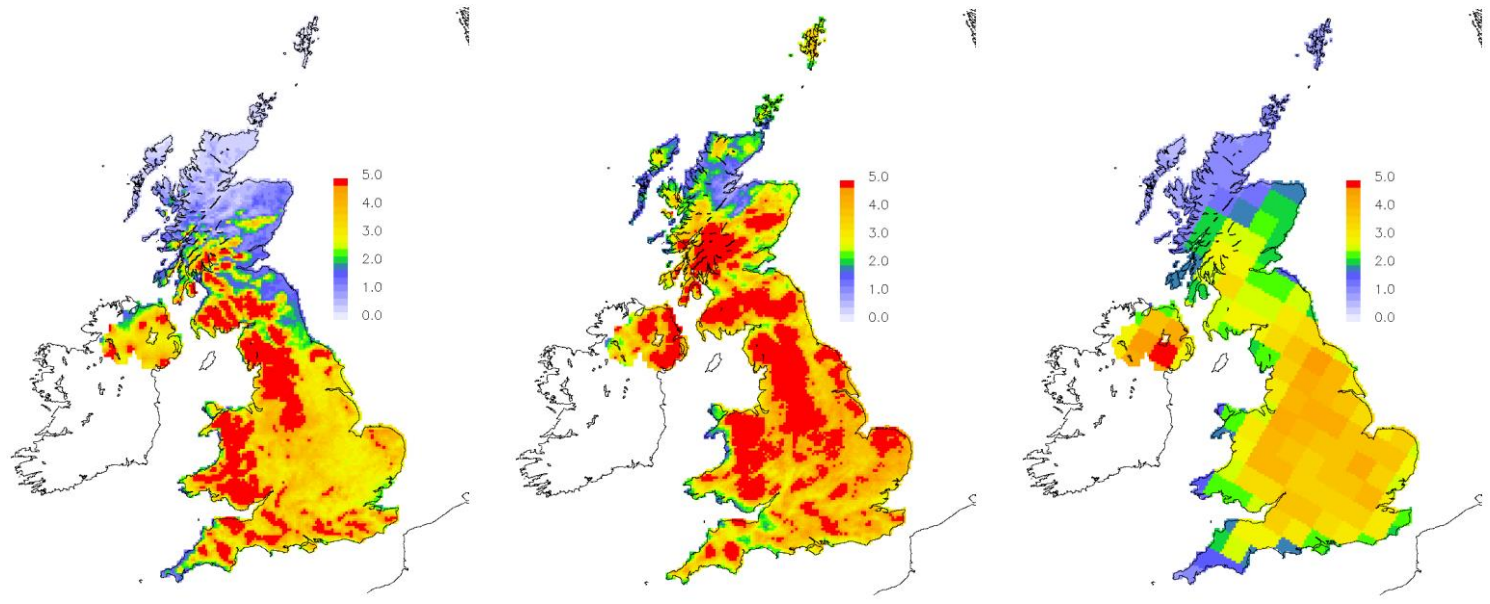


**Fig. 3.3(a)** FRAME 2002  $\text{NH}_x$  wet deposition  
[ $\text{kg N ha}^{-1} \text{yr}^{-1}$ ]

**Fig. 3.3(b)** CBED 2001-3  $\text{NH}_x$  wet deposition  
[ $\text{kg N ha}^{-1} \text{yr}^{-1}$ ]

**Fig. 3.3(c)** EMEP 2002  $\text{NH}_x$  wet deposition  
[ $\text{kg N ha}^{-1} \text{yr}^{-1}$ ]

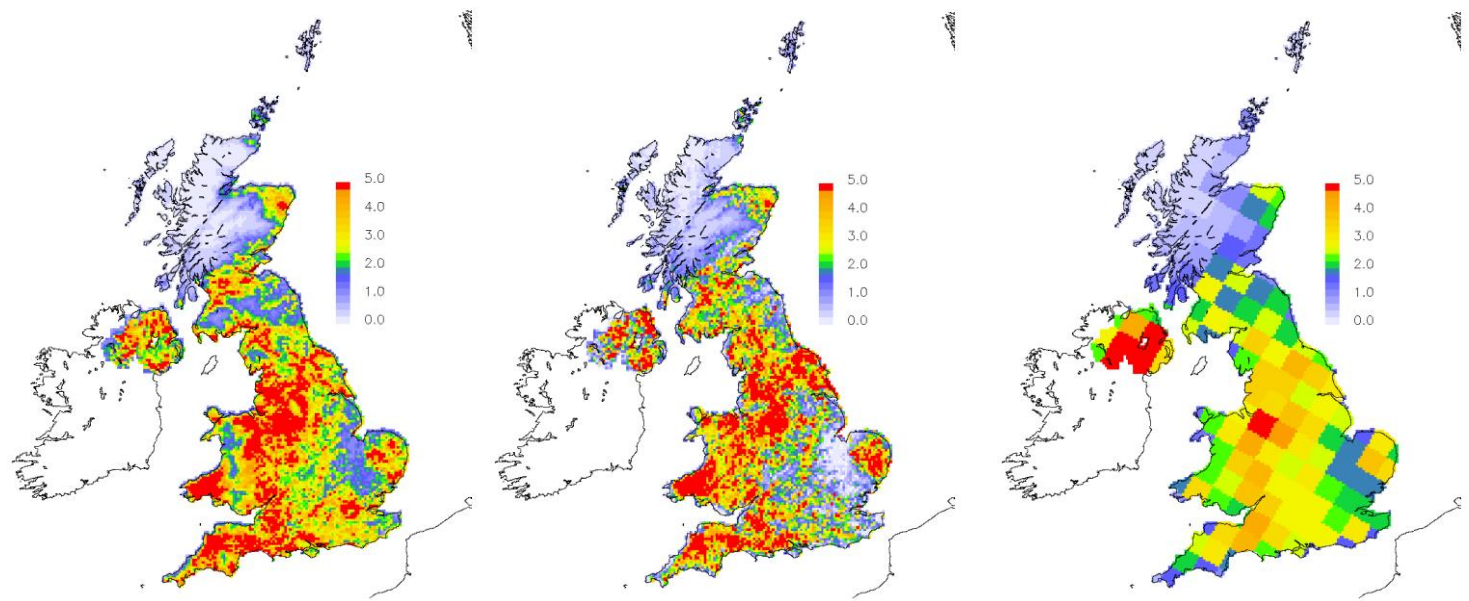


**Fig. 3.3(d)** FRAME 2002  $\text{NH}_x$  dry deposition  
[ $\text{kg N ha}^{-1} \text{yr}^{-1}$ ]

**Fig. 3.3(e)** CBED 2001-03  $\text{NH}_x$  dry deposition  
[ $\text{kg N ha}^{-1} \text{yr}^{-1}$ ]

**Fig. 3.3(f)** EMEP 2002  $\text{NH}_x$  dry deposition  
[ $\text{kg N ha}^{-1} \text{yr}^{-1}$ ]

## 4 Correlation of FRAME with measurements from the national monitoring networks

A direct assessment of the accuracy of FRAME in estimating atmospheric concentrations and deposition rates of gaseous and particulate compounds of nitrogen and sulphur can be made by comparison with measurements. For this purpose, data from the National Ammonia Monitoring Network and the National Nitric Acid Monitoring Network using monthly sampling from **DELT**A samplers (**D**Enuder for **L**ong **T**erm **A**nalysis) were employed (gas phase and aerosol concentrations), together with results from the rural SO<sub>2</sub> and NO<sub>2</sub> networks and the UK wet deposition network. The modelled data for the year 2002 have been compared with measurements of gas and aerosol concentrations. Concentrations of NO<sub>2</sub> were taken from the rural monitoring network using diffusion tubes. Wet deposition was obtained from the secondary acid precipitation monitoring network, comprising fortnightly collections of precipitation from 38 sites with ion concentrations analysed by ion chromatography. The data were averaged over the three-year period 2001-2003 to smooth out inter-annual anomalies. The results of these scatter plots are illustrated in Figures 4(a)-(g). A general feature of the plots is a good correlation between the measurements and the model, which suggests that FRAME is able to accurately represent the spatial distribution of gases and particles in the United Kingdom. Different monitoring networks with a more extensive set of measurement sites have been used to compare with FRAME air concentrations of SO<sub>2</sub>, NH<sub>3</sub> and NH<sub>4</sub><sup>+</sup> for the year 1999. The correlation plots are illustrated in Figures 4(k)-(m). Again a good correlation and slope is evident for these data.

A summary of the correlation parameters for the comparison between modelled and measured gas and particulate concentrations and wet deposition is given in Table 4. A good R<sup>2</sup> correlation coefficient (in the range 0.63 to 0.91) is evident for all parameters. The modelled NH<sub>3</sub> concentrations show an overestimate when compared to measurements whereas the modelled NH<sub>4</sub><sup>+</sup> concentrations show an underestimate. This suggests that the gas to particle conversion rate for ammonia may be proceeding too slowly in the model. NO<sub>3</sub><sup>-</sup> wet deposition is underestimated, which suggests that there is an underestimate in the washout coefficient for large nitrate aerosol. The concentration of HNO<sub>3</sub> is significantly underestimated. In part this may be attributed to the absence of nitric acid emissions in the model. Recent work at CEH Edinburgh suggests that nitric acid is co-emitted from slurry with ammonia. This source will be addressed in a future version of FRAME. The future expansion of the nitric acid monitoring network from 12 to 36 sites will permit a more detailed comparison between modelled and measured concentrations of nitric acid.

**Fig. 4(a)** Modelled SO<sub>2</sub> concentration correlation with measurements

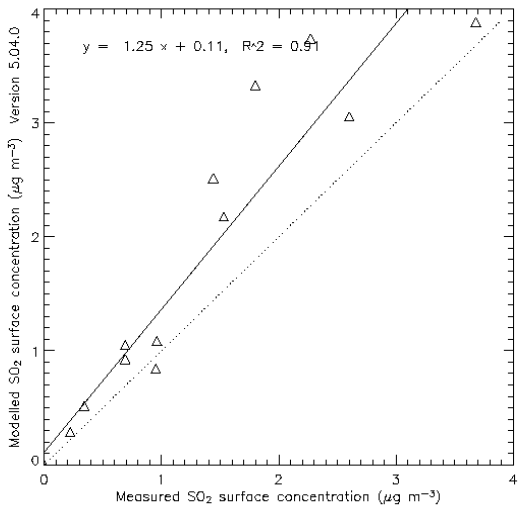


**Fig. 4(b)** Modelled SO<sub>4</sub><sup>2-</sup> concentration correlation with measurements

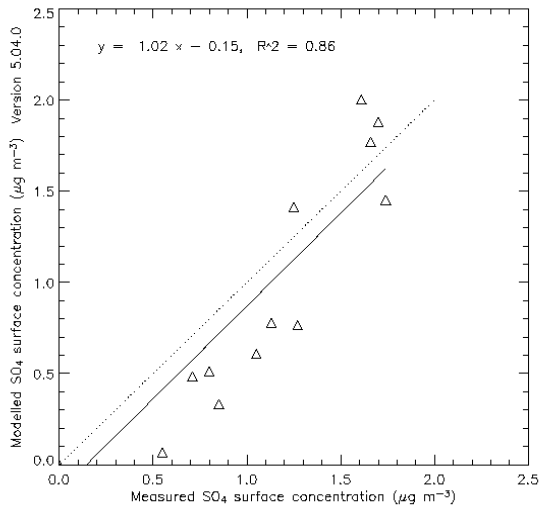


**Fig. 4(c)** Modelled NO<sub>2</sub> concentration correlation with measurements

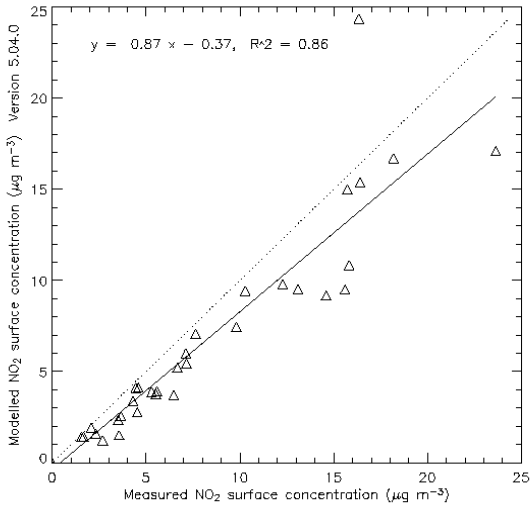


**Fig. 4(d)** Modelled NO<sub>3</sub><sup>-</sup> concentration correlation with measurements

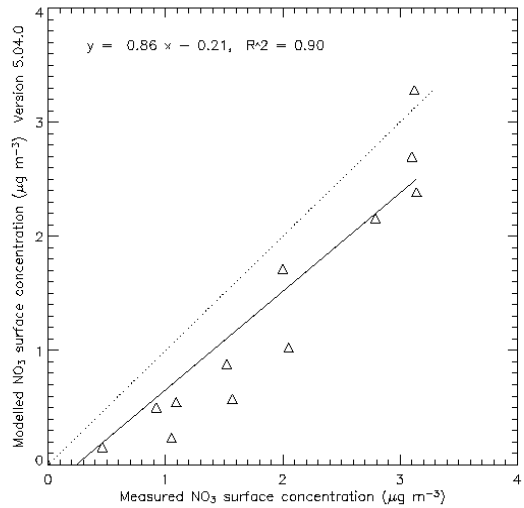


**Fig. 4(e)** Modelled NH<sub>3</sub> concentration correlation with measurements

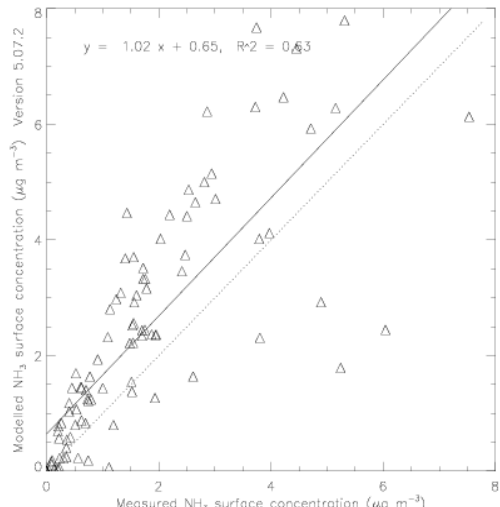


**Fig. 4(f)** Modelled NH<sub>4</sub><sup>+</sup> concentration correlation with measurements

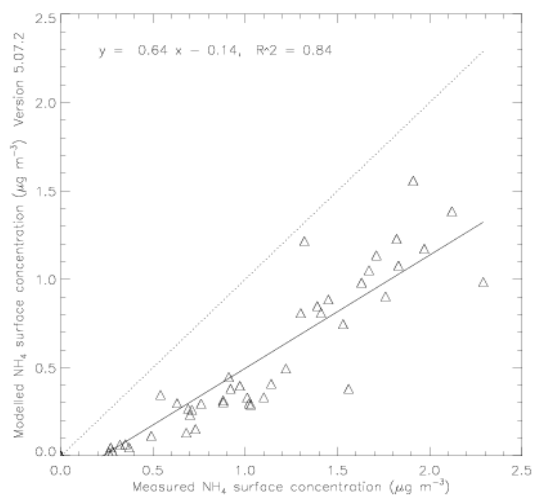


**Fig. 4(g)** Modelled HNO<sub>3</sub> concentration correlation with measurements

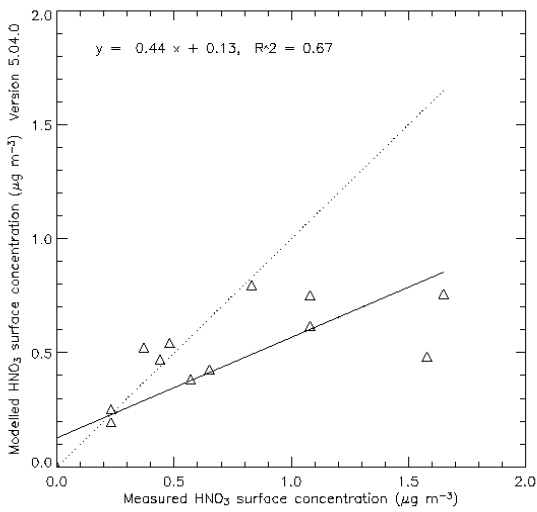


**Fig. 4(h)** Modelled NH<sub>4</sub><sup>+</sup> wet deposition correlation with measurements

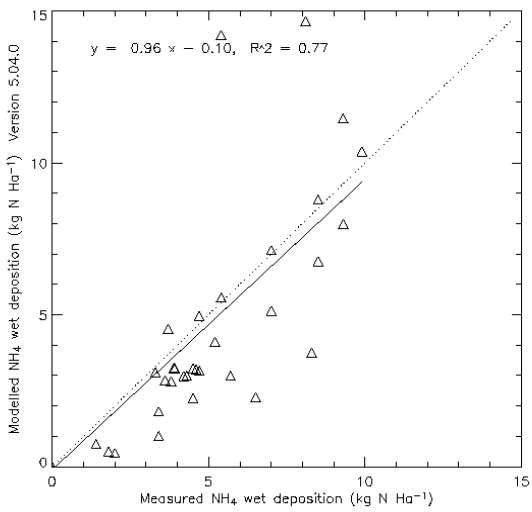


**Fig. 4(i)** Modelled NO<sub>3</sub><sup>-</sup> wet deposition correlation with measurements

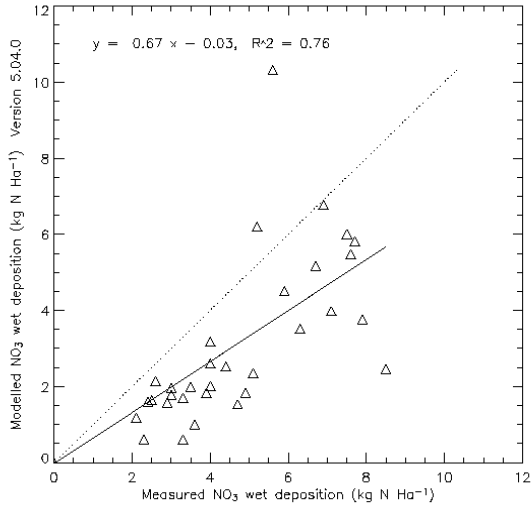


**Fig. 4(j)** Modelled SO<sub>4</sub><sup>2-</sup> wet deposition correlation with measurements

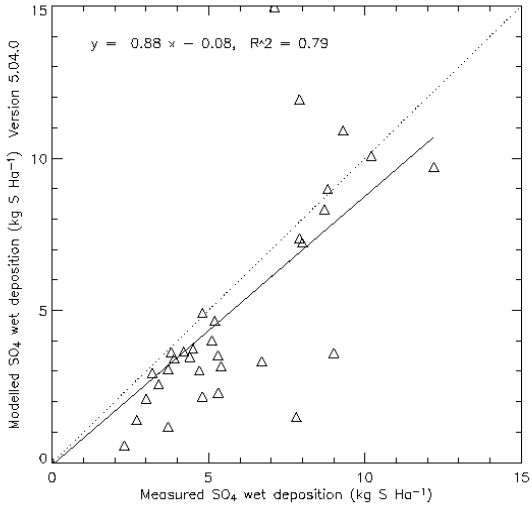


**Table 4:** Parameters for the linear regression  $y_{(\text{modelled})} = m * x_{(\text{measured})} + c$ ,  $R^2$  is the correlation coefficient

	m	C	$R^2$
SO <sub>2</sub> concentration	1.22	+0.11	0.88
SO <sub>4</sub> <sup>2-</sup> concentration	1.02	-0.15	0.86
NO <sub>2</sub> concentration	0.96	-0.24	0.87
NO <sub>3</sub> <sup>2-</sup> concentration	1.01	-0.25	0.91
NH <sub>3</sub> concentration	1.02	+0.65	0.63
NH <sub>4</sub> <sup>+</sup> concentration	0.64	+0.14	0.84
HNO <sub>3</sub> concentration	0.51	+0.14	0.65
SO <sub>4</sub> <sup>2-</sup> wet deposition	0.95	-0.09	0.81
NO <sub>3</sub> <sup>-</sup> wet deposition	0.75	-0.02	0.77
NH <sub>4</sub> <sup>+</sup> wet deposition	0.93	-0.10	0.79

## 5 Wind Frequency and Wind Speed Rose

### 5.1 Radiosonde Data

Radiosondes are routinely operated by national weather services to obtain vertical profiles of meteorological parameters (temperature, dew point temperature, wind speed and direction, with a 5° resolution). During 1991 to 2000, eight operational radiosonde stations in the United Kingdom provided data four times daily in addition to one station in the Republic of Ireland. The data are available in electronic format at the British Atmospheric Data Centre ([www.badc.nerc.ac.uk](http://www.badc.nerc.ac.uk)) with a 5° resolution. The aim of the present study was to generate a wind rose for the British Isles based on the available data set of radiosondes. In order to sample data from different geographical locations, four stations were selected in the British Isles. These were: Camborne (in Cornwall, south-west England); Hemsby (in East Anglia, east coast of England); Stornoway (in the outer Hebrides, north-west Scotland) and Valentia (on the west coast of the republic of Ireland). A ten-year data set covering the period 1991 to 2000 for the four stations was used. Although the time scale of a decade is not considered sufficient in meteorological terms for climatological mean data, averaging over this period serves to remove some of the inter-annual variations in wind. An appropriate altitude at which to extract wind data for analysis should be above the friction layer (as wind speed and direction can be strongly influenced by surface friction effects). Due to the significant vertical spacing between data points, which can be separated by depths of up to 200 m in some cases, it is further necessary to select a layer of atmosphere deep enough to have a strong probability of returning statistically significant wind data. In practice the most appropriate vertical layer was found to be the 950-900 hPa pressure level (approximately altitude layer 500-900 m.a.s.l.). For each radiosonde, any points within this layer were used to generate an average wind speed and direction. In all a total of 46000 radiosondes covering a ten-year period and four geographical locations were included in the study.

### 5.2 Wind Frequency Rose

Averaging the wind data over the four stations, and the ten year period, results in the wind rose, plotted at a fifteen degree angular resolution, illustrated in Figure 5.1. This is compared with the Jones wind rose. As can be seen, the radiosonde wind rose illustrates a peak in the WSW direction and is approximately symmetric around this axis. By comparison, the wind frequency rose of Jones (1981) exhibits a rather non-conventional peak in the northerly direction. In Figure 5.2, wind frequency roses are plotted averaged over the four stations for recent years. A greater incidence of easterlies in 1996 and south-easterlies in 1997 is evident whereas differences between the plots for years 1998, 1999 and 2000 are relatively small. In Figure 5.3 the wind roses are averaged over the ten year period for individual stations. The geographical variations are relatively small though the station at Stornoway features a greater incidence of south and SSW directions and a lower frequency of north-westerlies. Seasonal variations may also be analysed by averaging over the four stations and the ten-year period as a function of the month. Such monthly wind roses will be of importance for future model developments involving a canopy compensation point. This parameterisation considers the bi-directional exchange of ammonia, which is dependent on temperature and surface vegetation properties which vary seasonally and can be considered a function of the month of the year. A sample of four months (February, May, August and November) from each of the four seasons of the year is plotted in Figure 5.4. A strong incidence of north-easterlies is evident for the month of May. This is due to the occurrence of blocking anti-cyclones during the spring months of April and May.

### 5.3 Wind Speed Rose

The application of radiosonde wind-speed data to generate a wind-speed rose presents additional complications. As demonstrated by Singles (1996), the mean wind speed is inappropriate for use in an atmospheric transport model. The ‘optimised’ wind speeds calculated by Singles (1996) were the single wind speeds which were found to best reproduce the concentrations of ammonia and deposition of reduced nitrogen from a distribution of wind speeds based on the data of Jones *et al.* (1981). In this study a simple approach is sought for processing wind speed data to generate a value suitable for use in a transport model. Lower wind speeds are known to result in higher low-level concentration of gaseous species and greater deposition close to source regions. In dealing with a frequency distribution of wind speeds, one approach is therefore to apply a greater weighting to the low wind speeds in the averaging procedure. This is most simply achieved by taking the ‘harmonic mean’, or averaging the reciprocal wind speeds. Figure 5.5 shows a comparison between the wind speed rose used by Singles (1996) and that generated by calculating the harmonic mean from the ten year radiosonde data set. The radiosonde data exhibit stronger wind speeds from the south-west and lower values from the east, in contrast to the optimised wind speed data which show less pronounced directional dependence of wind speed, with the highest values from the north-west sector. The frequency-weighted mean value of wind speed from the Singles (1996) data is  $7.5 \text{ m s}^{-1}$  and the same value is also obtained from the harmonic mean of the radiosonde data. In addition, the same value has previously been adopted in the HARM (Metcalfe *et al.*, 2001) and TRACK (Lee *et al.*, 2000) models. Whilst the close agreement between these values may be considered fortuitous, this suggests that the use of the harmonic mean is a simple and effective procedure for generating a wind speed suitable for general application in a transport model. The previous use of the wind speed value  $7.5 \text{ ms}^{-1}$  in earlier modelling studies, in the absence of more detailed data, is also lent support by this agreement. The wind speed data may be analysed, as with the wind frequency data, for geographical and inter-annual variations. This analysis however reveals smaller variations between the wind speed roses than was observed for the wind frequency roses. The generation of a year-specific wind speed rose is therefore not considered to be of importance. Analysis of the seasonal variation of wind speed roses however produces more significant results with stronger wind speeds evident for a winter month (February) than for a summer month (August), as illustrated in Figure 5.6.

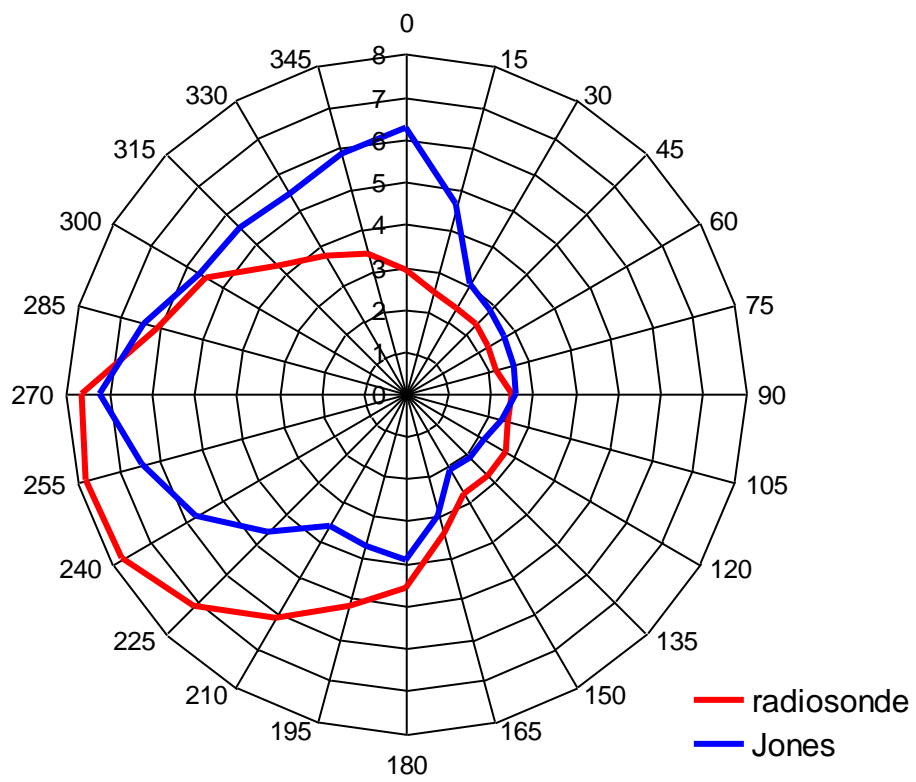


**Figure 5.1:** The 1991-2000 average radiosonde-generated wind frequency rose compared to the Jones (1981) wind frequency rose. Radial units are percent per 15° direction band.

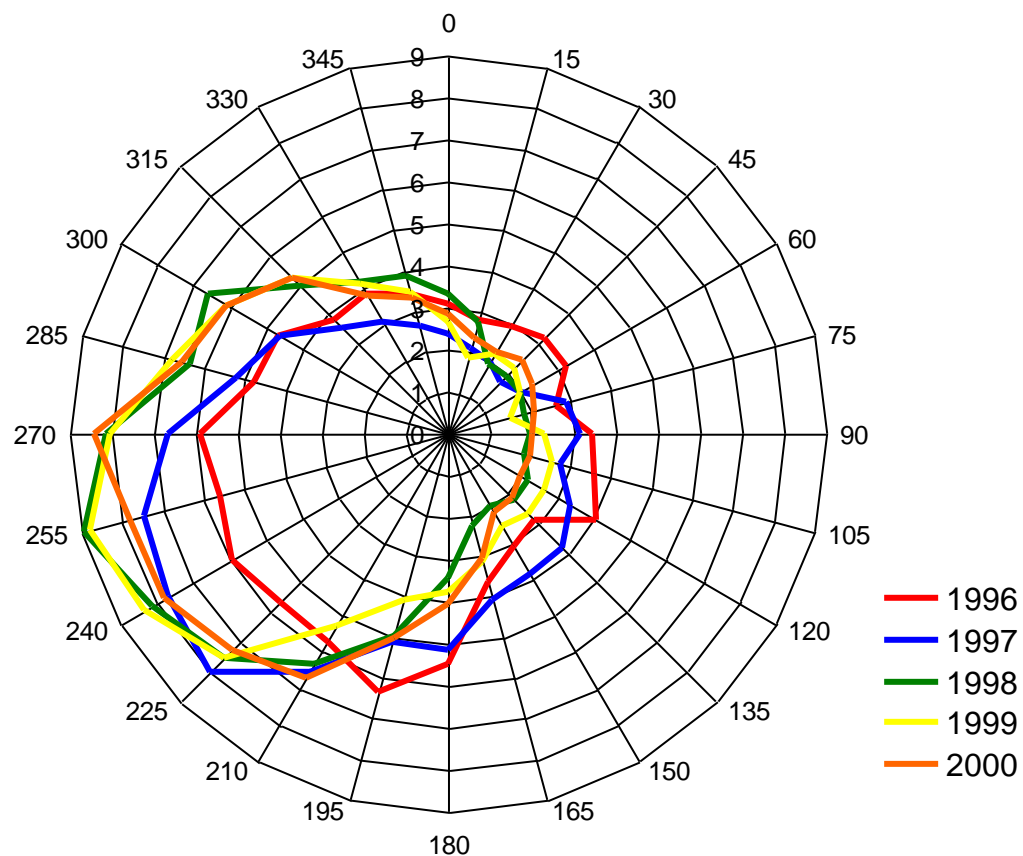


**Figure 5.2:** Annual variation in wind frequency rose (1996-2000) calculated from radiosonde data. Radial units are percent per  $15^\circ$  direction band

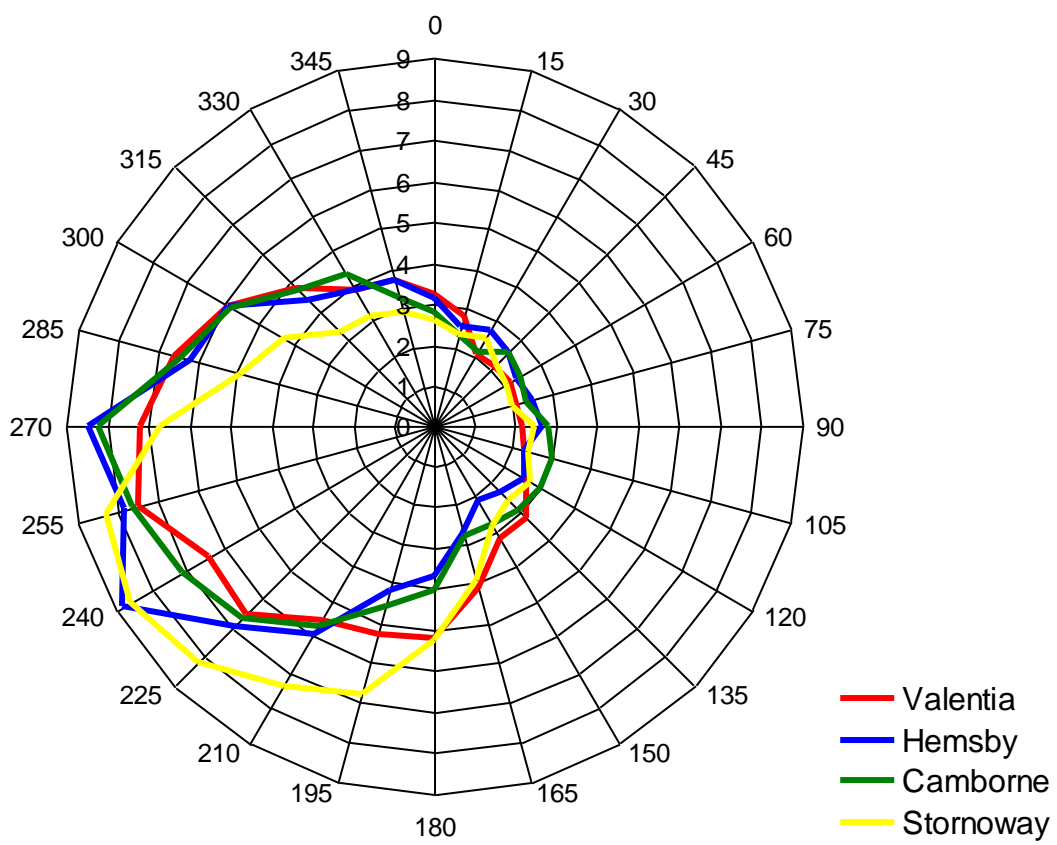


**Figure 5.3:** Average wind frequency rose for different stations calculated from 1991-2000 radiosonde data. Radial units are percent per 15° direction band

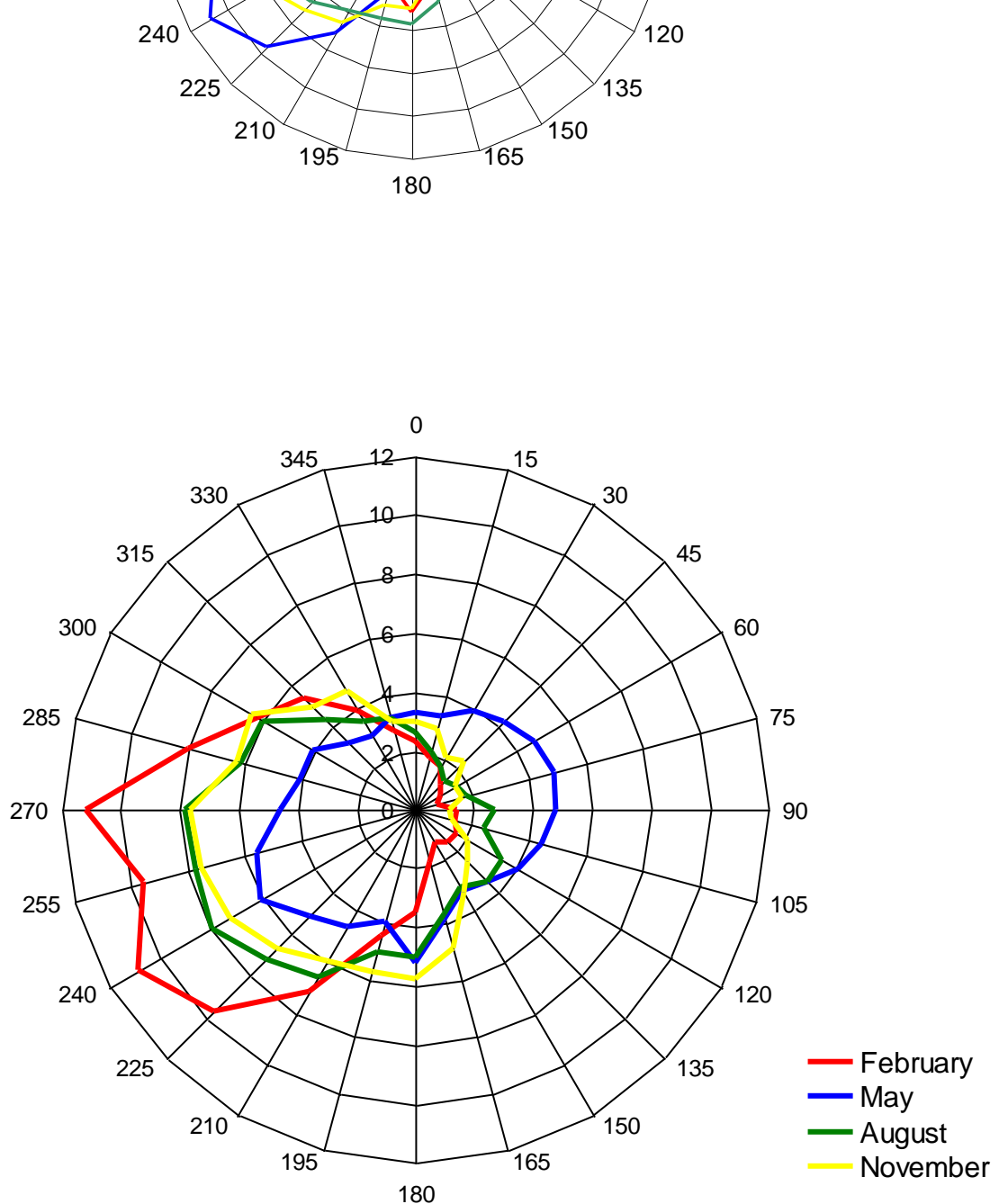


**Figure 5.4:** Seasonal variation in wind frequency roses for selected months calculated from 1991-2000 radiosonde data. Radial units are percent per  $15^\circ$  direction band

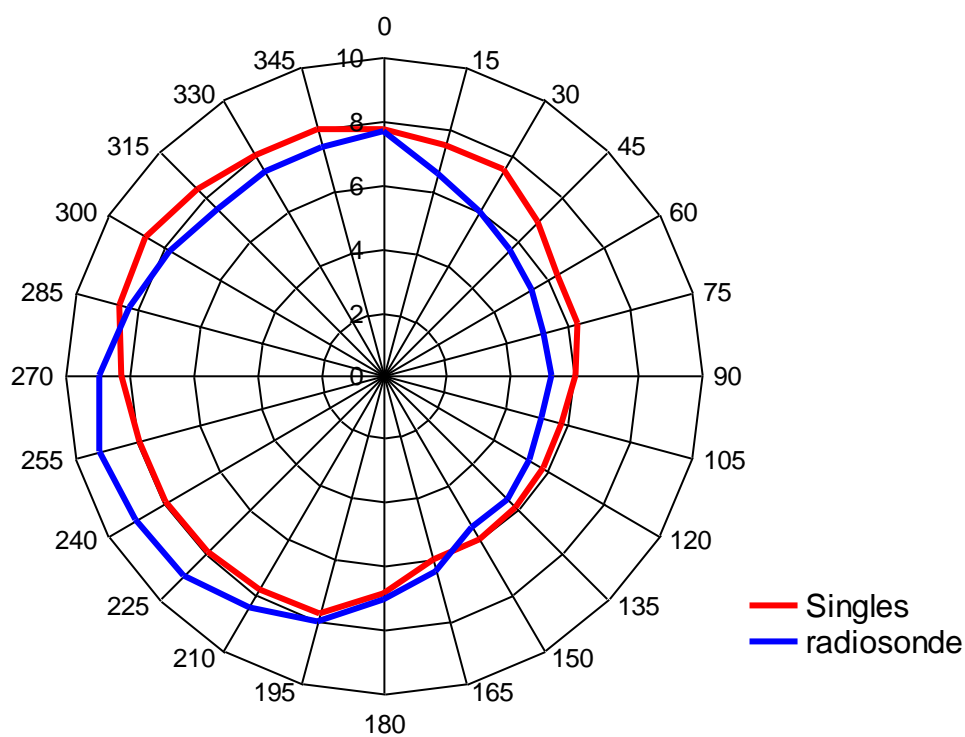


**Figure 5.5** The seasonal variation in wind speed rose for selected months calculated from 1991-2000 radiosonde data. Radial units are  $\text{m s}^{-1}$ .

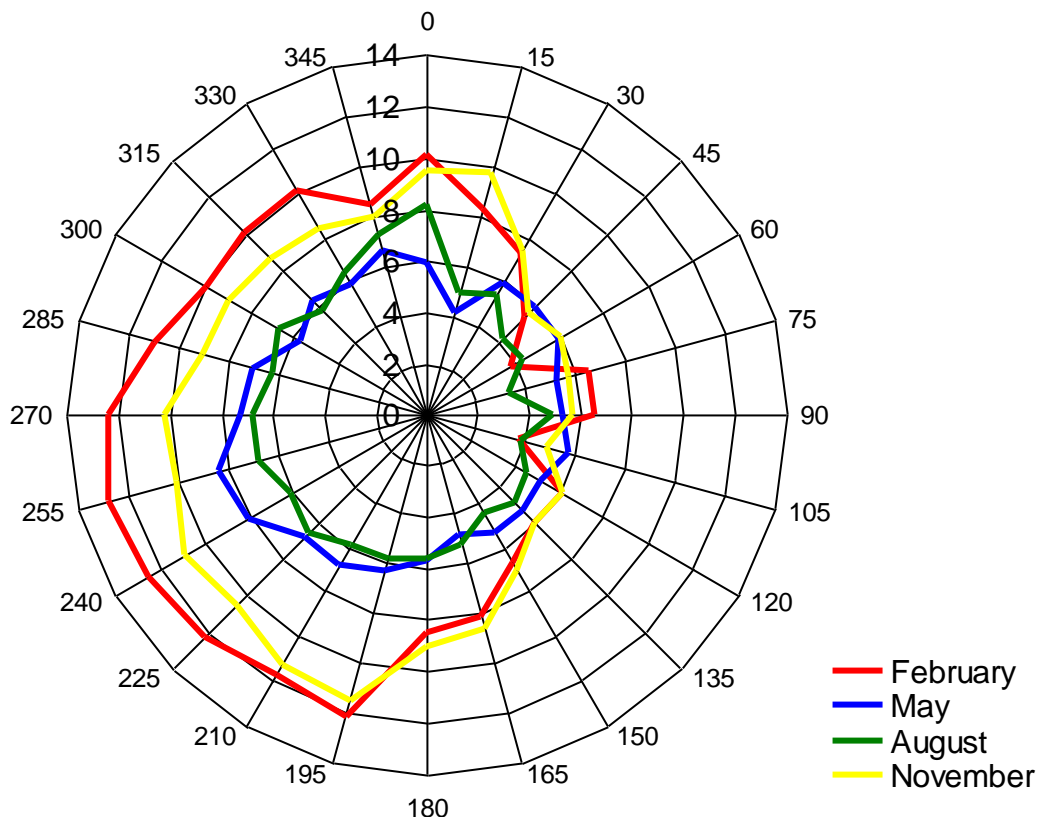


**Figure 5.6** The seasonal variation in wind speed rose for selected months calculated from 1991-2000 radiosonde data. Radial units are  $\text{m s}^{-1}$ .

## 5.4 Application of radiosonde wind data in FRAME

Version 5.3 of FRAME was run using emissions data from the year 1999 with (a) the radiosonde wind speed and wind frequency data and (b) the Jones wind speed and wind frequency data. The pollutants that have a deposition pattern most sensitive to the choice of wind parameters are those associated with long-range transport. In the context of modelling nitrogen and sulphur deposition with FRAME, SO<sub>2</sub> is therefore the most relevant gas to be considered. Approximately 80% of SO<sub>2</sub> emissions in the United Kingdom originate from high stacks and the gases emitted from these sources may travel significant distances before being deposited to ground.

The SO<sub>x</sub> dry deposition from a single point source (at Ironbridge in central England) was estimated with FRAME by calculating the difference between a simulation with all sources included and a simulations with the single point source emissions removed. The results are shown for both the radiosonde wind data and the Jones wind data in figure 5.7. The difference in the primary direction of transport between the two wind roses is highlighted by the different spatial distributions of SO<sub>x</sub> dry deposition. With the Jones data, more SO<sub>2</sub> is advected towards southern England. Many major point sources are located close to the east coast and with use of the radiosonde wind data, there will be a tendency for more of the gas to be advected out of the country towards the North Sea.

A comparison was made of FRAME data with measurements from the UK rural monitoring network for SO<sub>2</sub> concentration for both model simulations. It is evident that use of the radiosonde data results in a better agreement with the observations for all correlation parameters. With the radiosonde data, the correlation coefficient R<sup>2</sup> was 0.89, the slope was 0.92 and the intercept of the y-axis (0.12) was low. In contrast, use of the Jones wind data resulted in a marginally poorer R<sup>2</sup> of 0.87, a smaller slope of 0.89 and a higher intercept of the y-axis of 0.40.

The fate of sulphur in the model may be illustrated in terms of a set of budgets. The budgets show the total import and export as well as the total dry and wet deposition of sulphur for the United Kingdom (Fournier *et al.*, 2005b). The FRAME budget is strongly influenced by the choice of wind data, as illustrated in Table 5. The import in FRAME is calculated using FRAME-Europe and is not significantly influenced by the choice of wind rose. By contrast, it can be seen that the use of the radiosonde wind data results in generally lower deposition to the United Kingdom of 4 Mg NH<sub>x</sub>-N, 7 Mg NO<sub>y</sub>-N and 13 Mg SO<sub>x</sub>-S than with the Jones data. Export for NH<sub>x</sub>, NO<sub>y</sub> and SO<sub>x</sub> increased by 10 kg N ha<sup>-1</sup> y<sup>-1</sup>, 8 kg N ha<sup>-1</sup> y<sup>-1</sup> and 19 kg S ha<sup>-1</sup> y<sup>-1</sup>, respectively. Many large power stations in the UK are located close to the east coast. The result of this is that a significant proportion of the sulphur emitted from the country is exported to the northeast. The budget figures illustrate the importance of using accurate wind speed data in a statistical model, which is to be used to assess the balance between nationally deposited pollutants and the proportion which is exported towards other nations.

**Table 5:** UK budgets ( $\text{Mg y}^{-1}$ )

(a) Radiosonde wind data. (b) Jones` wind data. (c) Radiosonde – Jones.

		$\text{NH}_x\text{-N}$	$\text{NO}_y\text{-N}$	$\text{SO}_x\text{-S}$
a) Radiosonde	Import	39	53	55
	Dry deposition	75	60	69
	Wet deposition	88	61	109
	Export	143	397	474
b) Jones	Import	33	52	49
	Dry deposition	76	61	78
	Wet deposition	91	67	113
	Export	133	389	455
c) Radiosonde - Jones	Import	6	1	6
	Dry deposition	-1	-1	-9
	Wet deposition	-3	-6	-4
	Export	10	8	19

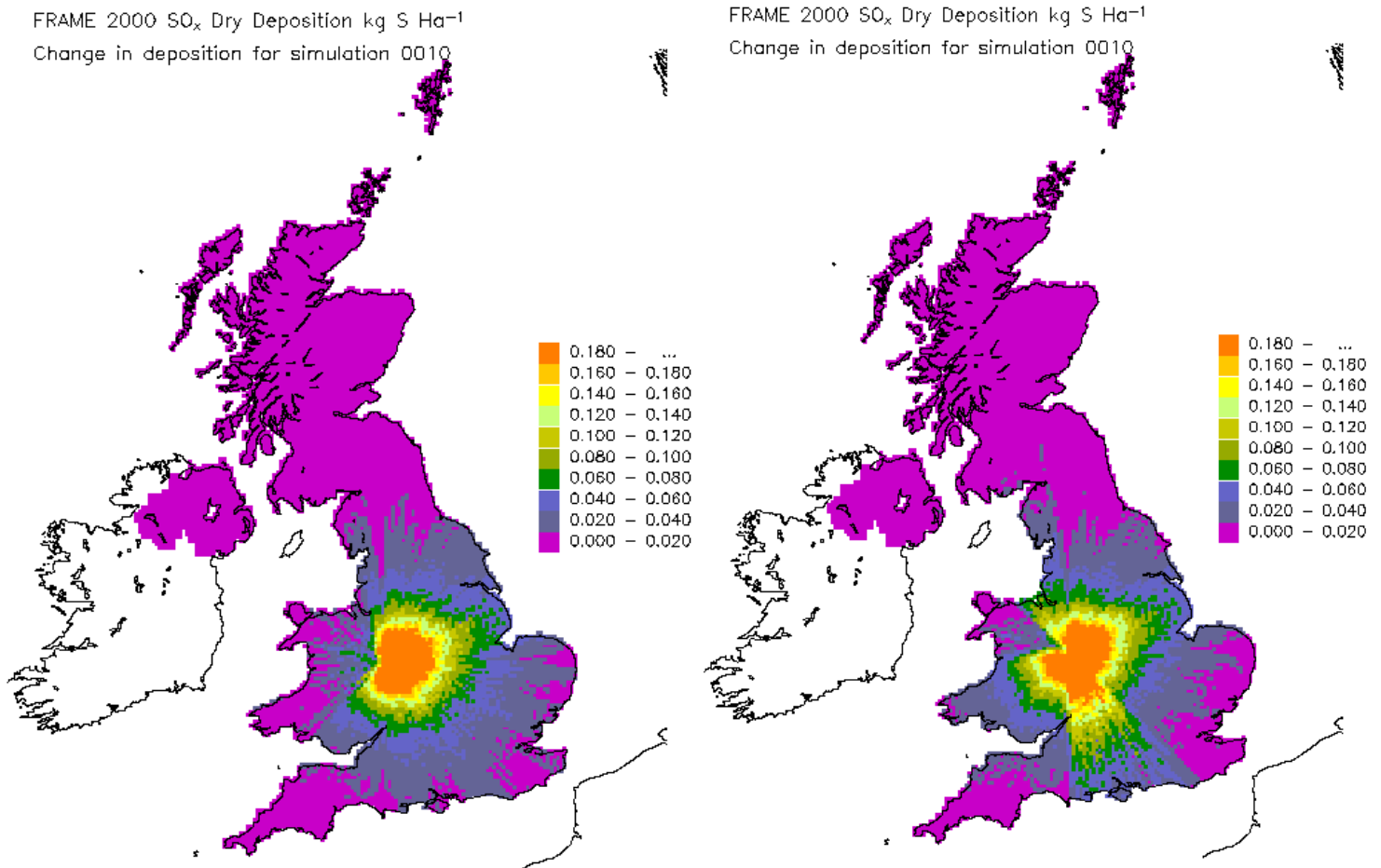


**Figure 5.7.**  $\text{SO}_2$  deposition footprint for a point source at Ironbridge using  
(a) the radiosonde wind rose ; (b) the Jones wind rose

## 6 Emissions from International Shipping

Versions of FRAME up till 4.19 employed a time saving device whereby trajectories were started over land. This was prior to the acquisition of powerful parallel processing facilities and the introduction of the fast finite volume solver for the vertical diffusion. A single FRAME run then took four days to complete, including approximately a 75% saving in computation time by avoiding running trajectories over marine areas. For FRAME 4.20, the run time on the Beowulf cluster, employing 50 processors was approximately 15 minutes so that this time saving was no longer required. In FRAME 4.21, shipping emissions of SO<sub>2</sub> and NO<sub>x</sub> were introduced. The trajectories were therefore set to run from the edge of the model domain. Based on a literature review (Joffre, 1988; Lee *et al.*, 1998; Barrett 1998) the following deposition velocities were selected for deposition of gases to the sea surface: 5 mm s<sup>-1</sup> for SO<sub>2</sub>, 5 mm s<sup>-1</sup> for NH<sub>3</sub>, 6 mm s<sup>-1</sup> for HNO<sub>3</sub>. Due to the insolubility of NO and NO<sub>2</sub>, their deposition velocities were set to zero.

A precipitation field was introduced over the sea. Although measurements of sea precipitation are unreliable, the basis of a marine precipitation field can be built from extrapolating coastal precipitation values. Along the Welsh coast, precipitation values are typically 1000 mm, increasing to 1200 mm in NW Scotland. It should be noted however that these west coastal values will be somewhat higher than marine precipitation due to the orographic triggering of the formation of new mesoscale precipitation systems many kilometres upstream of the coast. Annual precipitation along the east coast of England and Scotland is significantly lower (around 600 mm annually in East Anglia). A rain shadow effect exists whereby in westerly winds, precipitation falls mostly in the west of the country and the air has dried by the time it arrives at the east coast. This effect will also influence marine precipitation to the east of the UK coast. An increasing gradient in annual precipitation from south to north is evident. These features were captured by setting an annual precipitation rate of 1000 mm in the NW corner of the FRAME grid, 800 mm in the NE corner, 800 mm in the SW corner and 600 mm in the SE corner. Intermediate values were generated by interpolation. The resultant precipitation field is illustrated in Figure 6.1. Two important areas for transfer of pollutants between landmasses are the south-east where precipitation is set to approximately 600 mm year<sup>-1</sup> and the Irish sea where annual precipitation is approximately 800 mm.

Emissions of SO<sub>2</sub> from shipping for the year 2000 were introduced into the model (ENTEC, 2003). This required the development of a FORTRAN 90 routine to:

- Read in SO<sub>2</sub> emissions on an EMEP 50 km resolution grid
- Read in an array which correlated each FRAME grid point to the relevant EMEP coordinate
- Read in a land-sea mask for the British Isles
- Re-grid EMEP emissions onto the FRAME grid
- Re-grid emissions from the EMEP 50 km grid which were classified as land at a 5km resolution
- Output a 5km resolution emissions file on an ordnance survey grid

The Shipping emissions of SO<sub>2</sub> are illustrated in Figure 6.2 for the FRAME domain. The areas of heaviest emissions are evident in the English Channel and off the east coast of southern England. The budgets for import, export and deposition to the United Kingdom for the year 2000 are illustrated in Table 6. Total emissions of SO<sub>2</sub> by shipping within the FRAME domain amount to 74 kT S, of which 22 kT corresponds to coastal grid squares. Coastal grid squares contain a portion of both land and sea. However there is no sub-grid

variability in emissions, which are spread evenly across a grid square. The introduction of shipping emissions results in an increase in deposition to the United Kingdom of 17 kT S (comprising 5 kT dry deposition and 12 kT wet deposition) or 9.5%. Figure 6.3 illustrates the difference in sulphur deposition resulting from inclusion of shipping emissions. Deposition is tabulated in the first three columns for a simulation in which shipping emissions of SO<sub>2</sub> were included. The fourth column illustrates the deposition of sulphur with shipping emissions removed. It can be seen that the increase in dry deposition is most significant in coastal regions, particularly in the south-east. For wet deposition, the increases are largest in the south-east and in the high rainfall hill areas of Wales and northern England where changes in deposition exceeding 1 kg S ha<sup>-1</sup> can be observed.

**Table 6** Deposition budgets (Mg N or S) to the United Kingdom for sulphur and oxidised and reduced nitrogen for the year 2000 , illustrating the influence of including shipping emissions.

	NHx-N	NOy-N	SOx-S with shipping emissions	SOx-S without shipping emissions
Import	34	63	57	40
Export	135	465	465	443
Emissions	276	526	604	582
Dry Deposition	93	46	71	66
Wet Deposition	82	78	125	113

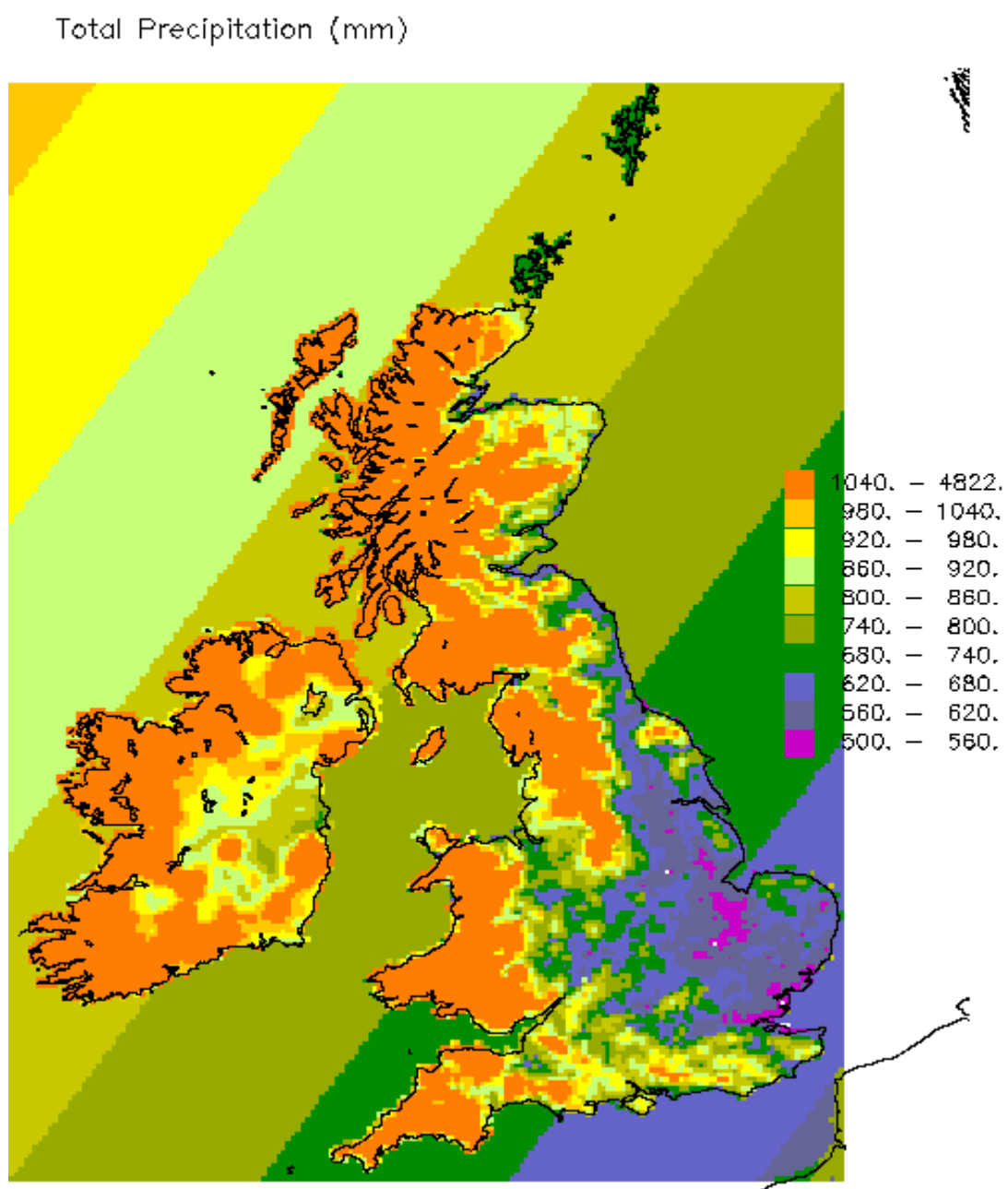


**Figure 6.1** Annual precipitation (mm) with inclusion of marine areas

SO<sub>2</sub> Shipping Emissions ( $\text{kg S Ha}^{-1}$ )

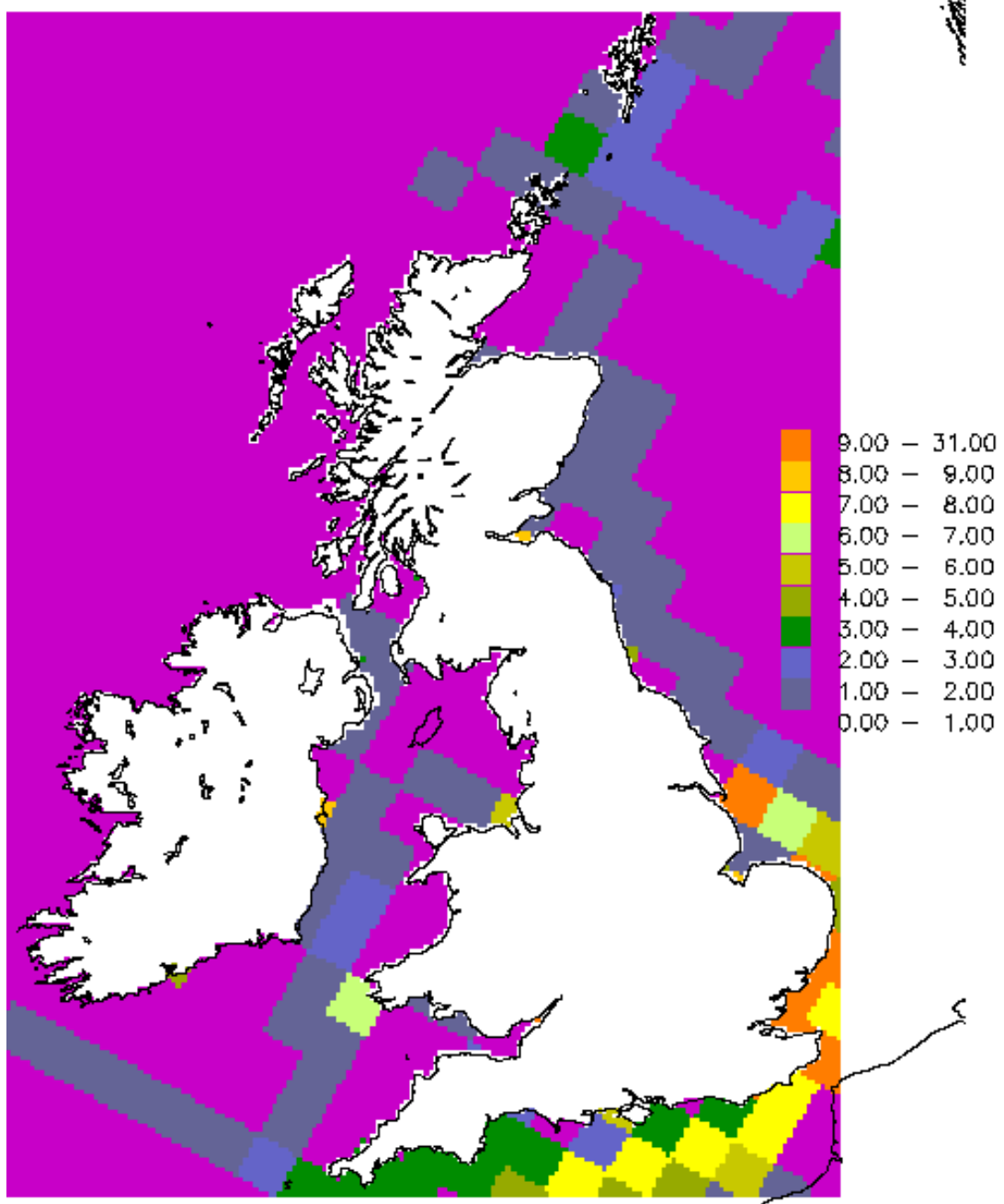


**Figure 6.2** Emissions of SO<sub>2</sub> from shipping for the year 2000 ( $\text{kg S Ha}^{-1} \text{ yr}^{-1}$ )

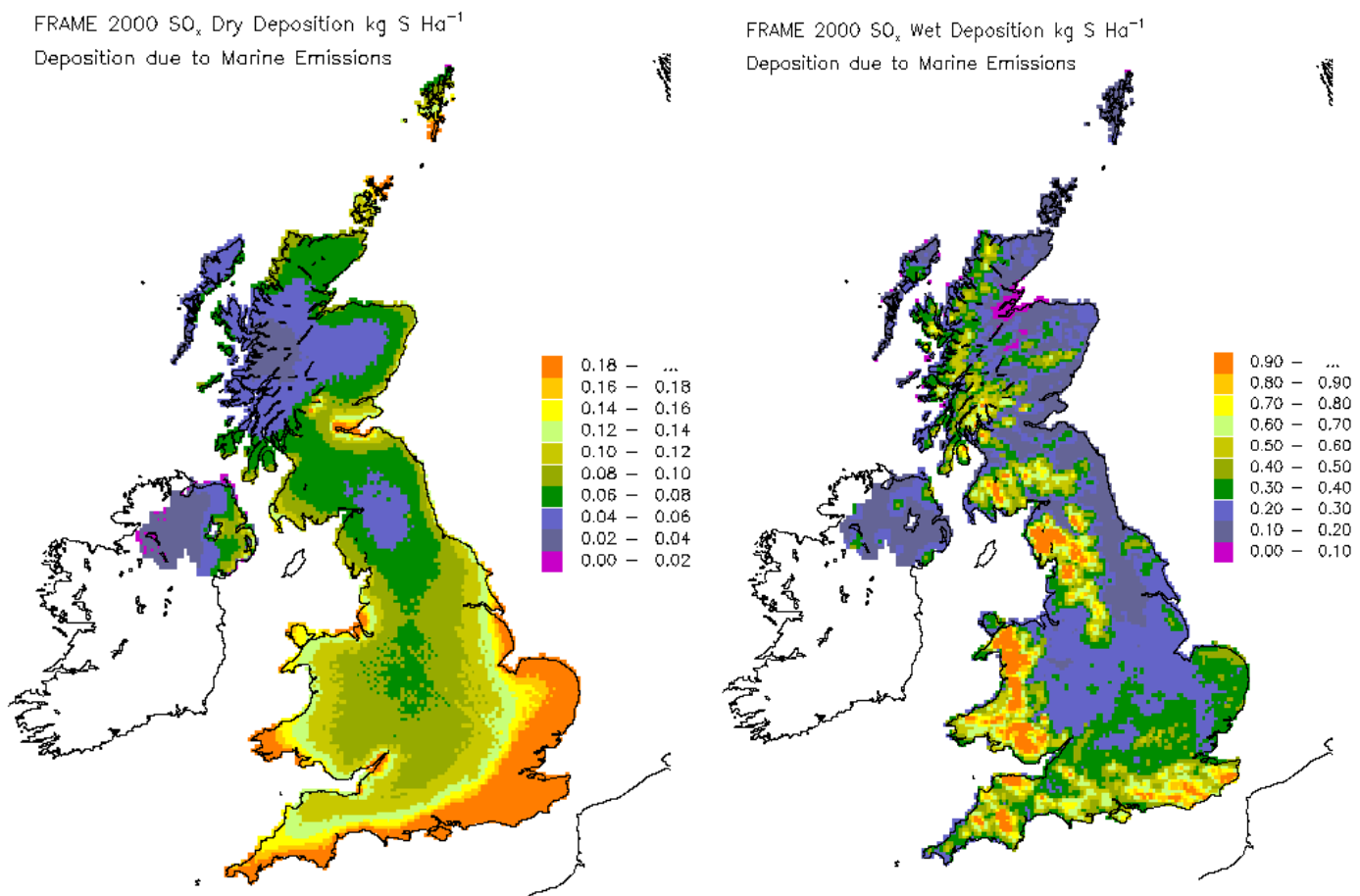


**Figure 6.3** Deposition footprints due to emissions from international shipping for the year 2000 (kg S ha<sup>-1</sup> yr<sup>-1</sup>)

## 7 Representation of Emissions Height in FRAME

In an atmospheric transport model such as FRAME, correct representation of the height at which pollutant gases are emitted to the atmosphere is an important consideration. With emissions heights underestimated, modelled concentrations close to the ground will be too high, resulting in overestimate of gaseous dry deposition in the vicinity of the source. With emissions heights set too high, the model will overestimate the fraction of emissions which escapes the local area and contributes to long range transport of pollutants. It also follows from this argument that the model requires a fine vertical grid spacing in order to resolve differences in emissions heights. In FRAME the depth of the surface layer is 1 m, allowing for a detailed treatment of  $\text{NO}_x$  emissions from vehicles and  $\text{NH}_3$  emissions from livestock. Improvements to the parameterisation of emissions of both point source emissions of  $\text{SO}_2$  and  $\text{NO}_x$  and low-level emissions of  $\text{NH}_3$  are considered here.

### 7.1 Plume Rise for Point Source Emissions of $\text{SO}_2$ and $\text{NO}_x$

In FRAME versions 4.6 and 4.7, major point source emissions of  $\text{SO}_2$  and  $\text{NO}_x$  were separated from background emissions and, where available, information on stack height data was employed to input the emissions at the appropriate vertical layer in the model. In reality, however, gases produced by combustion processes are injected into the atmosphere with significant vertical velocity and buoyancy due to their high temperature. An effective stack height may be calculated at which the emitted air is in equilibrium with its environment. In practice this is a function of the stack height and diameter, temperature and velocity of the emitted gas, and the atmospheric stability. In practice the effective emissions height is typically twice the stack height. A plume rise parameterisation was included in FRAME 4.17 for all point sources. Where stack parameters were not available, typical values were assigned.

Figure 7.1 shows the correlation with annual average measurements of  $\text{SO}_2$  and  $\text{NO}_2$  from the rural monitoring network for emissions year 1999. For both plots, introduction of the plume rise module is shown to result in an improved correlation with measurements. The improvement is most significant for  $\text{SO}_2$  as approximately 80% of emissions are associated with point sources. In particular, the modelled values of  $\text{SO}_2$  were found to significantly overestimate the measured concentrations at four sites located in northern England in a region of high emissions. Introduction of the plume rise module resulted in a significant lowering of the modelled concentrations at these sites which brought them closer to the measured values. This suggests that in the absence of a plume rise parameterisation, emissions from elevated point sources are mixed by the model too rapidly to the surface.

## SO<sub>2</sub> air concentration

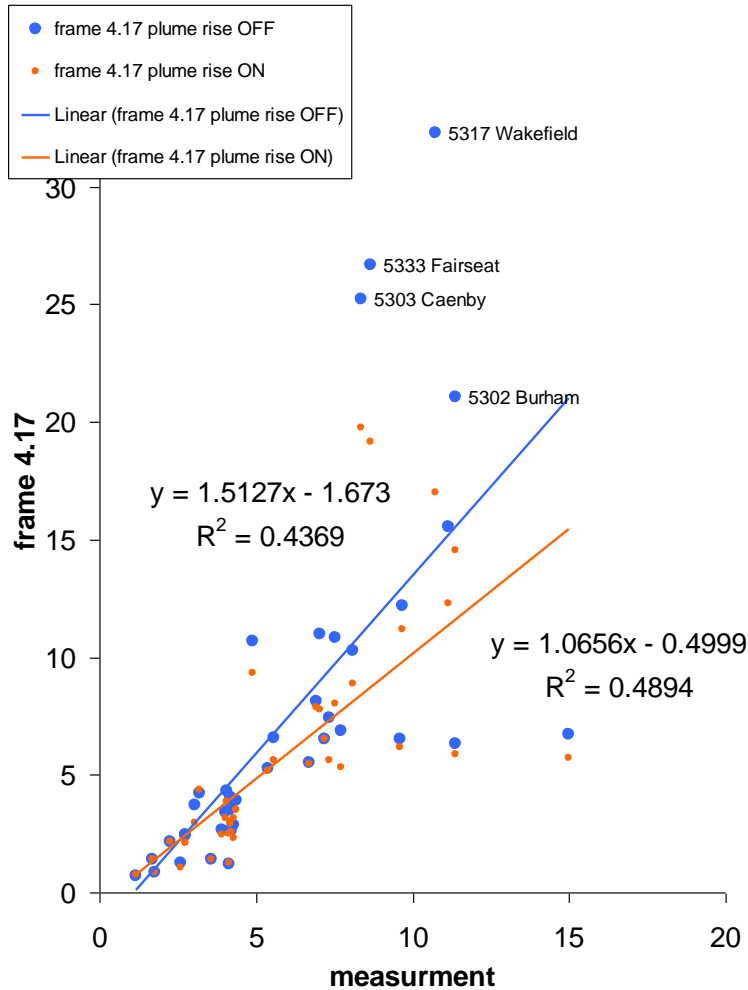


**Figure 7.1(a)** Correlation of modelled SO<sub>2</sub> concentrations ( $\mu\text{g m}^{-3}$ ) with measurements for the year 1999 with (i) no plume rise parameterisation and (ii) plume rise parameterisation included

## NO<sub>2</sub> air concentration

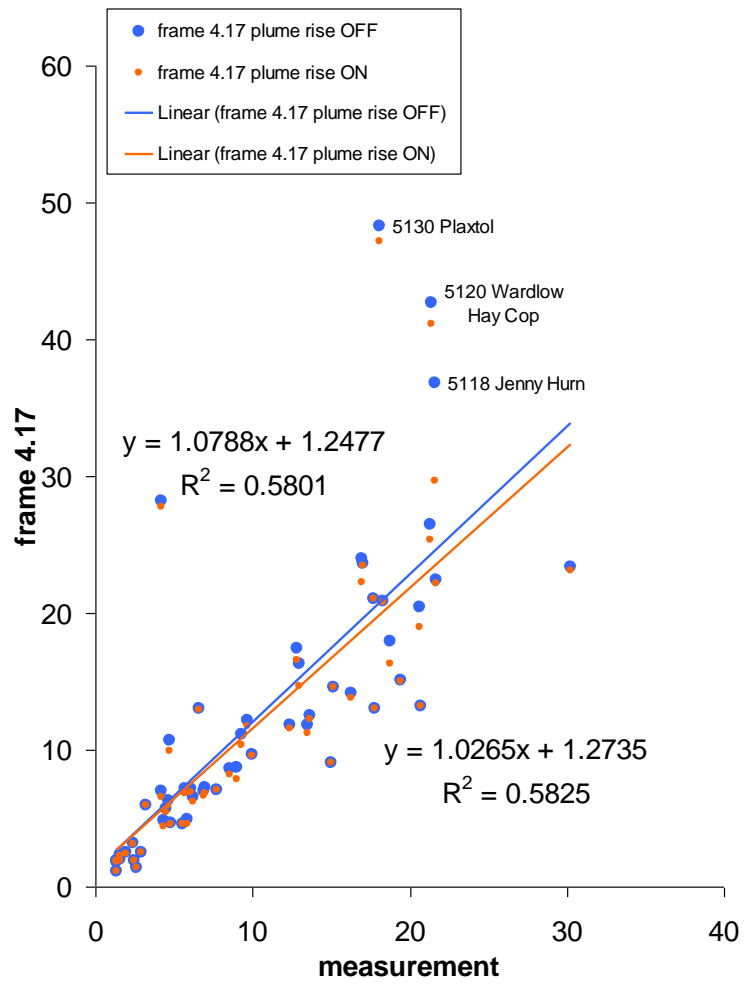


**Figure 7.1(b)** Correlation of modelled NO<sub>2</sub> concentrations ( $\mu\text{g m}^{-3}$ ) with measurements for the year 1999 with (i) no plume rise parameterisation and (ii) plume rise parameterisation included

## 7.2 Introduction of Sector Dependent Height of Ammonia Emissions

The height at which ammonia is emitted can have a significant influence on surface concentrations and therefore on dry deposition rates to vegetation. Ammonia is generally associated with low level emissions. However the precise height of emissions from livestock depends on whether the animals are housed or grazing. In FRAME 4.25 emissions of NH<sub>3</sub> were separated into its components. These included emissions from livestock (cattle, pigs, poultry and sheep), emissions from crops and grassland due to fertiliser application and emissions from non-agricultural sources. The latter comprise a large number of emissions sources (including vehicle exhaust, pets, sewage treatment, wild animals, sea birds, human sweat, cigarette smoke, babies' nappies etc). Each emissions sector was assigned a specific emissions height, depending on the nature of the source. Emissions from sheep, pigs, crops, grassland and non-agricultural sources were input to the surface layer. It was assumed that cattle are housed 50% of the time and grazing for 50% of the time so emissions were input to layers 1-5, the lowest 10 m. Poultry emissions were assumed to be from housing and were input to the layers 4-5 (height 4-10 m)

The correlation of modelled NH<sub>3</sub> concentrations with measurements from the ammonia monitoring network is illustrated in Figure 7.2, firstly with all NH<sub>3</sub> emissions assigned to the surface layer and secondly with the emissions sector height dependence employed. The new parameterisation is shown to result in a general lowering of NH<sub>3</sub> concentrations and a minor improvement in the correlation with measurements.

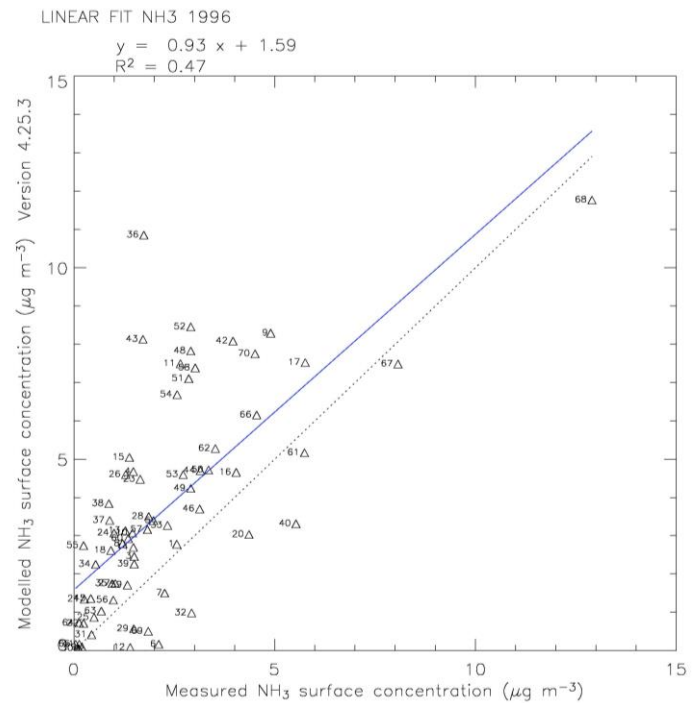
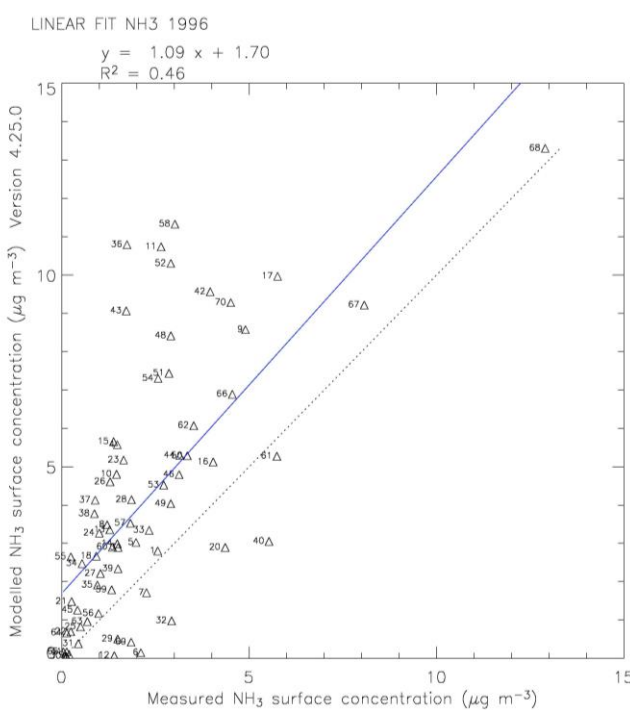


**Figure 7.2(a)** Correlation of modelled NH<sub>3</sub> concentrations ( $\mu\text{g m}^{-3}$ ) with measurements for the year 1996 with all emissions input to the surface layer

**Figure 7.2(b)** Correlation of modelled NH<sub>3</sub> concentrations ( $\mu\text{g m}^{-3}$ ) with measurements for the year 1996 with sector specific emissions height

## **8 Comparison of FRAME with measurements from the ammonia monitoring network**

Successfully modelling NH<sub>3</sub> concentrations is a significant challenge due to a combination of the solubility of the gas, its high reactivity and vegetation-sensitive deposition rate. Ammonia is characterised by having highly spatially variable and low-level emissions. Figure 8.1 shows the correlation of (i) FRAME modelled ammonia concentrations and (ii) measured concentrations with the corresponding 5 x 5 km<sup>2</sup> grid square ammonia emissions estimate. The modelled concentrations are highly correlated to the emissions ( $R^2 = 0.86$ ) whereas in contrast the observations have a much weaker correlation to the emissions ( $R^2 = 0.46$ ). This indicates that success in calculating ammonia concentrations is closely tied to resolving the fine scale spatial distribution of their emissions patterns. The introduction of a finer scale horizontal resolution in FRAME may therefore be expected to lead to a much improved correlation with measurements.

Observation sites of the UK national ammonia monitoring network can be grouped into three categories representative of: mixed agricultural, nature reserve and woodland. Figure 8.2 shows the correlation between the FRAME model predictions and the site observations for land-use specific sites. A strong difference in the gradient of the line of best fit is evident for the different groups of land categorisation. The model appears to be significantly over-estimating ammonia concentrations at nature sites. This occurs because nature sites tend to be ‘havens’ of low ammonia concentration within a model grid square which may have average emissions that are associated with intensive agricultural activity. On the other hand, it is noticeable that this division between different site types much improves the correlation between measurement and modelling for woodland and semi-natural areas (with  $R^2$  of 0.84, 0.91) compared with all the sites combined ( $R^2=0.48$ ). Sites in such woodland and semi natural areas will be less influenced by local sources than the sites in mixed agricultural landscapes ( $R^2$  0.58), demonstrating that natural spatial variability within each 5 km grid square is a key reason for the modest  $R^2$  values obtained between measured and modelled NH<sub>3</sub> concentrations.

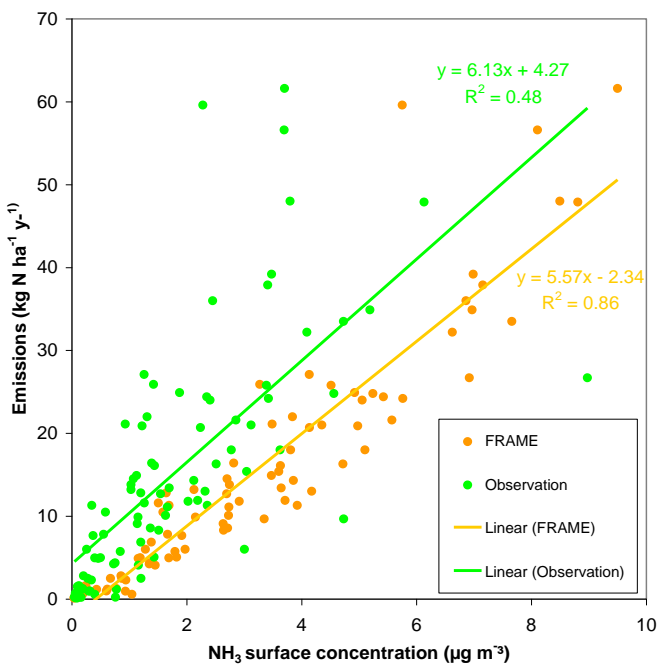


**Figure 8.1** FRAME model predicted NH<sub>3</sub> surface concentrations (orange, 1999) and observations from the UK national ammonia monitoring network (green, 1998-2001) versus the NH<sub>3</sub> 5 x 5 km<sup>2</sup> emissions estimate. Units are: concentrations µg m<sup>-3</sup> and emissions in kg N ha<sup>-1</sup> y<sup>-1</sup>.

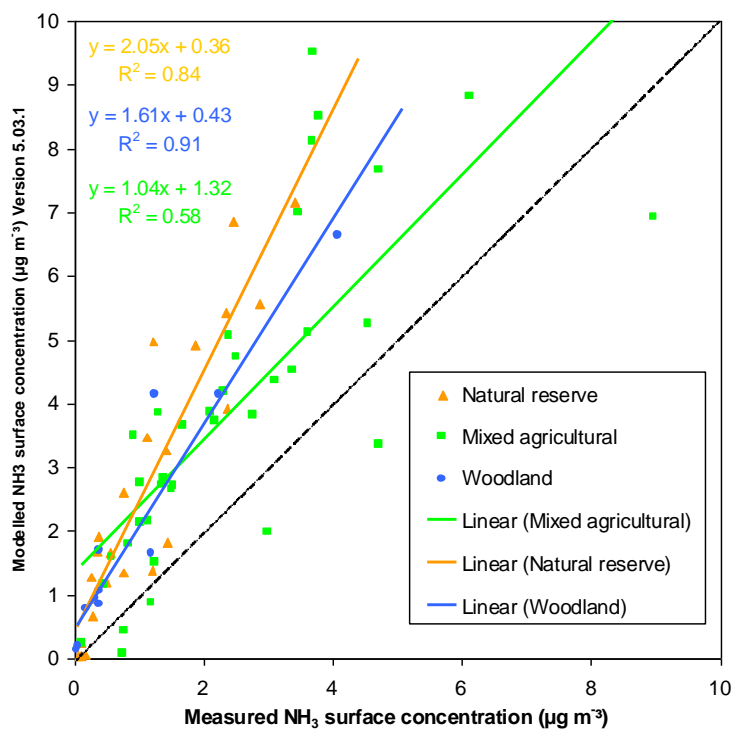


**Figure 8.2** FRAME NH<sub>3</sub> predictions versus UK National ammonia monitoring network. Units are µg m<sup>-3</sup>.

# 9 Sensitivity Study

## 9.1 Introduction

It is important to ascertain the uncertainty associated with model calculations of sulphur and nitrogen deposition. A large number of variables are incorporated into the model, including gaseous emission rates, chemical transformation rates, diffusion and advection rates, dry deposition velocities and washout coefficients. The uncertainty in setting these parameters will influence the accuracy with which the model can generate values of chemical deposition. An estimate of the uncertainty in acid deposition modelling was made by Abbott *et. al.* (2003) using the TRACK, FRAME and HARM models. Both a Monte Carlo analysis (with parameter values sampled from within the range of uncertainty) and a first order analysis (with single parameters varied individually) were carried out. The results suggested that the uncertainty in acid deposition might broadly be described as a ‘factor of two’. Page *et al.* (2004) applied a generalised likelihood uncertainty estimation methodology to the Hull Acid Rain Model. Two data sets of wet deposition from sites in Wales were used and the uncertainty prediction bounds were found to span the observed data satisfactorily.

The purpose of the work described here is to assess in more detail the sensitivity of deposition calculated by FRAME to the variation of the primary parameters within the limits of their uncertainty. For the purpose of this assessment the sensitivity analysis was conducted using FRAME version 4.21. The simulations were conducted with emissions, wind data and precipitation data representing the year 2000.

## 9.2 Parameters Studied

The chemical species represented within the FRAME model include SO<sub>2</sub>, (NH<sub>4</sub>)<sub>2</sub>SO<sub>4</sub>, H<sub>2</sub>SO<sub>4</sub>, NH<sub>3</sub>, NO, NO<sub>2</sub>, HNO<sub>3</sub>, NH<sub>4</sub>NO<sub>3</sub>, PAN and H<sub>2</sub>O<sub>2</sub>. The dry deposition velocity for NO and the wet deposition removal rates for NO, NO<sub>2</sub> and PAN are fixed at zero and therefore not included in the study. The FRAME parameters selected for uncertainty analysis are represented in Table 9.1. For each parameter, a separate model run was performed with the parameter increased by a percentage representative of the uncertainty associated with the knowledge of the model parameter. The percentage increases assigned to each parameter varied considerably. Certain parameters, such as cloud base height, wind-speed and mixing layer height can be measured quite accurately and therefore have a low uncertainty of 10 or 20% assigned to them. Other parameters (such as the seeder-feeder enhancement factor, the rate of nitric acid gas to nitrate particle conversion or the equilibrium constant for conversion of ammonia and nitric acid to ammonium nitrate) represent simple model parameterisations for atmospheric processes which are in reality much more complex. For such parameters, uncertainty limits with an increase of up to 100% have been selected. The percentage increases for each parameter are illustrated in Table 9.2. The choice of parameters 1 to 6 was influenced by the different representation of dry deposition velocities for various species within FRAME. In the case of NO<sub>2</sub> and SO<sub>2</sub>, dry deposition velocities are vegetation specific, being differentiated according to the land use categories *arable*, *forest*, *grass*, *moor-land* and *urban*, and for individual grid squares, are read in to the model as annual averages for those land use categories. By contrast, for the case of aerosols, dry deposition velocities are read in as constants, which do not vary according to grid square or vegetation type. Further, for ammonia, dry deposition velocities *VdVegNH3* are evaluated within FRAME 4.21 according to the equation:

$$VdVegNH3 = \frac{1}{R_a + R_b + R_c}, \quad (1)$$

where  $R_a$ ,  $R_b$  and  $R_c$  denote the aerodynamic, boundary layer and canopy resistance, respectively, all of which are land use dependent. The vegetation roughness length  $Z_0$  is used to calculate  $R_a$  and  $R_b$ , whilst the wind speed,  $vWindz$ , at a land use dependent reference height  $z$  above the zero plane displacement is used to calculate  $R_a$ . Thus, whilst the dry deposition velocities  $VdVegNO_2$ ,  $VdVegSO_2$  and  $DDry$  for  $NO_2$ ,  $SO_2$  and aerosols, respectively were varied directly in the study, it was considered sufficient to measure the influence of dry deposition velocity,  $VdVegNH_3$ , for ammonia by consideration of the typically dominant resistance component  $R_c$  of  $VdVegNH_3$ , together with  $Z_0$  and  $vWindz$ .

The wet scavenging coefficient is included in this study to assess its influence on wet deposition. The reaction rates and equilibrium constants 8, 9 and 11-14 of Tables 9.1 and 9.2 have been identified as representative of the main chemical reactions driving the FRAME model.

**Table 9.1:** FRAME parameters used in uncertainty study

	Parameter name	Parameter interpretation	Units
1	$VdVegNO_2$	$NO_2$ dry deposition velocity	$ms^{-1}$
2	$VdVegSO_2$	$SO_2$ dry deposition velocity	$ms^{-1}$
3	$DDry$	dry deposition of other species	$ms^{-1}$
4	$R_c$	Canopy resistance for ammonia deposition	$ms^{-1}$
5	$Z_0$	vegetation roughness length (used in calculation of $NH_3$ dry deposition velocity)	M
6	$VWindz$	Wind speed at a land use dependent height $z$ above the zero plane displacement	$ms^{-1}$
7	$\Delta_i$	wet scavenging ratio: $HNO_3$ , $SO_2$ , aerosols and $NH_3$	
8	$rrNOO_3$	reaction rate: $NO+O_3 \rightarrow NO_2+O_2$	$cm^3 s^{-1} molecule^{-1}$
9	$rrNO_2O_3$	reaction rate: $NO_2+O_3 \rightarrow NO_3+O_2$	$cm^3 s^{-1} molecule^{-1}$
10	$oxSO_2$	Oxidation reaction rate: $SO_2 \rightarrow H_2SO_4$	$h^{-1}$
11	$EquilC$	equilibrium constant: $NH_3+HNO_3 \leftrightarrow NH_4NO_3$	$mol^2 m^{-6}$
12	$FPhot$	daytime reaction rate: $NO_2+hv \rightarrow NO+O$ (night-time value is zero)	$s^{-1}$
13	$FGToP$	reaction rate: $HNO_3 \rightarrow NO^- + H^+$	$s^{-1}$
14	$rrNO_2OH$	reaction rate: $NO_2+OH^- \rightarrow HNO_3$	$cm^3 s^{-1} molecule^{-1}$
15	$peroxD$	daytime $H_2O_2$ production rate (night time value is zero)	$ppbh^{-1}$
16	$Sff$	Seeder feeder enhancement factor for wet deposition rate	
17	$emitNH_3$	$NH_3$ emissions	$kgNha^{-1}$
18	$EmitNOX$	$NO_x$ emissions	$kgNha^{-1}$
19	$EmitSOX$	$SO_2$ emissions and $H_2SO_4$ emissions	$kgSha^{-1}$
20	$wspeed$	optimised wind speed	$ms^{-1}$
21	$K_{max}$	maximum vertical diffusivity	$m^2 s^{-1}$
22	$HCldBd$	cloud base height	M
23	$h_{st}$	stack height	M
24	$hmix24$	diurnally variable mixing layer height	M
25	Heat	sensible heat flux	$Wm^{-2}$

Note: the aerosols include  $(NH_4)_2SO_4$ ,  $NH_4NO_3$  and a large  $NO_3$  category,

The percentage changes for all of the above reaction rates and for the equilibrium constant were selected with reference to Abbot *et al.* (2003) and using expert judgement. During the calculation of the wet deposition rate, the seeder-feeder factor,  $sff$ , is incorporated as follows:

$$\Lambda_i = \frac{\Delta_i}{hmix24} (rain_{nonor} + rain_{or} * sff), \quad (2)$$

Where  $\Lambda_i$  is the scavenging coefficient for chemical species  $i$  and  $\Delta_i$  denotes the scavenging ratio,  $h_{mix24}$  denotes the diurnally variable mixing layer height and for each 5 km grid square,  $rain_{nonor}$  denotes annual non-orographic rainfall and  $rain_{or}$  denotes annual directional orographic rainfall. The use of  $sff$  derives from the recognition that there is a higher ion concentration in rainfall in mountainous regions (Fowler *et al.*, 1988; Dore *et al.*, 1992), which needs to be accounted for by means of a correction coefficient during the calculation of the wet deposition rate. The rise in ion concentration derives from the formation of cloud around a hill summit through the orographic lifting of polluted air. This cloud, known as a ‘feeder cloud’, is efficiently washed out by precipitation falling from a higher level ‘seeder cloud’.

**Table 9.2:** Variation of FRAME parameters

	Parameter name	Parameter	Parameter implementation <sup>1</sup>	Increment (% increase)
1	<i>VdVegNO2</i>	dry deposition velocity of NO <sub>2</sub>	land use dependent	33
2	<i>VdVegSO2</i>	dry deposition velocity of SO <sub>2</sub>	land use dependent	100
3	<i>Ddry</i>	dry deposition velocity of other species	Species dependent	50
4	<i>Rc</i>	canopy resistance for ammonia deposition	land use dependent	100
5	<i>Z0</i>	vegetation roughness length	land use dependent	10
6	<i>Vwindz</i>	surface wind speed	land use dependent	20
7	$\Delta_i$	scavenging ratio for wet deposition	chemical variable dependent	100
8	<i>RrNOO3</i>	reaction rate: NO+O <sub>3</sub> → NO <sub>2</sub> +O <sub>2</sub>	$2.1 \times 10^{-12} \times e^{-1450/T}$	20
9	<i>rrNO<sub>2</sub>O<sub>3</sub></i>	reaction rate: NO <sub>2</sub> +O <sub>3</sub> → NO <sub>3</sub> +O <sub>2</sub>	$1.2 \times 10^{-13} \times e^{-2450/T}$	30
10	<i>OxSO2</i>	reaction rate: SO <sub>2</sub> + OH <sup>-</sup> → SO <sub>4</sub>	2 [daytime] ; 1 [night time]	100
11	<i>EquilC</i>	equilibrium constant: NH <sub>3</sub> +HNO <sub>3</sub> ↔ NH <sub>4</sub> NO <sub>3</sub>	temperature dependent	100
12	<i>Fphot</i>	reaction rate: NO <sub>2</sub> +hv → NO+O	$1 \times 10^{-2} \times e^{(0.39\sec(\text{zen}))} \times (1-6/16)$	40
13	<i>FGToP</i>	reaction rate: HNO <sub>3</sub> → NO <sub>3</sub> <sup>-</sup> + H <sup>+</sup>	$1 \times 10^{-5}$	100
14	<i>rrNO<sub>2</sub>OH</i>	reaction rate: NO <sub>2</sub> +OH <sup>-</sup> → HNO <sub>3</sub>	$1.1 \times 10^{-11}$	70
15	<i>PeroxD</i>	daytime H <sub>2</sub> O <sub>2</sub> production rate	0.08333	40
16	<i>Sff</i>	seeder feeder enhancement factor	2	100
17	<i>emitNH<sub>3</sub></i>	NH <sub>3</sub> emissions	spatially variable	30
18	<i>EmitNOX</i>	NO <sub>x</sub> emissions	spatially variable	20
19	<i>EmitSOX</i>	SO <sub>2</sub> emissions and H <sub>2</sub> SO <sub>4</sub> emissions	spatially variable	40
20	<i>Wspeed</i>	optimised wind speed	directionally variable (5-9 ms <sup>-1</sup> )	10
21	<i>K<sub>max</sub></i>	maximum vertical diffusivity	diurnally variable	100
22	<i>HCl<sub>dBd</sub></i>	cloud base height	250	20
23	<i>h<sub>st</sub></i>	stack height	spatially variable (50-260 m)	20
24	<i>h<sub>mix24</sub></i>	diurnally variable mixing layer height	diurnally variable	20
25	Heat	sensible heat flux	diurnally variable	20

<sup>1</sup>T and zen denote air temperature and zenith angle of the sun, respectively.

The assumption of a diurnally varying mixing height in equation (2) rather than, as in earlier versions of FRAME, a fixed mixing layer height of 1000 m, has led to a substantial improvement in the estimation of wet deposition levels to the British Isles and is thought to provide a more precise representation of the behaviour of the washout process (Fournier *et al.*, 2005a). From equation (2), it is evident that the two parameters *sff* (the seeder-feeder enhancement factor) and *h<sub>mix24</sub>* (the diurnally variable mixing layer height) as well as the orographic and non-orographic components of precipitation together determine the wet deposition rates. In this study, the sensitivity of the parameters *sff* and *h<sub>mix24</sub>* in determining wet deposition rates is assessed.

The levels of NH<sub>3</sub>, SO<sub>2</sub> and NO<sub>x</sub> emissions are expected to have a marked influence on deposition for most of the species represented in the FRAME model. One may assume, for example, that an increase in deposition levels for (NH<sub>4</sub>)<sub>2</sub>SO<sub>4</sub> and NH<sub>4</sub>NO<sub>3</sub> aerosol would

result from an increase in the emission levels of gaseous species following the atmospheric oxidation of SO<sub>2</sub> and NO<sub>x</sub>. In FRAME, the horizontal advection speed is assigned as a function of wind direction with a 1° resolution using long-term data series of wind-speeds from radiosonde data. In so far as it ultimately governs the estimation of the length of time taken by an air column to traverse an emission area and hence the amount of pollutant emitted to the column, *wspeed* is an important parameter to test.

The vertical diffusivity,  $K_z$ , for transfer of material between adjacent atmospheric layers, increases linearly with height up to a critical height at which it attains the value  $K_{max}$ . Above this height,  $K_z$  remains fixed at this maximum value up to the top of the mixing layer. The parameterisation of  $K_{max}$  itself depends on whether calculations are being performed a) over land at daytime, b) over land at night time or c) during either daytime or night time over sea regions. For each of the latter two categories,  $K_{max}$  is dependent on the geostrophic wind speed (to represent mechanical mixing). For the first category only,  $K_{max}$  is parameterised in terms of either geostrophic wind speed or (to represent convective mixing) both *hmix24* and the sensible heat flux, *Heat*, according as to which has the maximum effect. The parameters  $K_{max}$  and *Heat* have therefore been included in the sensitivity study as they will influence the vertical dispersion of gases and particles in the atmosphere and thus impact on both wet and dry deposition.

Aqueous phase chemistry in the model is performed only in layers, which are above the cloud-base height, *hCldBd*, as specified in Table 6. It is therefore of interest in the current study to assess whether modification of the parameter *hCldBd* is influential in altering chemical transformation rates and subsequent pollutant deposition levels. Version 4.21 of FRAME (used for the current study) includes specific treatment of point source emissions of SO<sub>2</sub> and NO<sub>x</sub> from chimney stacks (with heights varying from 50 m to 260 m) which are injected into the appropriate model layer. These point sources account for approximately 80% of SO<sub>2</sub> emissions. Stack heights are one of the model input parameters that can be defined with the greatest accuracy. However, the current study provides an opportunity to test the influence of varying stack height on wet and dry deposition of pollutants. For this reason, the stack height parameter *h<sub>st</sub>* has been included in the study

The FRAME output variables to be considered in terms of resultant annual average percentage change for the UK are:

- dry deposition rate for each of the species SO<sub>2</sub>, (NH<sub>4</sub>)<sub>2</sub>SO<sub>4</sub>, H<sub>2</sub>SO<sub>4</sub>, NH<sub>3</sub>, NO<sub>2</sub>, HNO<sub>3</sub>, NH<sub>4</sub>NO<sub>3</sub>, NO<sub>3</sub>, PAN, H<sub>2</sub>O<sub>2</sub>, NH<sub>x</sub>-N, NO<sub>y</sub>-N and SO<sub>x</sub>-S (Tables 2.4 and 2.10)
- wet deposition rate for each of the species SO<sub>2</sub>, (NH<sub>4</sub>)<sub>2</sub>SO<sub>4</sub>, H<sub>2</sub>SO<sub>4</sub>, NH<sub>3</sub>, HNO<sub>3</sub>, NH<sub>4</sub>NO<sub>3</sub>, NO<sub>3</sub>, NH<sub>x</sub>-N, NO<sub>y</sub>-N and SO<sub>x</sub>-S (Tables 2.5 and 2.10)

### 9.3 Results

The percentage changes in dry and wet deposition for each of the chemical species in FRAME associated with the changes in parameter values are tabulated in Tables 9.3 and 9.4 respectively (with the most sensitive two parameters for each chemical variable highlighted in bold red). In general the relative changes in deposition are not closely related to the relative changes in parameter values. From the data it is apparent that a number of parameters do not have a strong influence in determining wet or dry deposition.

**Table 9.3:** Annual average UK dry deposition % changes for the year 2000

Parameter	Parameter increase (%)	SO <sub>2</sub>	(NH <sub>4</sub> ) <sub>2</sub> SO <sub>4</sub>	H <sub>2</sub> SO <sub>4</sub>	NH <sub>3</sub>	NO <sub>2</sub>	HNO <sub>3</sub>	NH <sub>4</sub> NO <sub>3</sub>	NO <sub>3</sub>
VdVegNO2	33	-1.3	2.1	6.5	-0.28	<b>24</b>	-1.3	-3.5	-2.7
VdVegSO2	100	<b>36</b>	-1.6	-3.8	0.22 0	0	-0.13	0.2	0.01
Ddry	50	0.1	<b>36</b>	<b>52</b>	0	0	<b>25</b>	7.2	35.
Rc	100	-0.49	3.9	-7.1	<b>-23</b>	0	-4.3	8.3	-0.08
Zo	10	-1.3	2.0	6.7	-0.19	-1.1	-0.08	-0.7	-0.44
Vwindz	20	-0.04	0.31	-0.57	-1.7	0	-0.32	0.62	-0.01
Δ <sub>i</sub>	100	-4.5	<b>-32</b>	-30	-3.6	0	-21	-30	<b>-26</b>
RrNOO3	20	-1.3	2.1	6.6	-0.32	-1.1	-0.1	-0.61	-0.44
rrNO2O3	30	0.02	-0.1	0.1	-0.02	-3.7	1.6	3.5	21
EquilC	100	-0.01	0.53	-1.6	0.45	0	20	<b>-38</b>	0.2
Fphot	40	-0.03	0.17	-0.21	0.07	-1.7	-2.5	-6.5	0.12
FGToP	100	0.14	-0.66	0.67	-0.23	0	11.	24.	-4.2
rrNO2OH	70	0.37	-1.9	2.4	-0.84	-1.6	<b>28.</b>	<b>78</b>	-0.67
PeroxD	40	-0.59	0.26	5.0	-0.03	0	0.04	-0.07	0
Sff	100	-0.2	-7.6	-6.1	0.11	0	-3.2	-3.4	-5.5
EmitNH3	30	-1.3	11.	-20.	<b>32</b>	0	-9.5	18.	-0.19
EmitNOX	20	0.04	-0.31	0.6	-0.08	3.3	3.4	8.8	4.2
EmitSOX	40	<b>16</b>	4.7	<b>33</b>	-0.59	-1.7	0.08	-1.3	-0.71
Wspeed	10	-3.1	1.6	8.3	-9.1	-6.7	-0.65	-31.	1.1
K <sub>max</sub>	100	7.1	9.2	45.	-27.	<b>-14.</b>	23.	-16.	<b>-6.5</b>
HCldBd	20	0.01	-0.01	-0.01	0	0	0	0	0
h <sub>st</sub>	20	-4.3	-0.12	-2.5	0.01	-0.54	-0.14	-0.12	-0.3
hmix24	20	-3.5	-0.37	-0.41	0.29	-1.4	0.81	-1.4	0.48
Heat	20	-1.2	-0.72	0.53	-1.6	-1.2	-0.73	-4.3	-1.3

Parameters with increments that result in changes to deposition of less than 10% for all species can be categorised as ‘not strongly influential’. These include: the roughness length, the surface wind-speed, the reaction rate of NO with O<sub>3</sub>, the dissociation rate of NO<sub>2</sub>, the hydrogen peroxide production rate, the seeder-feeder enhancement factor, the NO<sub>x</sub> emissions rate, the height of cloud base, the stack height, the mixing layer height and the sensible heat flux.

An increase in the dry deposition velocity of a particular chemical species is found, as expected, to influence most strongly the mass dry deposition rate for that species (i.e. NO<sub>2</sub> & SO<sub>2</sub>). However the changes in mass deposition are significantly less than the changes in dry deposition velocity (i.e. a 33% increase in NO<sub>2</sub> dry deposition velocity leads to a 24% increase in NO<sub>2</sub> dry deposition and a 100% increase in SO<sub>2</sub> dry deposition velocity leads to an increase in SO<sub>2</sub> dry deposition of only 36%). The canopy resistance R<sub>C</sub> and the vegetation

roughness length  $Z_0$  are used to determine the deposition velocity of  $\text{NH}_3$ . A 100% increase in  $R_c$  was found to result in a 23% decrease in ammonia dry deposition with the  $Z_0$  uncertainty found to have only a small influence on dry deposition.

**Table 9.4:** Annual average UK wet deposition % changes for the year 2000

Parameter	Parameter increase (%)	SO <sub>2</sub>	(NH <sub>4</sub> ) <sub>2</sub> SO <sub>4</sub>	H <sub>2</sub> SO <sub>4</sub>	NH <sub>3</sub>	HNO <sub>3</sub>	NH <sub>4</sub> NO <sub>3</sub>	NO <sub>3</sub>
<i>VdVegNO2</i>	33	-1.0	0.86	2.4	-0.29	-1.1	-2.6	-1.8
<i>VdVegSO2</i>	100	-1.7	-7.5	1.7	-17.	1.1	-11.	-2.9
<i>Ddry</i>	50	-3.6	-1.6	-2.4	0.1	-0.64	0.79	-0.02
<i>Rc</i>	100	-0.4	5.3	-3.4	<b>19</b>	-4.6	6.1	-0.11
<i>Zo</i>	10	-1.0	0.72	2.5	-0.77	0.39	-0.97	-0.22
<i>vWindz</i>	20	-0.03	0.43	-0.28	1.42	-0.37	0.48	-0.01
$\Delta_i$	100	<b>81</b>	<b>19</b>	<b>32</b>	<b>56.</b>	<b>31</b>	12.	<b>24</b>
<i>RrNOO3</i>	20	-1.0	0.76	2.5	-0.52	0.31	-0.88	-0.22
<i>rrNO2O3</i>	30	0.01	-0.13	0.08	-0.32	1.2	2.2	<b>18</b>
<i>EquilC</i>	100	-0.01	0.23	-0.2	1.2	5.0	-8.2	0.12
<i>FPhot</i>	40	-0.04	0.25	-0.09	0.43	-3.3	-3.5	0.27
<i>FGToP</i>	100	0.13	-1.1	0.52	-2.5	16.	<b>18</b>	-4.5
<i>rrNO2OH</i>	70	0.47	-2.7	1.1	-4.8	<b>40</b>	<b>39</b>	-1.6
<i>PeroxD</i>	40	-0.83	0.1	3.2	-0.02	0.29	-0.36	0.01
<i>Sff</i>	100	-0.41	6.8	7.6	0.54	-3.8	5.7	5.6
<i>EmitNH3</i>	30	-1.0	<b>13</b>	-8.4	45.	-9.3	12.	-0.24
<i>emitNOX</i>	20	0.07	-0.33	0.09	-0.19	7.5	2.8	5.5
<i>emitSOX</i>	40	<b>24</b>	2.4	<b>19</b>	-1.6	1.9	-2.8	-0.2
<i>Wspeed</i>	10	-23	-1.3	-8.9	-10.	-18.	-9.7	-8.3
<i>K<sub>max</sub></i>	100	-4.9	<b>13</b>	-1.8	16	-7.4	7.2	0.52
<i>hCldBd</i>	20	0	0	-0.01	0	0	-0.01	0
<i>hst</i>	20	0.2	0.1	1.26	-0.1	0.1	-0.09	0.01
<i>hmix24</i>	20	-9.7	-3.2	1.1	-6.3	-2.6	0.32	-4.5
<i>Heat</i>	20	-3.1	0.61	3.3	-0.43	-2.1	0.06	-0.29

The large uncertainty in wet scavenging ratio of 100% was found to be associated with relatively large changes in wet deposition of the soluble species (81% for SO<sub>2</sub>, 56% for NH<sub>3</sub>, 32% for H<sub>2</sub>SO<sub>4</sub> and 31% for HNO<sub>3</sub>). Variation of the reaction rate for the oxidation of NO to NO<sub>2</sub> by O<sub>3</sub> appears not to greatly affect the results whereas a 30% increase in the rate of oxidation of NO<sub>2</sub> by ozone is correlated to a 21% increase in the deposition of the large nitrate aerosol. The uncertainty in the equilibrium constant *equilc* has an important influence

on the uncertainty in dry deposition of the ammonium nitrate aerosol. The gas to particle conversion rate uncertainty correlates to a 24% change in dry deposition of the ammonium nitrate aerosol. The reaction rate of NO<sub>2</sub> with the hydroxyl radical is shown to play a strong role in determining the dry deposition of nitric acid and ammonium nitrate.

**Table 9.5:** Annual average UK wet and dry NH<sub>X</sub>, NO<sub>Y</sub> & SO<sub>Y</sub> deposition % changes for the year 2000

Parameter	Parameter increase (%)	NH <sub>X</sub> dry	NO <sub>Y</sub> dry	SO <sub>Y</sub> dry	NH <sub>X</sub> wet	NO <sub>Y</sub> wet	SO <sub>Y</sub> wet
VdVegNO2	33	-0.23	<b>19</b>	-1.1	0.07	-1.8	1.1
VdVegSO2	100	0.17	-0.01	<b>34</b>	-0.23	0.02	-2.4
Ddry	50	<b>24</b>	3.4	2.2	-12	-3.4	-2.5
Rc	100	-22	-0.26	-0.4	11	0.15	0.57
Zo	10	-0.13	-0.98	-1.05	-0.02	-0.25	1.1
Vwindz	20	-1.6	-0.02	-0.03	0.81	0.01	0.04
Δ <sub>i</sub>	100	-4.4	-3.2	-5.9	<b>32</b>	<b>23</b>	<b>37</b>
RrNOO3	20	-0.26	-0.98	-1.1	0.11	-0.25	1.1
rrNO2O3	30	-0.02	-1.8	0.01	0.04	<b>15</b>	-0.02
EquilC	100	0.33	1.2	0	-0.25	-0.33	0.01
Fphot	40	0.05	-1.8	-0.03	-0.06	-0.41	0.05
FGToP	100	-0.16	0.72	0.12	0.3	-0.46	-0.18
rrNO2OH	70	-0.62	0.96	0.31	0.73	6.1	-0.52
PeroxD	40	-0.02	0	-0.49	0.01	-0.01	1.2
Sff	100	-0.09	-0.57	-0.55	4.3	4.8	5.6
EmitNH3	30	<b>32</b>	-0.58	-1.1	25	0.31	1.5
EmitNOX	20	-0.06	3.4	0.04	0.04	5.4	-0.08
EmitSOX	40	-0.46	-1.4	<b>15</b>	0.31	-0.28	<b>14</b>
Wspeed	10	-8.9	-6.3	-2.8	-5.6	-9.3	-9.0
K <sub>max</sub>	100	-26	<b>-10</b>	7.6	<b>14</b>	0.55	3.3
HClDbd	20	0	0	0	0	0	0
h <sub>st</sub>	20	0	-0.48	-4.1	0.01	0.01	0.6
hmix24	20	0.26	-1.2	-3.3	-4.0	-3.9	-2.8

Emission factors are found to be important in determining wet and dry deposition of ammonia and oxidised sulphur. Only a 10% variation was applied to the wind speed. However this was sufficient to effect significant changes in the deposition budgets, which were highly species dependent. Similarly, changing the maximum vertical diffusivity caused significant changes to the deposition of the chemical species, some positive and others negative.

In Table 9.5, the results of the deposition of individual chemical species are combined to show the changes to wet and dry deposition for reduced nitrogen, oxidised nitrogen and oxidised sulphur, which are the variables relevant for calculations of exceedance of critical loads. It is interesting to note that for this data, certain chemical transformation parameters, which were important for the variation in deposition of individual species (i.e.  $EquilC$ ,  $fGToP$ ,  $rrNO2OH$ ), are not of importance for deposition of combined species. This occurs because, in the case of variation of the equilibrium constant, for example, an increase in deposition of nitric acid is offset by a decrease in deposition of ammonium nitrate aerosol. The most important variables, highlighted in red are the deposition velocities, washout coefficients, emission rates and diffusivity rate

## 9.4 Conclusion

A sensitivity study was conducted with FRAME to investigate the influence on wet and dry deposition of making individual modifications to 25 different parameters including emissions rates, dry deposition velocities, wet scavenging ratios and chemical reaction rates. The parameters were all given increased values with the modifications being different for each parameter. The parameter increments were selected to correspond approximately to their limits of uncertainty. Certain parameters, when increased, were found not to have a strong influence on the results. These included: the roughness length, the surface wind-speed, the reaction rate of NO with O<sub>3</sub>, the dissociation rate of NO<sub>2</sub>, the hydrogen peroxide production rate, the seeder-feeder enhancement factor, the NO<sub>x</sub> emissions rate, the height of cloud base, the stack height, the mixing layer height and the sensible heat flux. For dry deposition, the most significant parameters were the deposition velocities (or the canopy resistance for ammonia). Additionally the gaseous emissions rates and the vertical diffusion rates were found to be sensitive parameters in influencing dry deposition. For wet deposition, the washout coefficients were responsible for introducing the greatest changes.

In this study, no attempt is made to assess the uncertainty in deposition resulting from uncertainty in the input parameters. However it does highlight the model parameters that are most sensitive in influencing the wet and dry deposition rates generated by FRAME. In general, it cannot be assumed that all model parameters interact independently from one another. A more detailed uncertainty analysis would thus require model runs in which a number of parameters are varied simultaneously, possibly using random variations and including both increases and decreases.

The results of this study suggest that, in order to reduce the uncertainty in estimates of deposition of nitrogen and sulphur, for a model such as FRAME, improved estimates of dry deposition velocities of gaseous species and their emission rates are important. Improved estimates of washout rates are important for reducing uncertainty in wet deposition. In general however, the various atmospheric chemical reaction rates were found to be less important in controlling deposition rates. Many of the chemistry model parameters considered in this study do not have a strong measurement base from which to assess an appropriate value for parameter uncertainty (such as the rate of nitric acid gas to nitrate particle conversion or the equilibrium constant for conversion of ammonia and nitric acid to ammonium nitrate). In such cases, the parameter values used in models may be those that are found by trial and error to produce good results. In this situation, assigning an uncertainty to a model parameter is a difficult task and relies on expert judgement.

Future uncertainty studies will focus on model simulations which simultaneously combine changes to a number of model parameters, including both increases and decreases. This may be achieved by randomly selecting the magnitude of the parameter change from within its range of uncertainty.

# 10. Improvement of the parameterisation of HNO<sub>3</sub> in FRAME

## 10.1 Introduction

The introduction of a nitric acid monitoring network in the United Kingdom ([www.nbu.ac.uk/cara](http://www.nbu.ac.uk/cara)) has allowed accurate measurement of this chemical compound at 12 sites in the United Kingdom. Monthly atmospheric sampling has been undertaken using **DELT**A samplers (**D**ENuder tubes for **L**ong **T**erm **A**nalysis). Interpolation of the measurements onto a 5 km resolution grid covering the United Kingdom combined with the application of appropriate deposition velocities allowed an assessment of the contribution of nitric acid to the dry deposition budget of oxidised nitrogen for the United Kingdom. The results revealed that nitric acid contributes 65 kT N compared to only 20 KT N for NO<sub>2</sub> (NEGTAP, 2001). As nitric acid therefore plays an important role in the processes of acidification and eutrophication, it is important that atmospheric transport models are able to accurately represent the measured concentrations. Models have, however, tended to significantly underestimate nitric acid concentrations. Here we investigate ways to improve the parameterisation in FRAME.

## 10.2 Changes to production and loss mechanisms of HNO<sub>3</sub>

The correlation of concentrations of HNO<sub>3</sub> calculated by FRAME with annually averaged measurements during the years 1998-2000 is illustrated in Figure 10.1. This plot shows that FRAME 5.0 underestimates HNO<sub>3</sub> concentrations by a factor of approximately 8. A number of production and loss mechanisms of HNO<sub>3</sub> in the model are involved in controlling the concentrations which may be altered to bring the modelled concentrations closer to the measured values. The principle production mechanism is the oxidation of NO<sub>2</sub> by the OH· free radical. Nitric acid is soluble and may be removed from the atmosphere by washout by precipitation. It is also rapidly removed from the surface layer by dry deposition, with deposition velocities typically in the range 30-40 mm s<sup>-1</sup>. In the sensitivity study described above, an increase in the vertical diffusion rate was also found to be an effective way to deplete surface concentrations of HNO<sub>3</sub>. Removal of HNO<sub>3</sub> by chemical transformation occurs via a gas to particle transformation, which represents the deposition of nitric acid vapour on to large dust particles to form large nitrate aerosol and through the equilibrium reaction of nitric acid with ammonia gas to form small ammonium nitrate aerosol. The modifications applied to the physical and chemical parameters in version 5.1 of FRAME are illustrated in Table 10

**Table 10** Parameter scaling factors applied to FRAME 5.1

Parameter	Modification
Dry deposition velocity of HNO <sub>3</sub>	No change
Washout coefficient of HNO <sub>3</sub>	0.5
Vertical diffusion rate	No change
Oxidation rate of NO <sub>2</sub> by OH·	2
Particle to gas conversion rate	2
Ammonium nitrate equilibrium	2

The chemical transformation rates were increased by a factor of 2. This was considered to be within the bounds of the uncertainty with which such reaction rates are known. The vertical diffusion rate was not modified as this would have a significant effect on the concentrations of other species. The dry deposition velocity of  $\text{HNO}_3$  was not modified as the value employed in FRAME of  $30 \text{ mm s}^{-1}$  was considered appropriate. Reducing this would lead to an underestimate in the deposition of nitric acid. The correlation plot for nitric acid concentrations calculated by FRAME version 5.1 (after parameter changes) is illustrated in Figure 10.2. A significant improvement is evident with the slope having increased to 0.23 when an intercept on the y-axis is permitted and to 0.47 when the best fit line is restrained to pass through the origin.

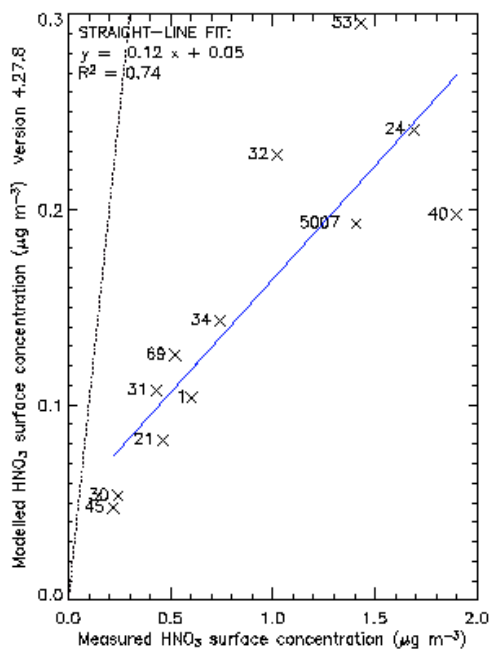


**Figure 10.1** Correlation of FRAME 5.0 concentrations of  $\text{HNO}_3$  with measurements before parameter changes

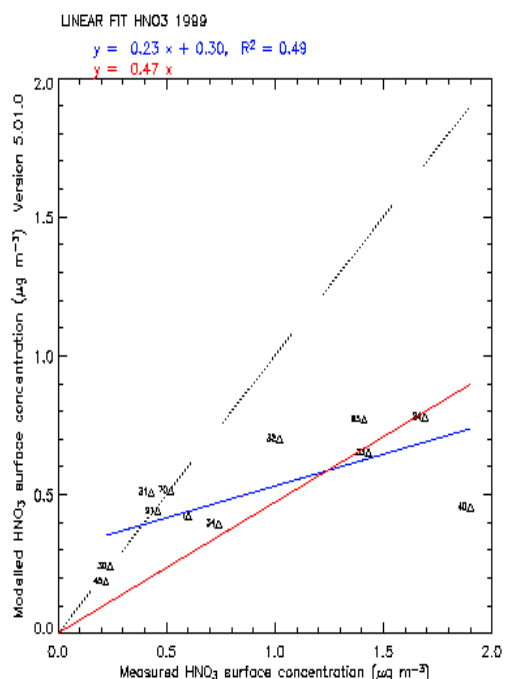


**Figure 10.2** Correlation of FRAME 5.1 concentrations of  $\text{HNO}_3$  with measurements after parameter changes

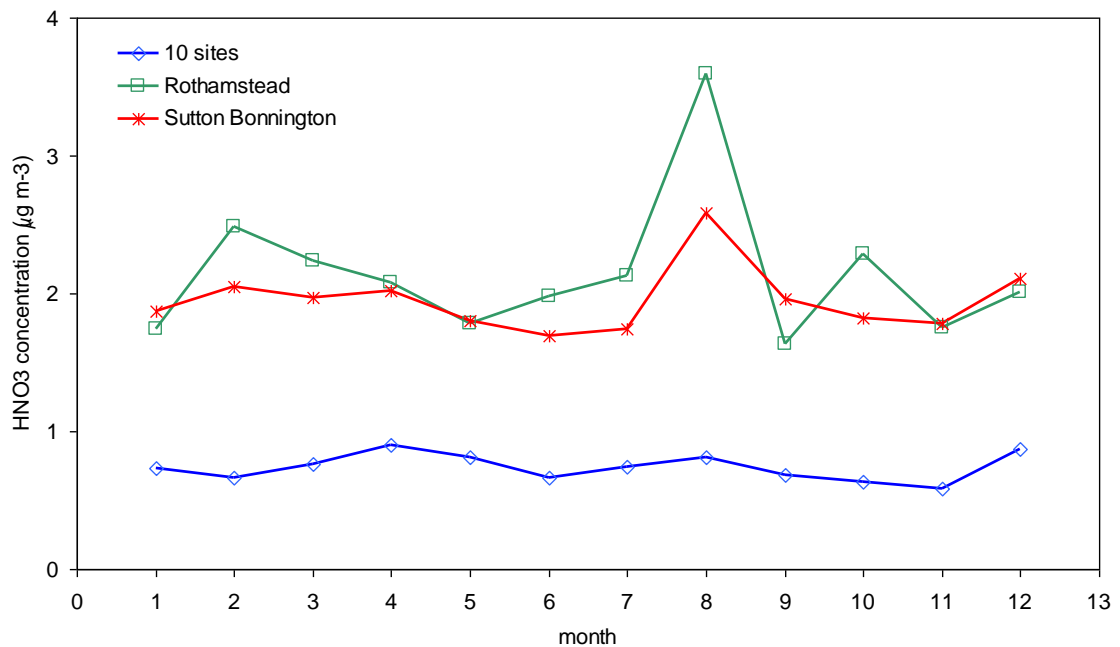


**Figure 10.3** Seasonal variation in  $\text{HNO}_3$  concentrations at individual sites and grouped sites

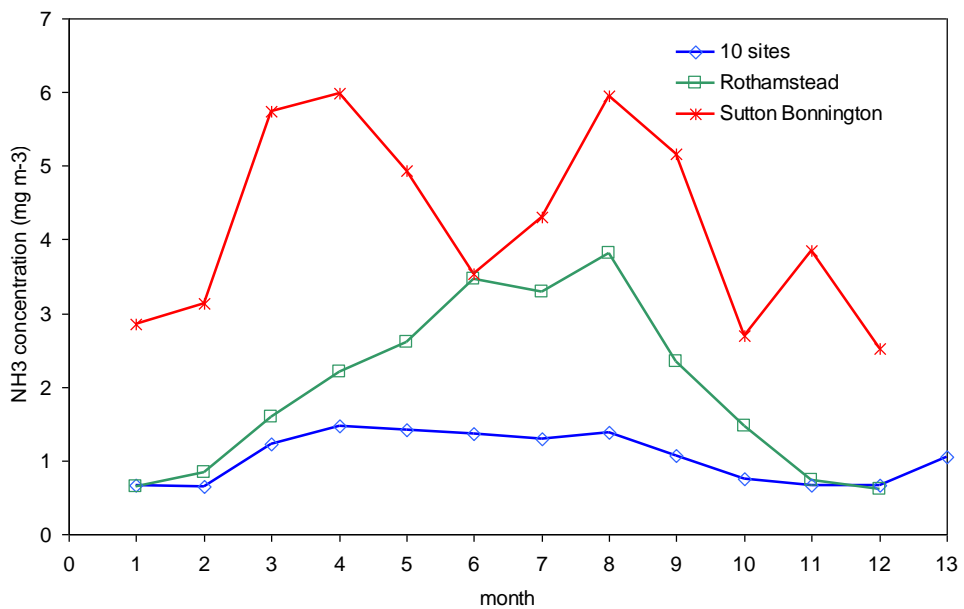


**Figure 10.4** Seasonal variation in  $\text{NH}_3$  concentrations at individual sites and grouped sites

The two sites at which FRAME most underestimates the measured  $\text{HNO}_3$  concentrations are Sutton Bonnington and Rothamstead, both of which are located close to agricultural activity. Closer analysis of the concentrations measured at these sites reveals an annual cycle with concentrations peaking during the month of August. The average concentrations for the remaining 10 sites however reveal no significant annual cycle (Figure 10.3). A similar analysis was conducted with the ammonia concentrations, also measured with DELTA samplers. The results, illustrated in Figure 10.4 show that ammonia emissions also peak during the month of August at both Sutton Bonnington and Rothamstead. A broad peak is associated with the annual trend at Rothamstead and a much narrower peak at Sutton Bonnington. The annual cycle in the measured nitric acid concentrations at these two agricultural sites, and the coincidence of the peaks with ammonia emissions may be evidence to support the theory that nitric acid is co-emitted with ammonia from agricultural sources. Removal of the sites 34 and 40 (which may be close to sources of nitric acid not included in the model emissions inventory) from the correlation plot results in improved correlation (Figure 10.5) with the slope of the graph increased from 0.47 to 0.6. The emissions of  $\text{HNO}_3$  from agricultural sources will be included in a future version of FRAME. Furthermore the current expansion of the nitric acid monitoring network from 12 to 36 sites will allow for a more detailed model-measurement comparison of nitric acid concentrations.

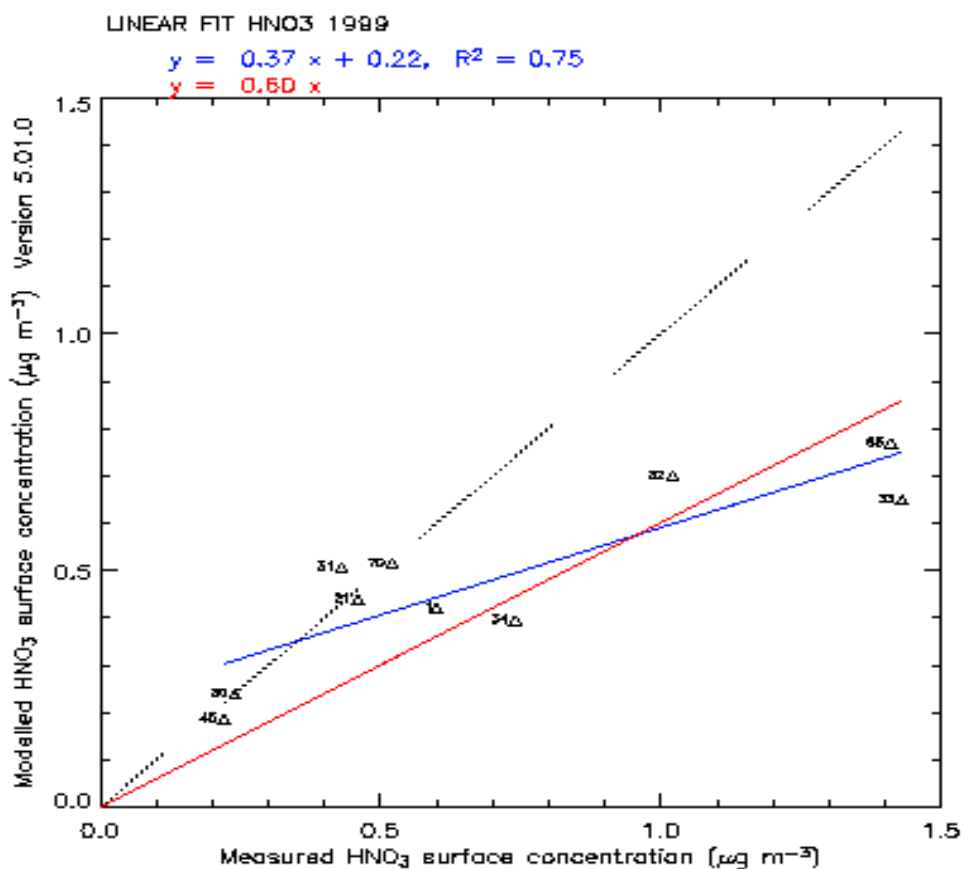


**Figure 10.5** Correlation of FRAME 5.1 concentrations of  $\text{HNO}_3$  with measurements with sites 34 and 40 removed

# 11 The Air Quality Strategy

## 11.1 Rationale and background

FRAME was used to calculate the deposition of SO<sub>x</sub>, NO<sub>y</sub> and NH<sub>x</sub> to the United Kingdom for future emissions scenarios defined by the Air Quality Strategy (AQS). A detailed inventory of emissions from 242 individual point sources for the year 2003 was provided by the Environment Agency, the Scottish Environmental Protection Agency the Environment Heritage Service Northern Ireland. The data included, where available, information on stack height, diameter, temperature and exit velocity of emissions, as well as annual emissions of SO<sub>2</sub> and NO<sub>x</sub>. Where stack parameters were missing, typical default values were assigned. Remaining emissions of SO<sub>2</sub> and NO<sub>x</sub> were taken from the National Atmospheric Emissions Inventory (NAEI) using data for a recent emissions year, 2002. These included a further 766 small point sources as well as gridded background emissions for different snap codes (Energy production and transformation; Commercial, institutional and residential combustion; Industrial combustion; Industrial processes; Production and distribution of fossil fuels; Road transport; Other transport; Waste treatment and disposal). The input of ammonia emissions to the model used the AENEID inventory of Dragosits *et al.* (1998), which separately calculates spatial emissions from cattle, pigs, poultry, sheep, crops and grassland and non-agricultural sources. Future emissions of NH<sub>3</sub> for the year 2020 were set to the National Emissions Ceiling Directive (NECD) target for the UK. The Republic of Ireland is included in the FRAME domain and future emissions of SO<sub>2</sub>, NO<sub>x</sub> and NH<sub>3</sub> for the year 2020 were set according to the NECD targets. The initial concentrations of trajectories in FRAME are set the edge of the domain according to calculations from the European scale model FRAME-Europe. For the year 2020, European emissions were assumed to be at the levels determined by the NECD.

The future emissions estimates supplied by AEA Technology for the year 2020 were used to generate scaling factors for each snap code emissions sector. These scaling factors were used to convert the 2002 emissions maps to a 2020 scenario. Emissions of SO<sub>2</sub> and NO<sub>x</sub> from international shipping were assumed to increase from 2002 by a rate of 2.5% per annum, according to the assessment of Johnson *et al.* (2000). Eight emissions abatement strategies were investigated with FRAME, as well as the baseline 2020 scenario (Table 11.1) and the 2002 scenario used to represent a ‘recent emissions year’. Emissions abatement factors were applied to individual snap code sectors according to the total emissions forecast as a result of applying the emissions controls.

## 11.2 Results

The emissions scenarios were used as input to the FRAME model and maps of wet and dry deposition of SO<sub>x</sub>, NO<sub>y</sub> and NH<sub>x</sub> were generated at a 5 km resolution for three vegetation types: moor-land, forest and grid-averaged deposition. Grid-averaged dry and wet deposition of SO<sub>x</sub>, NO<sub>y</sub> and NH<sub>x</sub> are illustrated in Figures 11.1(a)-(f) for the year 2002 (representing a ‘recent emissions year’) and in Figures 11.2(a)-(f) for the year 2020 baseline projection. Dry deposition occurs in the vicinity of the major sources (road transport for NO<sub>y</sub> and industrial regions and power stations for SO<sub>y</sub>). Wet deposition is associated with the longer-range transport of aerosols and occurs in upland regions where annual precipitation is highest. According to future emissions projections, significant reductions in UK emissions of SO<sub>2</sub> (from 501 to 180 kT S) and NO<sub>x</sub> (from 481 to 265 kT N) are forecast during the period 2002 to 2020. These changes are reflected in the maps of deposition. In 2002 significant areas of eastern England are subject to dry deposition in excess of 3 kg S ha<sup>-1</sup> and wet deposition in

excess of 5 kg S ha<sup>-1</sup>. For 2020, the dry deposition remains above these thresholds only in localised areas, particularly in southeast England due to the increased influence of shipping

**Table 11.1** Air Quality Strategy emissions abatement scenarios for the year 2020

Scenario number	Abatement measure
<b>Base case</b>	Base case scenario with no additional measures applied
<b>A</b>	<b>Euro low:</b> Proposes a 20% reduction in NOx emissions from all new diesel <b>Light Duty Vehicles (LDVs)</b> and a 50% reduction in NOx emissions from new diesel <b>Heavy Duty Vehicles (HDVs)</b> to be introduced in 2010 and 2013 respectively.
<b>B</b>	<b>Euro high:</b> Proposes: reductions of NO <sub>x</sub> emissions of 50% from new petrol LDVs and 40% from new diesel LDVs from 2010 and 68% reduction in NO <sub>x</sub> emissions from all new LDVs from 2015; a 75% reduction in NO <sub>x</sub> emissions from new HDVs from 2013.
<b>C</b>	<b>Early Euro low:</b> Assumes a programme of incentives for early introduction of measure A is introduced in 2006 for LDVs and 2010 for HDVs.
<b>K</b>	<b>Large Combustion Plant (LCP):</b> Assumes power stations and combustion plants fit low NO <sub>x</sub> burners and introduce other combustion modifications by 2010.
<b>N</b>	Shipping: Assumes that international shipping in the North Sea will use low sulphur fuel (1% instead of 1.5%) and the reduction of NO <sub>x</sub> emissions by 25% from new ships from 2010.
<b>O</b>	<b>Early Euro Low &amp; LEV:</b> Assumes a combination of measure C and a programme of incentives to increase the penetration of <b>Low Emission Vehicles</b>
<b>P</b>	<b>Early Euro Low &amp; SCP:</b> Assumes a combination of measure C and a 50% reduction in NO <sub>x</sub> and SO <sub>2</sub> emissions from <b>Small Combustion Plants</b> from 2013.
<b>Q</b>	<b>Early Euro Low &amp; LEV &amp; SCP:</b> Assumes a combination of measures P and Q.

emissions. The areas with wet deposition exceeding 5 kg S ha<sup>-1</sup> have retreated to upland areas by 2020. A similar situation is apparent for NO<sub>y</sub> deposition, with significant areas of the country subject to wet and dry deposition in excess of 5 kg N ha<sup>-1</sup> for 2002. By 2020, only restricted areas near major urban centres or subject to heavy annual precipitation have NO<sub>y</sub> deposition in excess of 5 kg N ha<sup>-1</sup>. A different picture emerges, however, for deposition of NH<sub>x</sub>. In the absence of detailed future emissions scenarios for NH<sub>3</sub>, only a small reduction in emissions of 4% has been applied for the future 2020 scenario. The move from a 2002 scenario to a 2020 scenario therefore represents a change in which deposition of potentially acidifying and eutrophying pollutants is increasingly shifted towards reduced nitrogen.

The results of the FRAME simulations can be illustrated simply in the form of tables of total UK deposition of oxidised nitrogen and sulphur (Table 11.2). Significant changes in deposition are forecast between 2002 and 2020 with SO<sub>x</sub> deposition falling by 45%, a decrease in NO<sub>y</sub> deposition of 35% and a small decrease in NH<sub>x</sub> deposition of 5%. In comparison, the additional emissions reductions scenarios result in much smaller changes in deposition. The greatest change occurs due to the implementation of scenario B (Euro high) with an 11.7% reduction in NO<sub>y</sub> deposition. Scenario Q with a combination of emissions

reduction measures (Euro low, LEV and SCP) results in a 7.6% reduction in NO<sub>y</sub> deposition and a 1.5% reduction in SO<sub>x</sub> deposition. The implementation of measures to abate emissions from international shipping (scenario N) leads to a 5.9% reduction in SO<sub>x</sub> deposition and a 1.7% reduction in NO<sub>y</sub> deposition.

### 11.3 Calculation of Exceedance of Critical Loads

Calculation of exceedance of critical loads for a ‘recent year’ was undertaken using the **Concentration Based Estimated Deposition (CBED)** deposition data set, which is based upon interpolation of measurements of gas concentrations and ion concentrations in precipitation averaged over the three years 2001-2003 (Smith *et al.*, 2000; Smith and Fowler, 2001; NEGTAP, 2001). Deposition plots from the CBED data set are illustrated in Figures 3(a)-(f).

Where FRAME deposition data is to be used for calculations of critical loads exceedance, a standard technique is to apply a ‘calibration procedure’ (NEGTAP, p91). This approach is based on the convention that the official data set of mapped deposition of nitrogen and sulphur for the United Kingdom is obtained from measurements of wet deposition and gas concentrations for a recent year. FRAME may be used to provide estimates of deposition for future years (i.e. using projected emissions changes to inventories for the year 2020). In estimating changes in pollutant deposition over time, it is important to compare equivalent data sets. Comparing FRAME deposition estimates for the year 2020 with CBED deposition for the period 2001-03 could result in misleading conclusions due to the differences in the approaches used. It is for this reason that a calibration is applied to FRAME deposition to normalise the modelled data to the CBED estimates. In essence ‘calibration’ means that FRAME is used to estimate the relative change to deposition for each 5 km grid square in the UK during a specified time period. Future estimates of deposition are calculated by applying the modelled change to the CBED measurement-based deposition for a recent year for each individual UK 5km grid square. For this work, the calibration procedure used is described in equation (11).

$$\text{DEP}_{(\text{CAL},2020)} = \text{DEP}_{(\text{UNC},2020)} * (\text{DEP}_{(\text{CBED},2001-2003)} / \text{DEP}_{(\text{UNC},2002)}) \dots \dots \dots \quad (11)$$

Where DEP<sub>(UNC,2002)</sub> refers to uncalibrated FRAME deposition data for the emissions simulation year 2002, DEP<sub>(UNC,2020)</sub> refers to uncalibrated FRAME deposition data for the emissions simulation year 2020, DEP<sub>(CBED,2001-2003)</sub> is the CBED deposition data for the period 2001-2003 and DEP<sub>(CAL,2020)</sub> is the calibrated deposition for the year 2020.

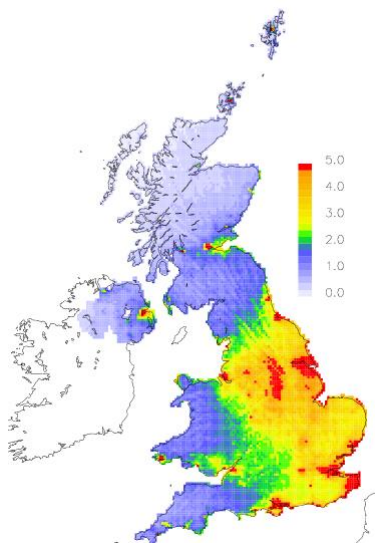


**Figure 11.1(a)** FRAME 2002 SO<sub>x</sub> dry deposition ( $\text{kg S ha}^{-1} \text{ yr}^{-1}$ )

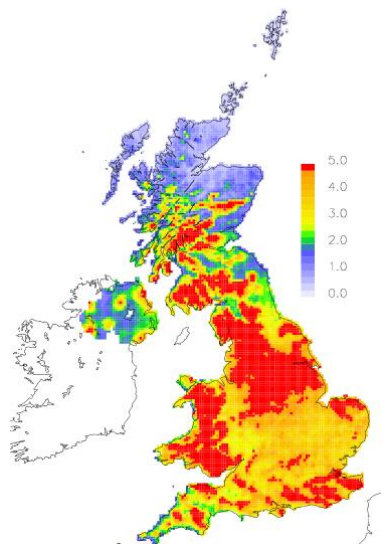


**Figure 11.1(b)** FRAME 2002 SO<sub>x</sub> wet deposition ( $\text{kg S ha}^{-1} \text{ yr}^{-1}$ )

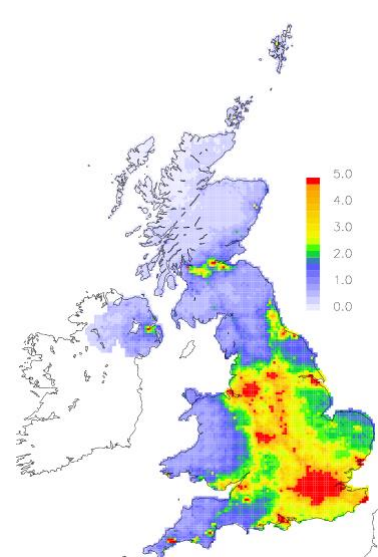


**Figure 11.1(c)** FRAME 2002 NO<sub>y</sub> dry deposition ( $\text{kg N ha}^{-1} \text{ yr}^{-1}$ )

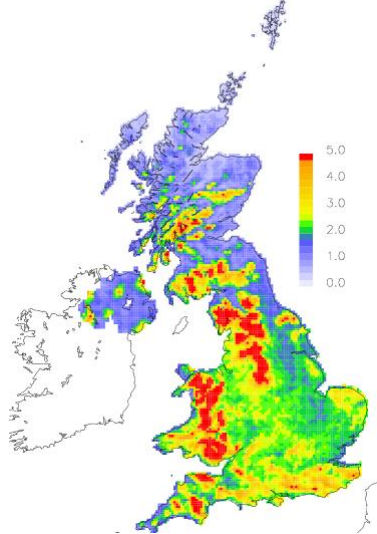


**Figure 11.1(d)** FRAME 2002 NO<sub>y</sub> wet deposition ( $\text{kg N ha}^{-1} \text{ yr}^{-1}$ )

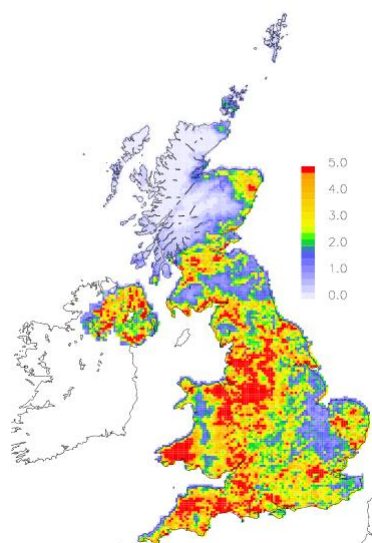


**Figure 11.1(e)** FRAME 2002 NH<sub>x</sub> dry deposition ( $\text{kg N ha}^{-1} \text{ yr}^{-1}$ )

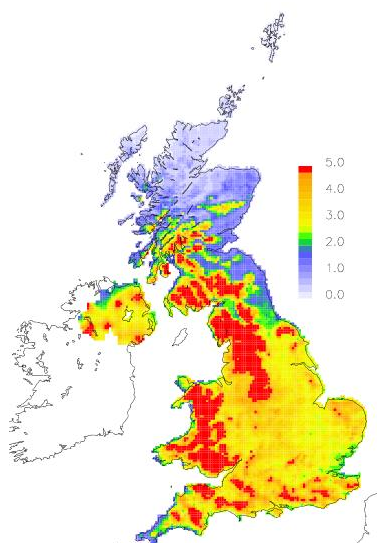


**Figure 11.1(f)** FRAME 2002 NH<sub>x</sub> wet deposition ( $\text{kg N Ha}^{-1} \text{ yr}^{-1}$ )

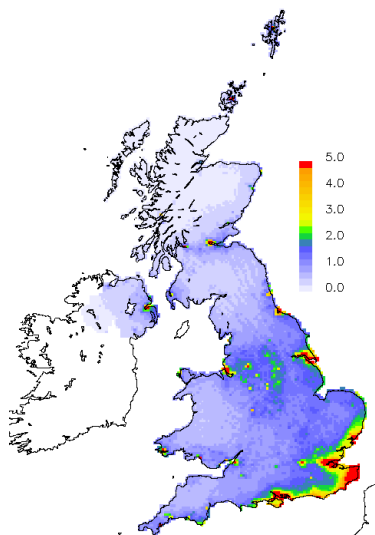


**Figure 11.2(a)** FRAME 2020 SO<sub>x</sub> dry deposition (kg S ha<sup>-1</sup> yr<sup>-1</sup>)

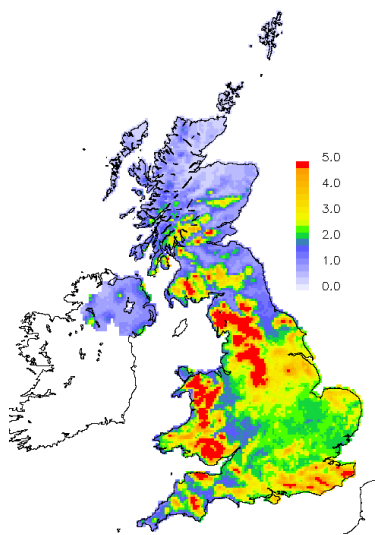


**Figure 11.2(b)** FRAME 2020 SO<sub>x</sub> wet deposition (kg S ha<sup>-1</sup> yr<sup>-1</sup>)

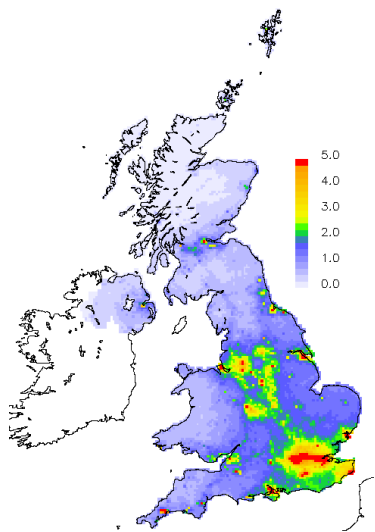


**Figure 11.2(c)** FRAME 2020 NO<sub>y</sub> dry deposition (kg N ha<sup>-1</sup> yr<sup>-1</sup>)

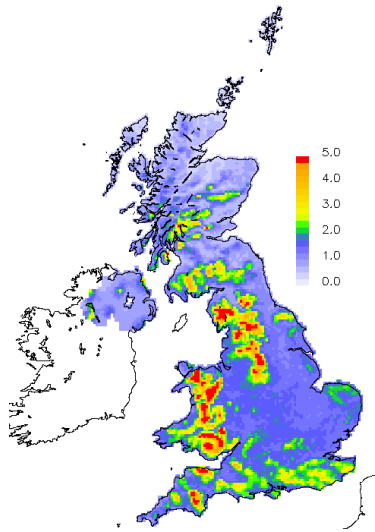


**Figure 11.2(d)** FRAME 2020 NO<sub>y</sub> wet deposition (kg N ha<sup>-1</sup> yr<sup>-1</sup>)

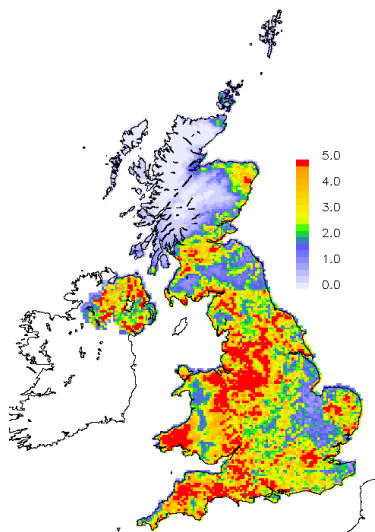


**Figure 11.2(e)** FRAME 2020 NH<sub>x</sub> dry deposition (kg N ha<sup>-1</sup> yr<sup>-1</sup>)

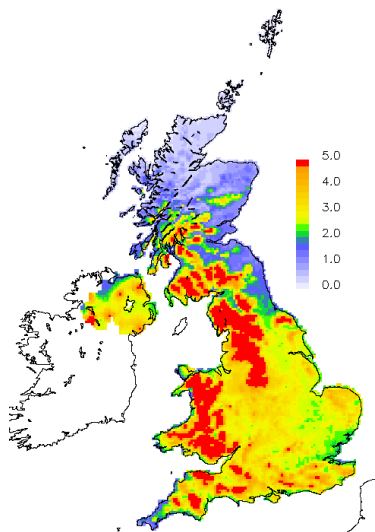


**Figure 11.2(f)** FRAME 2020 NH<sub>x</sub> wet deposition (kg N ha<sup>-1</sup> yr<sup>-1</sup>)

**Table 11.2** UK deposition budgets (kT N and kT S)

Scenario	SO <sub>x</sub> dry deposition	SO <sub>x</sub> wet deposition	SO <sub>x</sub> total deposition	NO <sub>y</sub> dry deposition	NO <sub>y</sub> wet deposition	NO <sub>y</sub> total deposition
2002	55.9	103.7	159.6	46.7	64.8	111.5
2020	27.9	59.6	87.5	29.9	42.8	72.7
A	27.8	59.7	87.5	27.9	40.9	68.8
B	27.8	59.8	87.6	25.5	38.7	64.2
C	27.8	59.7	87.5	27.8	40.8	68.6
K	27.8	60.0	87.8	28.2	38.3	66.5
N	25.6	56.7	82.6	29.5	42.0	71.5
O	27.8	59.7	87.5	27.4	40.4	67.8
P	27.1	59.1	86.2	27.4	40.5	67.9
Q	27.0	59.2	86.2	27.0	40.2	67.2

## 12 Past and Future Trends for Nitrogen and Sulphur

In section 11, FRAME was used to make estimates of nitrogen and sulphur deposition using future emissions scenarios for the year 2020. Here we consider historical and future changes in emissions of SO<sub>2</sub>, NH<sub>3</sub> and NO<sub>x</sub> during the period 1970 to 2020. FRAME is applied to calculate the changing pattern of sulphur and nitrogen deposition to the United Kingdom and the deposition data are used to assess the changes to exceedance of critical loads for acidic deposition and nutrient nitrogen deposition during the 50 year time period.

### 12.1 Past and Future Trends in Emissions of SO<sub>2</sub>, NO<sub>x</sub> and NH<sub>3</sub>

The historical series of total UK emissions of SO<sub>2</sub>, NO<sub>x</sub> and NH<sub>3</sub> (Chris Dore, AEA Technology, personal communication) as well as future predictions of emissions of SO<sub>2</sub> and NO<sub>x</sub> for the years 2010, 2015 and 2020 (John Stedman, AEA Technology, personal communication) are illustrated in Figure 12.1. Over 80% of SO<sub>2</sub> emissions are associated with the power generating industry and industrial combustion, emitted mostly from large stacks. The implementation of cleaner technologies has resulted in a strong decrease in emissions of 88% from 3200 Mg S-SO<sub>2</sub> in 1970 to 400 Mg S-SO<sub>2</sub> in 2005. A further 55% reduction is forecast between 2005 and 2020. During recent years, road transport has accounted for approximately 50% of national NO<sub>x</sub> emissions. Due to an increase in volume of traffic, NO<sub>x</sub> emissions peaked during 1979 at 820 Mg N-NO<sub>x</sub>. A combination of reduced emissions from the power generating industry and the introduction of catalytic converters for motor vehicles has resulted in a 47% reduction to 430 Mg N-NO<sub>x</sub> for 2005. NO<sub>x</sub> emissions are forecast to fall by a further 38% between 2005 and 2020. The time series for NH<sub>3</sub> emissions covers a shorter time span (1990 to 2003). During this period, emissions have fallen by 19% from 305 Mg N-NH<sub>3</sub> to 247 Mg N-NH<sub>3</sub>. Future estimates of NH<sub>3</sub> emissions have not been included in this study.

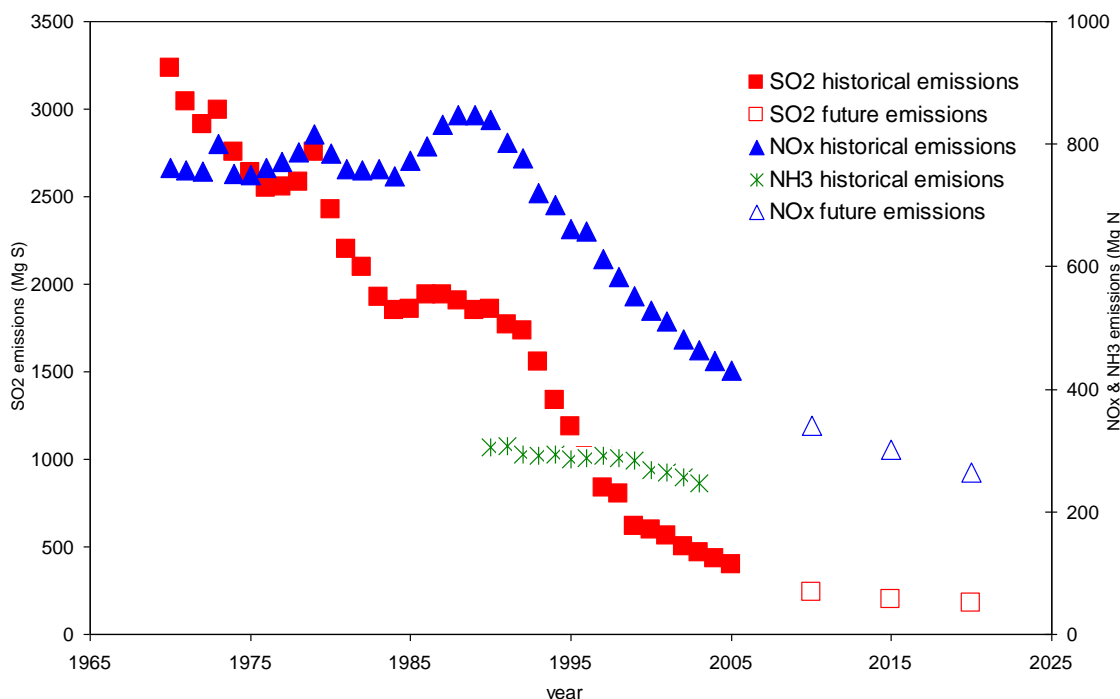


**Figure 12.1** Historical and future trends in total emissions of SO<sub>2</sub>, NO<sub>x</sub> and NH<sub>3</sub> from the UK during 1970 to 2020

## 12.2 Trends in Deposition of Sulphur and Nitrogen

In order to calculate past and future deposition of sulphur and nitrogen to the UK, it is necessary to generate historical and forecast emissions maps. Although some historical emissions maps are available (i.e. for the year 1990), much of these data are incompatible with more recent emissions data as it is gridded at a coarser resolution (10 km for 1990 and 1 km for 2005) and is lacking in separate information on point source emissions. In estimating the temporal trends in deposition to the UK, it is important for input emissions data for different years to be identically formatted otherwise artificial changes in modelled deposition may be generated. The background and point source emissions files for the year 2002 were taken to be the baseline year. The data for total emissions in Figure 12.1 were used to scale emissions backwards and forwards in time and generate new emissions files for the years 1970, 1980, 1990, 2005, 2010 and 2020. Background emissions data were divided into eight different **SNAP** codes (Selected Nomenclature for Air Pollution): energy production and transformation; commercial, institutional and residential combustion; industrial combustion; industrial processes; production and distribution of fossil fuels; road transport; other transport; Waste treatment and disposal. Year-dependent scaling factors were assigned to each SNAP emissions data set and to point source emissions. The UK NH<sub>3</sub> emissions for the years 1970 and 1980 were set at the 1990 level and future emissions for the years 2010, 2015 and 2020 were set at the 2005 level. Emissions from the Republic of Ireland are also included explicitly in the FRAME domain and these were scaled backwards in time in a similar manner to the UK emissions. Future emissions for the years 2010, 2015 and 2020 for the Republic of Ireland were set at the levels defined by the National Emissions Ceiling Directive. Emissions of SO<sub>2</sub> and NO<sub>x</sub> from international shipping were also included in the domain. These were scaled forwards and backwards in time from the baseline year 2000 according to the assumption that emissions are increasing at 2.5% per year (Vestreng and Fagerli, 2005). The concentrations at the start of a FRAME-UK simulation were initialised from a European scale model, FRAME-Europe. The European emissions were scaled according to year in a similar manner to emissions from the UK and the Republic of Ireland.

A relatively simple approach was adopted to generating past and future emissions fields. It is therefore important to consider the consequences of these approximations. Total deposition of nitrogen and sulphur is comprised of two parts: dry (principally gas) deposition and wet deposition (mainly washout of aerosol particles). The latter is associated with long range transport and can therefore be assumed not to be sensitive to local scale changes in source location. Dry deposition of NO<sub>y</sub> is strongly correlated with emissions from major roads and urban centres. Although road construction has taken place during recent decades, it can be assumed that the location of major urban areas and their connecting roads have not undergone major change. Similarly, the location of agricultural areas associated with NH<sub>3</sub> emissions is assumed not to have undergone a major national redistribution during the last few decades. Emissions of SO<sub>2</sub> are principally from power generation and industrial combustion. In this case some redistribution of sources will have taken place during the time scale of the study as certain industrial units were closed and others built. In general, the emissions data used in this study are considered suitable for use in the national scale study considered here, but not appropriate for use in a local scale study.

The deposition of sulphur and oxidised nitrogen calculated by FRAME for the year 1970 is illustrated in figure 12.3. These can be compared with deposition maps for a recent year (2002, figures 11.1(a)-(d)) and for a future year (2002, figures 11.2(a)-(d)). A striking change in deposition is apparent during the 50 year time period. For sulphur, both dry and wet deposition in 1970 exceeded 20 kg S ha<sup>-1</sup> yr<sup>-1</sup> in much of the country. By the year 2002, dry deposition exceeds 5 kg S ha<sup>-1</sup> yr<sup>-1</sup> only in some industrial areas of northern England and in

the south-east although many areas have wet deposition of sulphur in excess of  $5 \text{ kg S ha}^{-1} \text{ yr}^{-1}$ . By 2020, only a restricted region receives annual deposition in excess of  $5 \text{ kg S ha}^{-1} \text{ yr}^{-1}$ , corresponding to the high rainfall areas of the Pennines and some coastal regions which are strongly influenced by shipping emissions. A similar pattern is apparent for NO<sub>y</sub> deposition. Upland regions and areas influenced by vehicle emissions are subject to deposition in excess of  $10 \text{ kg N ha}^{-1} \text{ yr}^{-1}$ . By 2020 the regions where deposition exceeds  $5 \text{ kg N ha}^{-1} \text{ yr}^{-1}$  are restricted to a small number of coastal sites, urban regions and some upland sites.

The trend in average UK deposition to a single vegetation type (forest) is illustrated for the period 1970-2020 in Figure 12.4(a). Total acid deposition is the sum of the depositions of SO<sub>x</sub>, NO<sub>y</sub> and NH<sub>x</sub> and total nitrogen deposition is the sum of the NO<sub>y</sub> and NH<sub>x</sub>. A rapid decline in acidic deposition occurs from 1970 to 1980 driven by the fast decline in SO<sub>x</sub> deposition. The rate of decline slows between 1980 and 1990 due to increases in NO<sub>y</sub> deposition and is high between 1990 and 2005 due to significant decreases in both SO<sub>x</sub> and NO<sub>y</sub> deposition. Beyond 2005, despite further reductions in NO<sub>y</sub> and SO<sub>x</sub> deposition, reductions in total acid deposition are less significant as NH<sub>x</sub> is forecast to make a relatively more important contribution to acidic deposition. The trend in nitrogen deposition follows closely the trend in NO<sub>y</sub> emissions, peaking in 1990 and decreasing steadily to 2020. In figure 12.4(b) the data are plotted to show the change in the relative contributions of SO<sub>x</sub>, NO<sub>y</sub> and NH<sub>x</sub> deposition to acidic deposition and of NO<sub>y</sub> and NH<sub>x</sub> to total nitrogen deposition to forest. During this 50 year period, the role of sulphur is found to change from being the most important to the least important in contributing to acid deposition. Primarily due to the high deposition velocity of ammonia to forest, NH<sub>x</sub> deposition makes an important contribution to both acid and nitrogen deposition. By 2005, 78% of nitrogen deposition and 64% of acid deposition is due to NH<sub>x</sub> deposition. In the absence of emissions controls to ammonia, its relative importance as an acidifying and eutrophying pollutant is forecast to become more important.

## 12.3 Past and Future Trends in the Exceedance of Critical Loads

Total acid deposition was calculated to be the sum of the deposition of SO<sub>x</sub>, NO<sub>y</sub> and NH<sub>x</sub> (which assumes that NH<sub>x</sub> is oxidised in soil) and total nitrogen deposition as the sum of the deposition of NO<sub>y</sub> and NH<sub>x</sub>. For the year 1970, sulphur was found to account for over half of total acid deposition to forest (Figure 12.4(b)). During the period 1970-1990, oxidised nitrogen accounted for 30% of total nitrogen deposition to forest. However, for a recent emissions year (2005), reductions in emissions of SO<sub>2</sub> and NO<sub>x</sub> lead to a changing importance of pollutants, with NH<sub>x</sub> making the greatest contribution to both acid deposition (64%) and total nitrogen deposition (78%) to forest. Without future reductions in ammonia emissions, NH<sub>x</sub> deposition is forecast to increasingly dominate acid and total nitrogen deposition. A description of the methods used to derive and calculate critical loads is given in Hall *et al.* (2004). The exceedances of critical loads of acidity and nutrient nitrogen across the UK were calculated using the FRAME data for 1970, 2002 and 2020. The significant reduction in the areas with exceedance is mapped in Figures 12.5(a) and 12.5(b). Figure 12.6 illustrates the change in the percentage area of sensitive UK habitats for which critical loads of acidity and nutrient nitrogen were exceeded. For acidity, the habitat areas with deposition exceeding critical loads are seen to fall significantly between 1970 and 2020 (from 96% to 22% for dwarf shrub heath). However, for nutrient nitrogen, the percentage area of unmanaged forest exceeded falls only marginally, from 98% to 94% between 1970 and 2020. This is due to the dominant role of dry deposition of ammonia to tall vegetation. The total area of sensitive UK habitats exceeded fell from 89% to 39% for acidity and from 69% to 48% for nutrient nitrogen.

Reductions in acid deposition and total nitrogen deposition may provide the conditions in which chemical and biological recovery of sensitive habitats can begin, but the timescales of these processes are often very long relative to the timescales for reductions in emissions. The study demonstrates the importance of the ability to control emissions of ammonia. Future work will focus on comparison with measurements of changes in wet deposition and air pollutant concentrations in the UK and on changing patterns in atmospheric oxidation rates and incorporation of future emissions estimates for ammonia.

**Figure 12.3(a)** FRAME 1970 SO<sub>x</sub> dry deposition ( $\text{kg S ha}^{-1} \text{yr}^{-1}$ )

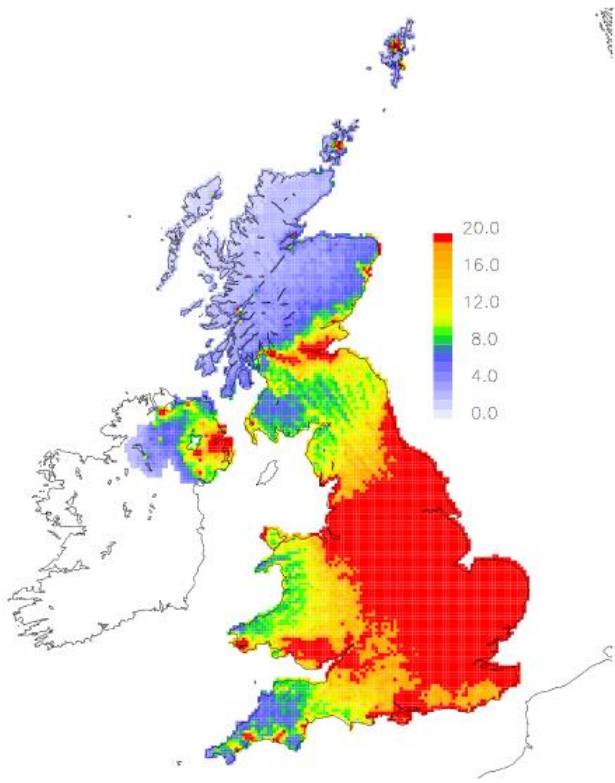


**Figure 12.3(b)** FRAME 1970 SO<sub>x</sub> wet deposition ( $\text{kg S ha}^{-1} \text{yr}^{-1}$ )

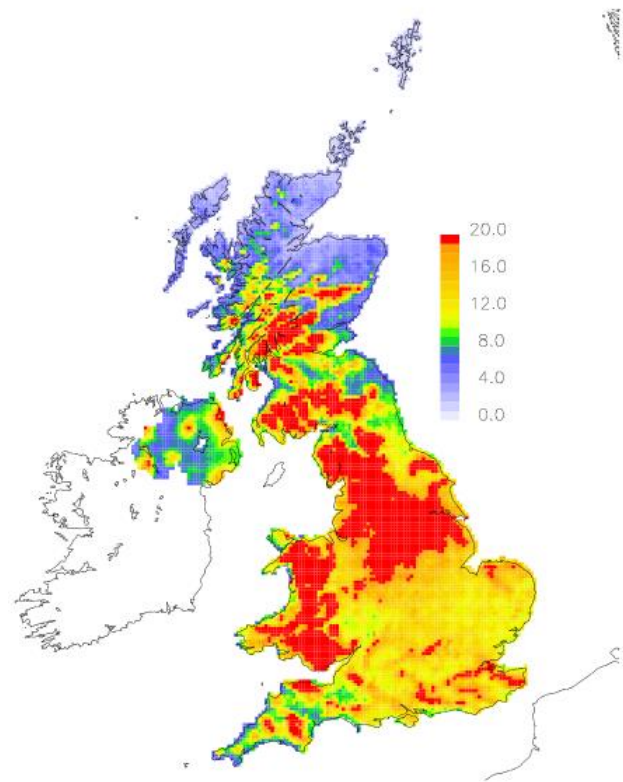


**Figure 12.3(c)** FRAME 1970 NO<sub>y</sub> dry deposition ( $\text{kg N ha}^{-1} \text{yr}^{-1}$ )

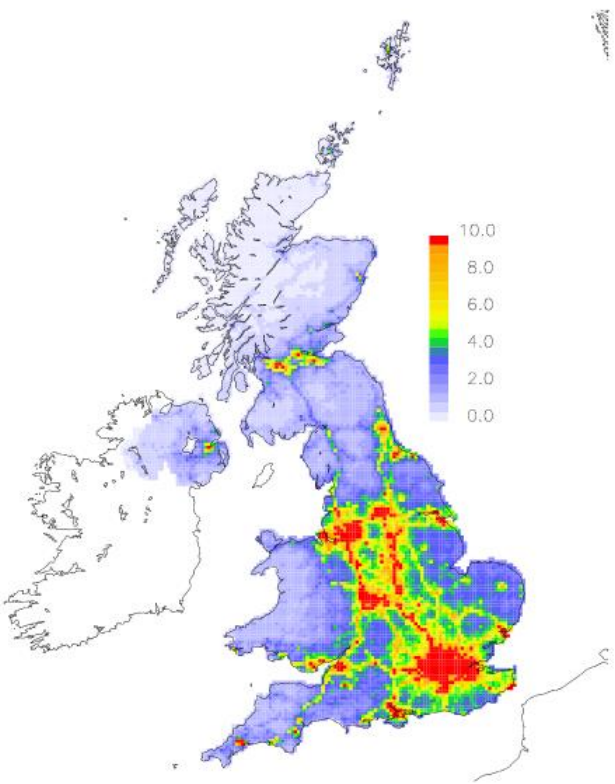


**Figure 12.3(d)** FRAME 1970 NO<sub>y</sub> wet deposition ( $\text{kg N ha}^{-1} \text{yr}^{-1}$ )

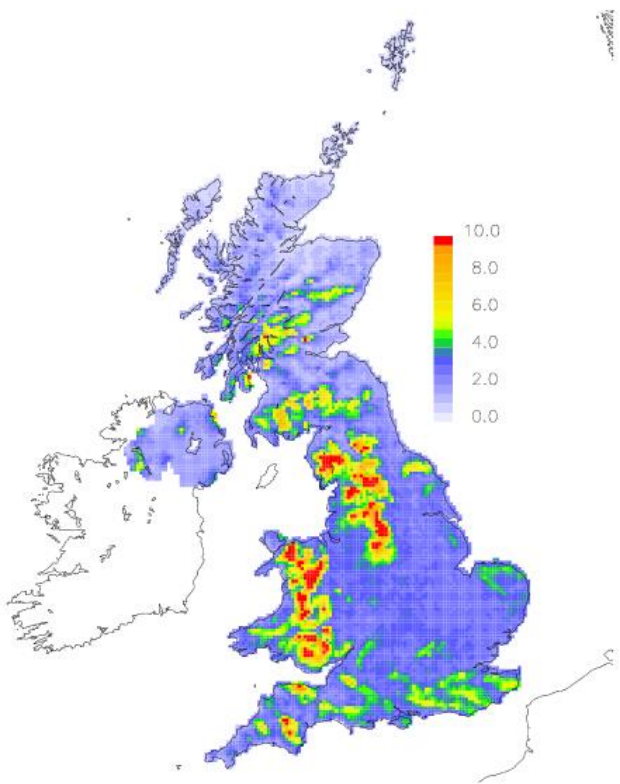


**Figure 12.4(a)** Average deposition to forest in the UK of SO<sub>x</sub>, NO<sub>y</sub> and NH<sub>x</sub> during the period 1970 to 2020

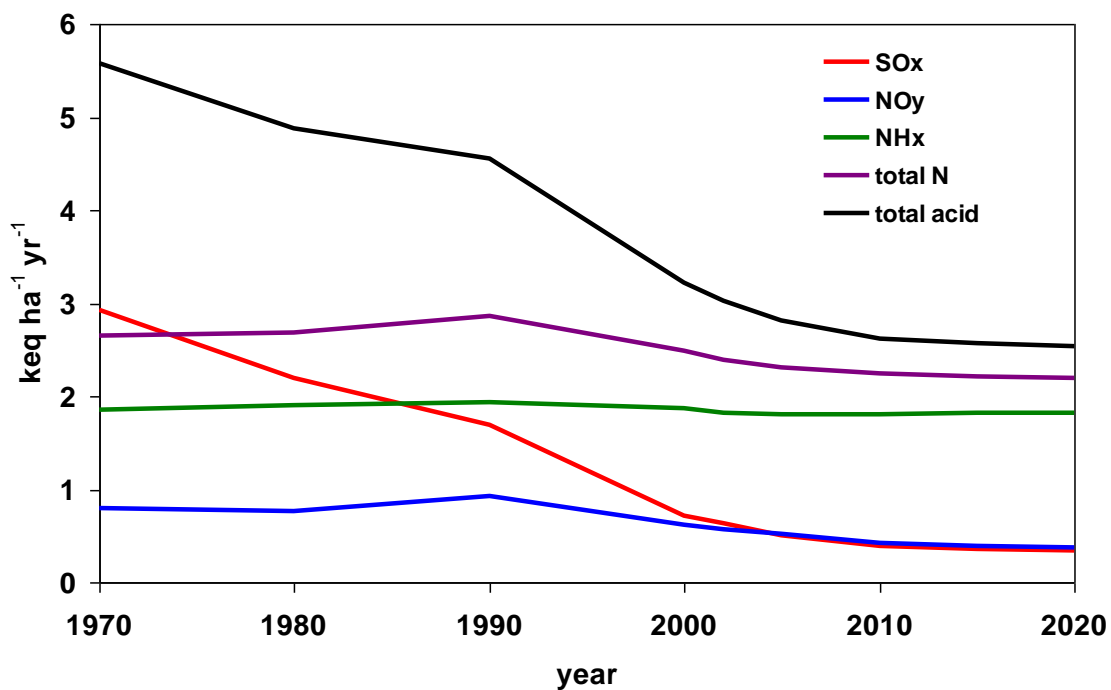


**Figure 12.4(b)** The relative contributions to acidic and nitrogen deposition to forest of SO<sub>x</sub>, NO<sub>y</sub> and NH<sub>x</sub> in the UK during the period 1970 to 2020

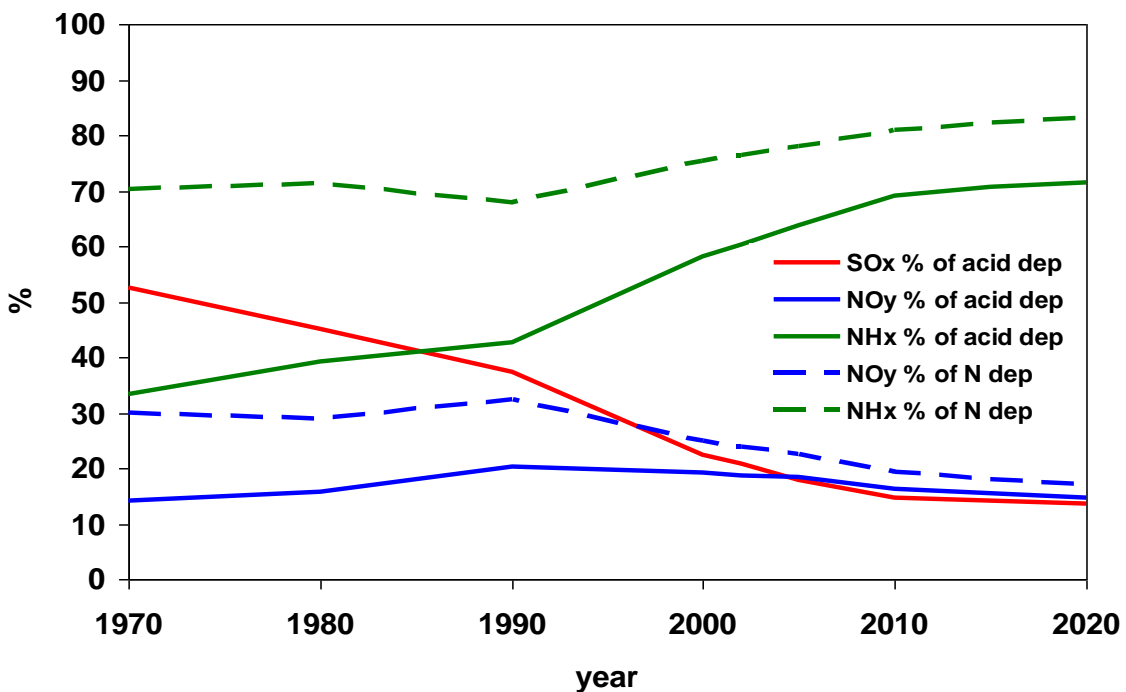


**Figure 12.5(a)**

**Exceedance of 5<sup>th</sup> percentile acidity critical loads by acid deposition for:**

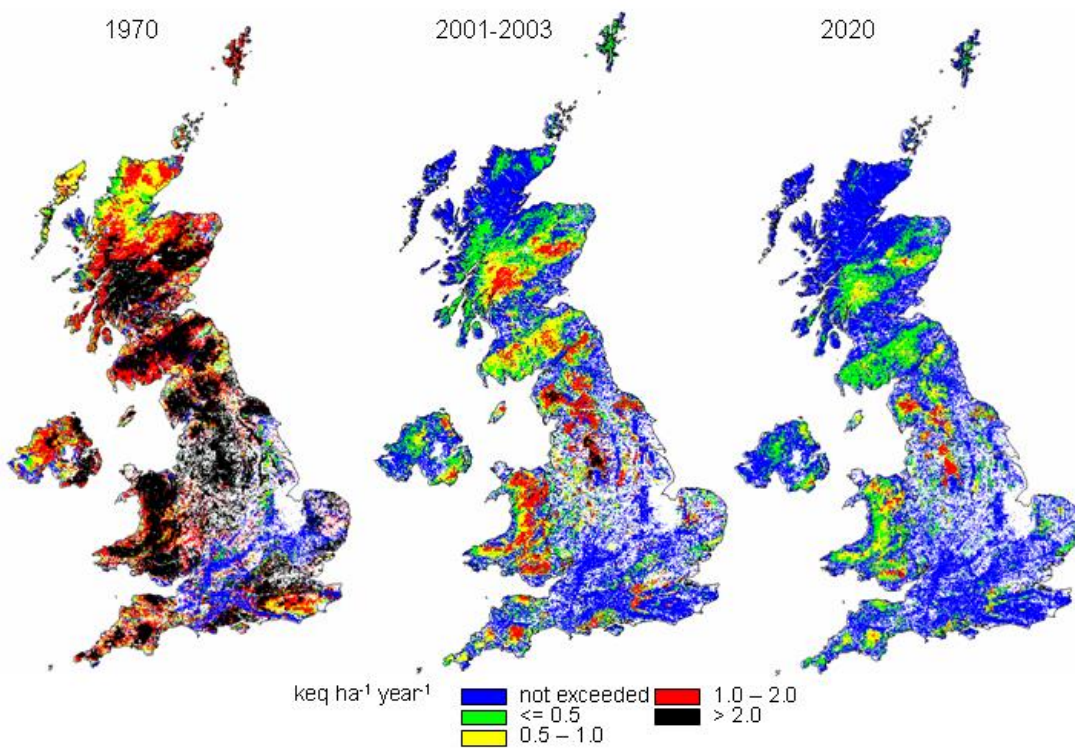


**Figure 12.5(b)**

**Exceedance of 5<sup>th</sup> percentile nutrient nitrogen critical loads by nitrogen deposition for:**

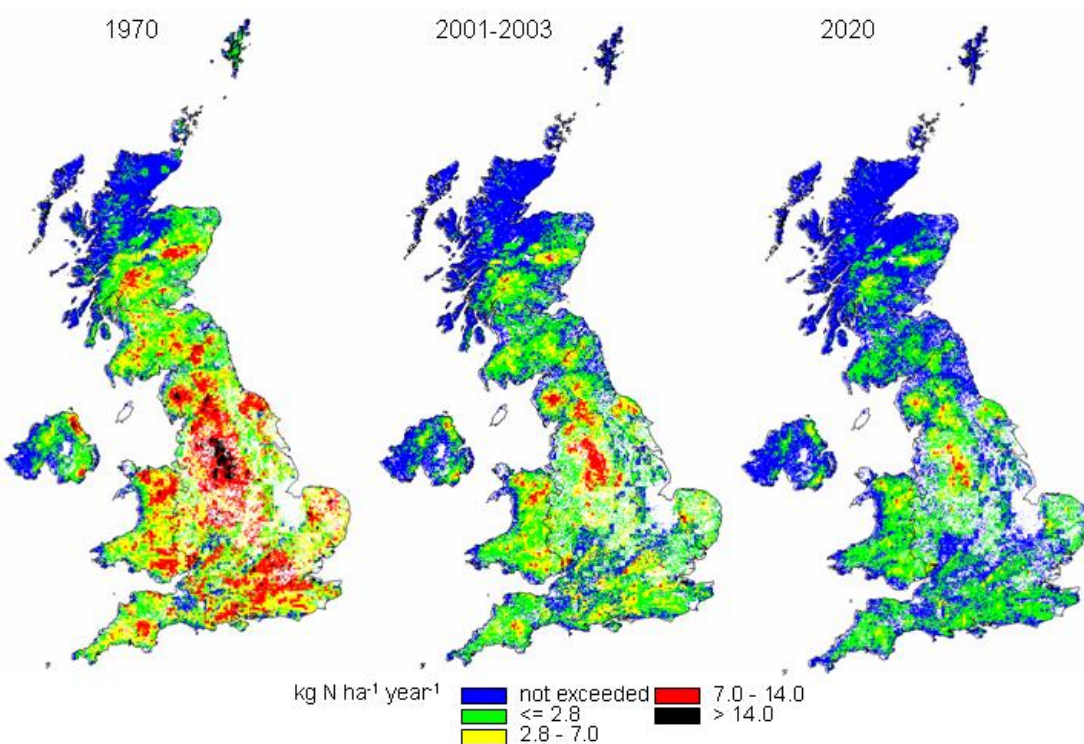
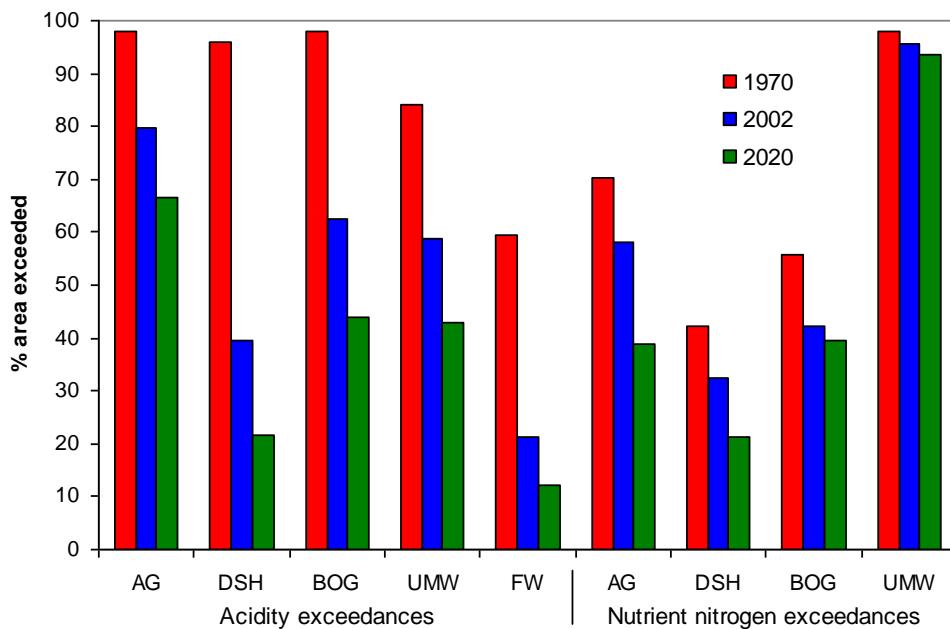


**Figure 12.6** The percentage of ecosystem area in the UK with exceedance of critical loads for deposition of acidity and nitrogen during 1970 to 2020 (AG: Acid Grassland, DSH: Dwarf Shrub Heath, BOG: bog, UMW: unmanaged woodland, FW: freshwater)



## 13 Source-Receptor Relationships for the UKIAM

FRAME was applied to generating source-receptor relationships for input to the United Kingdom Integrated Assessment Model (**UKIAM**). Integrated assessment is a procedure used to estimate the most cost effective measures of protecting the environment from the effects of air pollution by reduction of emissions. Such studies combine atmospheric transport modelling with procedures for environmental assessment and financial estimates for the costs of introducing clean technologies. A source-receptor relationship correlates an air pollutant emissions source to a receptor of the pollutant, in this case a mapped deposition ‘footprint’. An emissions source footprint may be calculated with FRAME by running two model simulations: firstly with all sources included; secondly with a single source removed. The receptor footprint is the difference in deposition between the first and second simulations.

For this study the following source deposition footprints of sulphur and reduced and oxidised nitrogen were modelled separately:

- Emissions from the 75 counties in the United Kingdom
- Emissions from 20 major point sources
- Emissions from international shipping
- Import of pollutants from European sources

Analysis of these data is not included here, but is described in detail in Oxley *et al.*, (2003)

## 14. FRAME web site

A web site dedicated to FRAME ([www.frame.ceh.ac.uk](http://www.frame.ceh.ac.uk)) has been developed and includes the following information:

- Background, including the development of different versions of the model.
- Model description, including the parameterisation of emissions, chemical transformation, trajectories and wet and dry deposition processes.
- Deposition maps of wet and dry deposition of sulphur and reduced and oxidised nitrogen.
- Correlation plots of modelled data compared to data from the national monitoring networks for gas and aerosol concentrations and wet deposition.
- Critical Loads Exceedances, including a description of calculation procedures and results for past and future years
- Reports, including a status report, prepared at the start of the current contract and the final contract report.

## 14. References

- Abbott J., Hayman G., Vincent K., Metcalfe S., Dore T., Skeffington P., Whyatt D., Passant N., Woodfield M. (2003) Uncertainty in acid deposition modelling and critical load assessments. R & D Technical Report TR4-083(5)/1, Environment Agency, Bristol, UK.
- ApSimon, H.M., Barker, B.M. and Kayin, S. (1994). Modelling studies of the atmospheric release and transport of ammonia in anticyclonic periods. *Atmos.Env.* **28(4)**, 665-678.
- Barrett, K. (1998) Oceanic emissions in Europe and their transboundary fluxes. *Atmos.Env.*, **32(3)**, 381-391
- Barrett, K. and Seland, O. (1995). European Transboundary Acidifying Air Pollution – Ten years calculated field data and budgets to the end of the first Sulphur Protocol. EMEP report 1/95. Norwegian Meteor. Inst. Oslo, Norway.
- COMEAP (2001) Statement on long-term effects of particles on mortality, Committee On the Medical Effects of Air Pollution, <http://www.advisorybodies.doh.gov.uk/comeap>
- DETTR. 2000. Department of the Environment, Transport and the Regions, The Scottish Executive, The National Assembly for Wales and The Department of the Environment in Northern Ireland. The Air Quality Strategy for England, Scotland, Wales and Northern Ireland. January 2000.
- Dore A.J., Choularton, T.W. and Fowler, D. (1992) An improved wet deposition map of the United Kingdom incorporating the seeder-feeder effect over mountainous terrain. *Atmos.Environ.* **26A**, 1375-1381.
- Dore, A.J., Vieno, M., Fournier, N., Weston, K.J. and Sutton, M.A. (2005) Development of a new wind rose for the British Isles using radiosonde data and application to an atmospheric transport model. *Q.J.Roy.Met.Soc.* (under review).
- Dore, A.J., Mousavi-Baygi, M., Smith, R.I., Hall, J., Fowler, D. and Choularton, T.W. (2006) A model of annual orographic precipitation and acid deposition and its application to Snowdonia. *Atmos.Env.*, (in press)
- Dragosits, U., Sutton, M.A., Place, C.J. and Bayley A. (1998) Modelling the spatial distribution of ammonia emissions in the UK. *Environ. Pollut.* **102**, S1, 195-203.
- ENTEC (2003) Investigation into Benefits of Proposals on the Sulphur Content of Marine Fuels, Final Report for DEFRA, August 2003.
- Fournier, N., Pais, V.A., Sutton, M.A., Weston K.J., Dragosits U., Tang Y.S., and Aherne, J. (2003) Parallelization and application of a multi-layer atmospheric transport model to quantify dispersion and deposition of ammonia over the British Isles. *Environmental Pollution*, **116(1)**, 95-107.
- Fournier, N., Dore, A.J., Vieno, M., Weston, K.J., Dragosits, U. and Sutton, M.A. (2004) Modelling the deposition of atmospheric oxidised nitrogen and sulphur to the United Kingdom using a multi-layer long-range transport model. *Atmos.Env.*, **38(5)**, 683-694.
- Fournier, N., Weston, K.J., Dore, A.J. and Sutton, M.A. (2005a) Modelling the wet deposition of reduced nitrogen over the British Isles using a Lagrangian multi-layer atmospheric transport model. *Q.J.Roy.Met.Soc.*, **131**, 703-722.
- Fournier, N., Tang, Y.S., Dragosits, U., de Kluizenaar, Y. and Sutton, M.A. (2005b) Regional atmospheric budgets of reduced nitrogen over the British Isles assessed using an atmospheric transport model. *Water, Air and Soil Pollution*, **162**, 331-351
- Fowler D., Cape J., Leith I.D., Choularton T.W., Gay M.J., Jones A. (1988) The influence of altitude on rainfall composition. *Atmos.Env.* **22**, 1355-1362.

- Fowler, D., Smith, R.I., Muller, J.B.A., Hayman, G. and Vincent, K.J., (2005) Changes in the atmospheric deposition of acidifying compounds in the UK between 1986 and 2001. *Environmental Pollution*, **137**, 12-25.
- Hall, J., Ulyett, J., Heywood, L., Broughton, R. & 12 UK experts. (2004) Update to: The Status of UK Critical Loads – Critical Loads Methods, Data and Maps, February 2004. Report to DEFRA (Contract EPG 1/3/185). (<http://critloads.ceh.ac.uk>)
- Joffre, S.M. (1988) Modelling the dry deposition velocity of highly soluble gases to the sea surface. *Atmos.Env.*, **22(6)**, 1137-1146.
- Johnson, J.E., Tarrasón, L. and Bartnicki, J. (2000). Effects of international shipping on European pollution levels. EMEP/MSC-W Note 5/00. EMEP, Meteorological Synthesizing Centre – West, Norwegian Meteorological Institute, Oslo, Norway ([www.emep.int](http://www.emep.int))
- Lee, D.S., Halliwell, C., Garland, J.A., Dollard, G.J. & Kingdom, R.D. (1998) Exchange of ammonia at the sea surface – A preliminary study. *Atmos.Env.*, **32**, 431-439.
- Lee, D.S., Kingdom, R.D., Jenkin, M.E. and Garland, J.A. (2000) Modelling the atmospheric oxidised and reduced nitrogen budgets for the UK with a Lagrangian multi-layer long-range transport model. *Environmental modelling and assessment*. **5**, 83-104.
- Metcalfe, S.E., Whyatt, J.D., Broughton, R., Derwent, R.G., Finnegan, D., Hall, J., Mineter, M., O'Donoghue, M. and Sutton, M.A. (2001) Developing the Hull Acid Rain Model: its validation and implication for policy makers. *Environmental Science & Policy*, **4**, 25-37.
- NEGTAP (2001) Transboundary Air Pollution: Acidification, Eutrophication and Ground Level ozone in the UK. Report of the National Expert Group on Transboundary Air Pollution, DEFRA, London.
- Oxley, T., ApSimon, H., Dore, A.J., Sutton, M.A. Hall, J., Heywood, E., Gonzales del Campo, T. and Warren, R. (2003) The UK Integrated Assessment Model, UKIAM: A National Scale Approach to the analysis of strategies for abatement of atmospheric pollutants under the convention on long-range transboundary air pollution *Integrated Assessment*, **4**, 236-249.
- Page T., Whyatt J.D., Beven K.J., Metcalfe S.E. (2004) Uncertainty in modelled estimates of acid deposition across Wales: a GLUE approach *Atmos.Env.*. **38**, 2079-2090.
- Singles, R.J. (1996) Fine resolution modelling of ammonia dry deposition over Great Britain. Ph.D. thesis, Department of Meteorology, University of Edinburgh. pp 278.
- Singles, R.J., Sutton, M.A. and Weston, K.J. (1998) A multi-layer model to describe the atmospheric transport and deposition of ammonia in Great Britain. *Atmos.Env.*, **32**, 393-399.
- Smith, R.I., Fowler, D., Sutton, M.A., Flechard, C. and Coyle, M. (2000) Regional estimation of pollutant gas deposition in the UK: model description, sensitivity analyses and outputs. *Atmos.Env.* **34**, 3757-3777.
- Smith, R.I. and Fowler, D. (2001) Uncertainty in wet deposition of sulphur. *Water, Air and Soil Pollution: Focus* **1**: 341-354.
- Tarrasón, L., Fagerli, H., Eiof Jonson, J., Klein, H., van Loon, M., Simpson, D., Tsyro, S., Vestreng, V., Wind, P., Posch, M., Solberg, S., Spranger, T., Cuvelier, K., Thunis, P., White, L. (2003) Transboundary Acidification, Eutrophication and Ground Level Ozone in Europe. PART I Unified EMEP Model description. EMEP Status Report 2003
- Van den Beuken R. (1997) Mapping emission and dry deposition of ammonia for Ireland. FERG Report 24. Dept ERM, Univ. College Dublin.
- Vestreng, V. and Fagerli, H. (2005) The role of past, present and future shipping emissions in European acidification, eutrophication and ozone levels. 1<sup>st</sup> ACCENT symposium, Urbino, September 12-16 2005, p215
- Vieno, M. (2005) The use of an Atmospheric Chemistry-Transport Model (FRAME) over the UK and the development of its numerical and physical schemes. PhD thesis, University of Edinburgh

# **Appendix 1: Summary log of major developments in FRAME in relation to model versions**

The following lists the major developments on FRAME as they have been incorporated into the model. Prototype versions have also been developed to consider a number of other features, such as bi-directional ammonia exchange, modified wind roses and alternative model diffusion schemes. In addition, to the application of FRAME to acid and nitrogen deposition, a second version of FRAME, referred to as Metal-FRAME has been developed for the analysis of heavy metal deposition over the UK.

## **FRAME 1.0 : Great Britain (1993-1996)**

The first version of the FRAME model resulted from the work of Singles (1998). FRAME was established as being the first UK model of  $\text{NH}_x$ ,  $\text{NO}_y$  and  $\text{SO}_2$  to be: a) 5 km grid resolution, b) multi-layer (33 layers in the vertical), c) incorporate ecosystem specific deposition to different receptors for ammonia, allowing critical loads exceedances to be calculated. FRAME 1.0 covered only Great Britain, as no spatial  $\text{NH}_3$  emission inventory was available at that stage for Northern Ireland.

## **FRAME 1.1: United Kingdom (1998-1999)**

This version corresponded to the extension of the domain of the model from Great Britain to the United Kingdom by including Northern Ireland, using the inventory developed by Dragosits *et al.* (1998).

## **FRAME 2.0: British Isles (1999-2000)**

A limitation of FRAME 1.1 was that the treatment of Northern Ireland was inaccurate because of important trans-boundary fluxes with Eire not being adequately treated. Given the rectangular domain of FRAME it was evident that Eire should be incorporated explicitly in the model domain. This extension was accomplished in FRAME 2.0, including the 5 km ammonia emissions from van den Beuken (1997), together with emissions of  $\text{SO}_2$  and  $\text{NO}_x$  from the Irish EPA. With this change, FRAME became the first British Isles scale atmospheric transport model of  $\text{NH}_3$ ,  $\text{NO}_x$  and  $\text{SO}_2$ . The model was further developed to allow treatment of sub-domains. With this extension, it became possible to calculate atmospheric budgets for the UK as part of the British Isles model, as well as for devolved regions, such as Wales, Scotland etc.

## **FRAME 3.0: Parallelisation (1999-2000)**

A key limitation of the previous versions of FRAME was the slow model run time, being 6 days for FRAME 1.0 and 8 days for FRAME 2.0 on a Sun Workstation. The model was therefore re-built to allow it to be run using parallel processing, with High Performance Fortran. On the EPCC Cray T3E this provided a run time of about one hour, although more practical (due to access restrictions) was the running of the parallel version (FRAME 3.0) on a 4 processor Sun workstation, allowing a run time of 2 days.

## **FRAME 3.1: Parallelisation and load-balance (2000)**

The load-balance was improved by considering the length of the trajectories before distributing them to the processors of the parallel computer.

## **FRAME 4.0: Finite Volume method (2000-2001)**

FRAME versions 1 to 3 were established with the multi-layer diffusion being calculated using the 4<sup>th</sup> order Runge-Kutta method. This was computationally inefficient, and as a complement to the development of a parallel version of FRAME, a new diffusion scheme was developed using the implicit Finite Volume Method. On the four-processor parallel Sun workstation, this provided a run time of 2.5 hours. This much improved run-time provided the basis for subsequent model developments to be conducted effectively.

## **FRAME 4.1: Directional orographic rainfall (2000-2001)**

FRAME 4.1 was developed to incorporate directional orographic rainfall using a precipitation model. This allowed for increased orographic precipitation on the upwind side of hilly areas, providing an advance on the previous non-directional orographic enhancement of wet deposition. The initial parameterisation was consolidated with other model changes at Version 4.9.

## **FRAME 4.2: Variable depth of the mixing layer (2001)**

FRAME 4.2 considered a new parameterisation of the scavenging coefficients. In earlier versions a constant height of the mixing layer was used to calculate scavenging coefficients. Strictly, however this is dependent on mixing depth, which is calculated diurnally (on an hourly basis) within FRAME. The scavenging calculation was therefore modified to take account of the variable height of the mixing layer.

## **FRAME 4.3: Dry deposition velocities revision (2001)**

In FRAME 4.3 deposition velocities of the model were modified for oxidized nitrogen species.

## **FRAME 4.4: HNO<sub>3</sub> dry deposition (2001)**

This version revised the dry deposition velocity of HNO<sub>3</sub> to 30 mm s<sup>-1</sup> instead of the value of 10 mm s<sup>-1</sup> used in FRAME 4.3.

## **FRAME 4.5: NO<sub>x</sub> emissions height (2001)**

This version upgraded FRAME 4.4 by distributing the NO<sub>x</sub> emissions throughout the lowest 100 m instead of 300 m.

## **FRAME 4.6: SO<sub>2</sub> point sources (2001)**

FRAME 4.6 included SO<sub>2</sub> emissions from high-level point sources at the height of each stack (according to site based information from the National Atmospheric Emissions Inventory). This provided the basis to extend the approach to NO<sub>x</sub> (FRAME 4.7) and develop a plume rise module in future versions.

## **FRAME 4.7: NO<sub>x</sub> point sources (2002)**

FRAME 4.7 included high-level NO<sub>x</sub> point sources based on stack height information from the NAEI on a site basis.

## **FRAME 4.8: NO<sub>3</sub><sup>-</sup> night-time formation (2002)**

In FRAME 4.8, the reaction rate ( $k_{12}$ ) of NO<sub>3</sub><sup>-</sup> at night-time was updated to a value more consistent with the latest scientific literature.

#### **FRAME 4.9: Directional orographic rainfall (2002)**

In FRAME 4.9 the directional orographic rainfall from FRAME 4.1 was consolidated with the other changes up to FRAME 4.8.

#### **FRAME 4.10-4.14: Operational changes (2002)**

A series of changes was made to streamline the FRAME code and make it operationally more efficient, including use of input data and generation of output data in forms required by FRAME users.

#### **FRAME 4.15 : 1 degree resolution of the wind rose (November 2002)**

FRAME 4.15 introduced a fine 1° resolution in the trajectories (which was previously 15°). This was effective in removing problems caused by the ‘wheel spoke effect’.

#### **FRAME 4.16: Vegetation specific deposition of NO<sub>2</sub> and SO<sub>2</sub> (January 2003)**

Vegetation specific deposition of NO<sub>2</sub> and SO<sub>2</sub> (for forest, moor land, grassland, arable and urban) was introduced to FRAME.

#### **FRAME 4.17: Plume rise of point source emissions (February 2003)**

A parameterisation for plume rise of emissions from point sources, dependent on stack height, diameter, temperature, exit velocity and atmospheric stability class was introduced to FRAME.

#### **FRAME 4.18: Receptor option with trajectories starting at domain edge (June 2003)**

Trajectories were set to start at the edge of the model domain rather than the UK coast (allowing inclusion of shipping emissions over the North Sea). A receptor option was introduced allowing quick test simulations with only the trajectories covering pre-defined ‘receptor’ squares initialised.

#### **FRAME 4.19: Improvement to import, export and emissions routines (July 2003)**

The subroutines representing export, import and emissions in FRAME were streamlined.

#### **FRAME 4.20: Separate UK and Eire input files, batch simulation option (August 2003)**

Emissions files for the Republic of Ireland and the UK were separated. An option to execute multiple simulations (for application to source-receptor calculations) using a progressive numbering system for output files was introduced.

#### **FRAME 4.21: Shipping emissions of SO<sub>2</sub> and dry deposition of gases to sea water (August 2003)**

Emissions of SO<sub>2</sub> from international shipping and dry deposition of gases to sea water were introduced to the FRAME domain.

#### **FRAME 4.22: Improvement to emissions files input and input parameter file (September 2003)**

Operational improvements were made to emissions files input and the format of the FRAME parameter options file.

#### **FRAME 4.23: Bi-directional exchange of ammonia option (October 2003)**

An option was introduced to FRAME to allow for the bi-directional exchange of ammonia using a canopy compensation point formulation.

#### **FRAME 4.24: Plume spread emissions option & f90 standardisation (December 2003)**

An option was introduced to allow the spreading of point source emissions from one grid cell to 3\*3 grid cells (resulting in further reductions of trajectory anomalies due the wheel spoke effect). The code was standardised according to FORTRAN 90.

#### **FRAME 4.25: Option to read ammonia sector emissions separately (January 2004)**

Ammonia emissions were input to the model according to sector (pigs, poultry, cattle, sheep, and fertiliser, non-agricultural). Due to confidentiality of these farm derived data from DEFRA and the devolved administrations (from the CEH AENEID model, Dragosits *et al.* 1998), it became necessary for FRAME modellers to sign a confidentiality agreement, covering the terms already ready signed between CEH, DEFRA and the Devolved administrations.

#### **FRAME 4.26: Operational improvements (February 2004)**

Reorganisation of input files and removal of redundant options

#### **FRAME 5.0: Unified FRAME (August 2004)**

The model was set up to allow three separate simulation options for: (i) acidifying species & radiatively active gases (ii) heavy metals (iii) base cations. The calibration procedure for deposition data was automated.

#### **FRAME 5.1: Improvements to HNO<sub>3</sub> representation (September 2004)**

Changes to chemical reaction rates and removal rates were introduced resulting in improved correlation of HNO<sub>3</sub> concentrations with measurements.

#### **FRAME 5.2-5.3 SNAP-code dependent specific emissions input (March /2005)**

Background emissions of SO<sub>2</sub> and NO<sub>x</sub> were input according to snap code with height of emission formulated according to sector. The point source emissions data base was updated to include 900 point sources with detailed stack parameters for 250 sources.

#### **FRAME 5.4 Reformatting of emissions files and shipping emissions of NO<sub>x</sub> (June 2005)**

The emissions files were all re-formatted to a common \*.csv formulation, shipping emissions of NO<sub>x</sub> were introduced and over-shooting of the boundary layer by the plume rise routine was suppressed.

#### **FRAME 5.5: Calibration update and additional emissions years (November 2005)**

The CBED calibration data standard was updated from 1998-2000 to 2001-03. The option for running different emissions years was extended to include 1970, 1980, 1990, 1996, 1999, 2000, 2002, 2003, 2005, 2010, 2015, 2010, 2015 and 2020.

## Appendix 2: Flow chart illustrating the FRAME mechanism

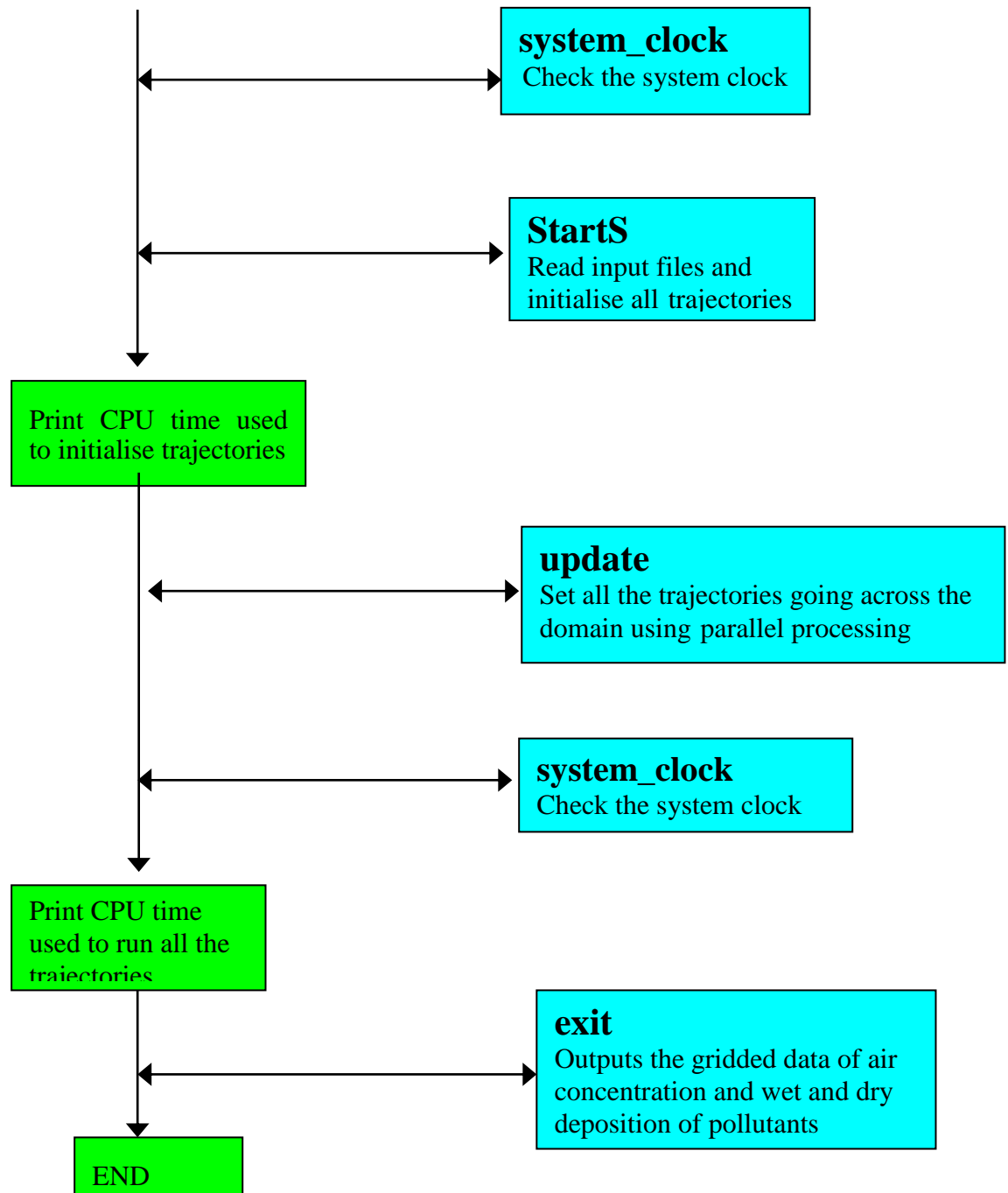
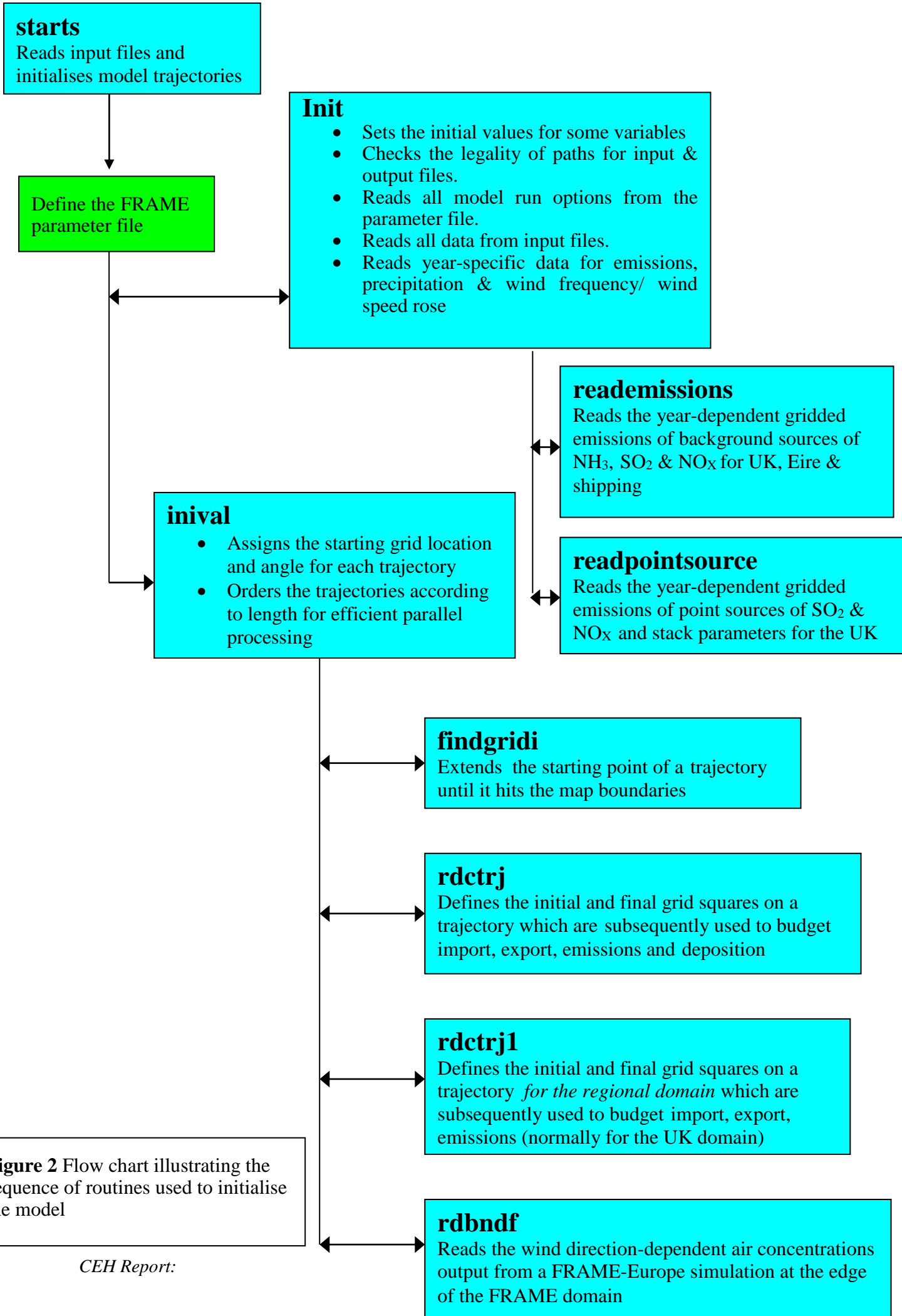


**Figure1.** Flow chart illustrating the overall layout of the major routines in the FRAME code



## update

Updates chemical and physical variables according to the location of the air column

**Figure 3** Flow chart illustrating the sequence of routines used to advect trajectories and update physical and chemical variables

